

University of Dundee

MASTER OF SCIENCE

Soil erosion risk along a buried hydrocarbon pipeline in Scotland

Kats, Kayleigh

Award date:
2022

Licence:
Copyright of the Author. All Rights Reserved

[Link to publication](#)

General rights

Copyright and moral rights for the publications made accessible in the public portal are retained by the authors and/or other copyright owners and it is a condition of accessing publications that users recognise and abide by the legal requirements associated with these rights.

- Users may download and print one copy of any publication from the public portal for the purpose of private study or research.
- You may not further distribute the material or use it for any profit-making activity or commercial gain
- You may freely distribute the URL identifying the publication in the public portal

Take down policy

If you believe that this document breaches copyright please contact us providing details, and we will remove access to the work immediately and investigate your claim.



Soil erosion risk along a buried hydrocarbon pipeline in Scotland

Kayleigh Kats

A thesis submitted for the degree of Master of Science by Research

University of Dundee

May 2022

Acknowledgments

Throughout this degree I have received great support and guidance. I would like to thank my supervisors Professor Glyn Bengough and Dr Andrew Black whose expertise and knowledge in bringing the research topic together during the COVID pandemic.

I would also like to acknowledge my colleagues and staff from the NERC Oil and Gas programme for their support and training opportunities. In particular I would like to give thanks to Mrs Lorna Morrow and Ms Anna Clark for your support during the course and field work excursions. In addition I would also like to thank my family, both the Kats, Skippers, and Milnes, who have been supportive throughout the research and write up of this thesis.

This thesis is in dedication to my father Michael who was proud and supportive of my passion for geoscience, and left this world knowing the outcome of this research.

Signed declaration

I, Kayleigh Kats, as the candidate am the author of this thesis; that, unless otherwise stated, all references cited have been consulted by me; that the work of which the thesis is a record has been done by me, and that it has not been previously accepted for a higher degree. The thesis is not based upon joint research.

Kayleigh Kats
30th September 2021

Abstract

Onshore buried pipelines are potentially at risk of soil erosion by heavy rainfall events that may decrease pipeline cover and increase the risk of pipeline failure. The National Grid gas pipeline that runs throughout Scotland was studied in relation to the number and change in heavy (≥ 4 mm/h) rainfall events per annum at three locations (Dyce, Leuchars and Eskdalemuir) along the pipeline route. Eskdalemuir experienced more than double the number of heavy rainfall events per year with a mean value of 30, compared to Dyce at 11 and Leuchars at 9. The number of rainfall events was highly variable, with the 2015 winter period alone at Eskdalemuir experiencing 21 heavy rainfall events. The G.I.S. analysis of the pipeline showed that 740 km of the 1611 km length of the pipeline was classified as arable land cover. Crop records attributed to 531 km of the pipeline length to spring and winter cereals, oilseed rape and potatoes sown in light-textured loamy soils. These arable soils are relatively vulnerable to soil erosion and are located mainly in the (drier) North of the pipeline route. The much wetter Eskdalemuir region, in the south west, is much less agriculturally active but also has steeper slopes.

Eskdalemuir was selected to evaluate ground displacement using Sentinel-1 radar imagery as this area experiences intense rainfall events and is in elevated terrain and erosion of even a few metres of pipeline is a potentially serious hazard. Fifty-four image pairs were processed for the winter periods of 2015 to 2018: the top 10% of ground displacement points along the pipeline route ranged from -43mm to -11 mm and indicated locations where significant erosion may have occurred. Ground displacements immediately above the pipeline appeared similar to those on either side of the pipeline corridor. Risk factors (slope, soil grouping and land use) were mapped to compare with a published European soil erosion risk map and the ground displacements map. The G.I.S.-based risk mapping and monitoring of ground displacement all indicated areas of potential concern, but showed few areas of complete agreement. Whilst all methods highlight areas at risk they mainly indicate sites that require field visits for local assessment of soil conditions.

Contents

Acknowledgments	i
Abstract	ii
1 Introduction	1
1.1 Onshore oil and gas pipelines	1
1.2 The challenges facing buried Onshore infrastructure	2
1.3 Problem identification	2
1.4 Aims and objectives	3
2 Literature review	5
2.1 Geohazards contributing to pipeline failure	5
2.1.1 Liquid pipeline failure	6
2.1.2 Gas pipeline failures	6
2.2 Pipeline integrity	7
2.2.1 Fluid category and API gravity	8
2.2.2 Thermal and pressure regimes	9
Heavy and extra heavy oil	10
Key global pipelines	10
2.2.3 Pipeline installation and typical burial depths	11
2.3 Monitoring and estimating depth of cover	12
2.3.1 Identifying soil erosion risk	13
2.3.2 Lidar as a technique estimating depth of cover	13
2.4 Threats to changes in depth of cover	14
2.4.1 Increase in precipitation	14
2.4.2 Changes in the oil and gas industry	15
2.4.3 Vegetation and climate	16
2.5 Pipeline thermal regime and vegetation growth	17
2.6 Soil erosion along pipeline right of way	18
2.7 Pipeline uplift	20
2.7.1 Vertical displacement	21
2.7.2 Lateral displacement	22
2.8 Conclusion	23

3	Evaluating the change in patterns of heavy rainfall events in Eastern Scotland	24
3.1	Introduction	24
3.1.1	Peak over threshold selection	25
3.1.2	Aims and objectives	25
3.2	Materials and methods	26
3.2.1	Study location	26
3.2.2	Data sources and methods	27
	Data acquisition	28
3.2.3	Method	28
	MIDAS data processing and quality checking	29
	UKCP18 data processing	29
3.3	Results	31
3.3.1	Annual rainfall (MIDAS)	31
	Total annual rainfall and exceedance over time (MIDAS)	32
3.3.2	Historical seasonal rainfall patterns (MIDAS)	33
	Autumn and summer exceedance events(MIDAS)	33
	Winter and spring exceedance events (MIDAS)	34
	Eskdalemuir changes by 20 year period	35
3.3.3	Future annual rainfall projections (UKCP18)	36
3.4	Discussion	37
3.4.1	Annual trend	37
3.4.2	Seasonal change in heavy rainfall events and possible drivers	38
3.4.3	Future simulations and pipeline risk mapping	39
3.5	Conclusion	39
4	Evaluating the soil erosion risk to a hydrocarbon pipeline using G.I.S	41
4.1	Introduction	41
4.1.1	Aims and objectives	42
4.2	Study area	42
4.3	Data sources and methods	43
4.3.1	Methods	44
4.3.2	G.I.S analysis	44
4.4	Results	45
4.4.1	Environment along the pipeline route	45
4.4.2	Changes in crops grown during 2015 to 2019	48
4.4.3	Identifying points of high risk	49
4.5	Discussion	51
4.5.1	Land cover and crop change	51
4.5.2	Identification of vulnerable areas	52
4.5.3	Improving soil erosion mapping for pipelines	53

4.6	Conclusion	53
5	Estimating ground surface displacement along a hydrocarbon pipeline in Scotland	55
5.1	Introduction	55
5.1.1	Interferometric synthetic-aperture radar	56
5.1.2	Aims and objectives	56
5.1.3	Study area and reference site	56
5.1.4	Pipeline slope profile	57
5.2	Data sources, software and methods	58
5.2.1	Database sources and software	58
	Processing each image pair	59
	GIS analysis	60
5.3	Results	62
5.3.1	Data processing	62
5.3.2	Weather station - reference point for all image pairs	62
5.3.3	Pipeline corridor	63
	Zone comparison	65
	Spatial analysis	67
5.4	Discussion	69
5.4.1	Challenges and uncertainties in the InSar technique	69
5.4.2	Ground displacement along the pipeline route	70
5.5	Conclusion and potential use	71
6	Discussion and conclusion	72
6.1	Results in context	72
6.2	Implications for the oil and gas pipeline sector	74
6.3	Limits of this study	75
6.4	Conclusion	76
A	Autumn results	95
B	Winter results	98
C	Spring results	101
D	Summer results	104
E	Sentinel-1 dates	107

List of Figures

2.1	The frequency of pipeline failure in relation to depth of cover. (European Gas Pipeline Incident Group 2018)	7
2.2	Diagram showing the types of pipelines in the gas industry (U.S. Energy Information Administration 2020).	8
2.3	The relationship between API gravity and density published by Bahadori (2016).	9
2.4	Aerial image and example of the results from the depth of cover report. Colours along the pipeline indicate cover depth Published in Finley et al. (2018a).	14
2.5	Global rainfall erosivity. Published by Panagos et al. (2017)	15
2.6	Estimation of proven crude oil reserves globally. (British Petroleum 2018)	16
2.7	Lateral displacement for dimensionless depth H/D Jung et al. (2013)	22
3.1	The location of the study area, gas pipeline (National Grid 2018) and weather stations based on OSGB1936 British National Grid coordinate system (m).	27
3.2	Flow chart outlining the different data formats sourced and the steps with justification taken to ensure the data (for MIDAS) is sufficient for data analysis. Microsoft Excel and R Studio (RStudio Team 2021) were used throughout the data mining process.	28
3.3	Boxplot showing the total rainfall depths (mm) for a given water year across all three weather stations.	31
3.4	Boxplot showing the total rainfall amount for a given water year for all three weather stations.	32
3.5	Line graph showing total annual rainfall over time	32
3.6	Line graph showing the total number of heavy rainfall events over time	33
3.7	Summer exceedance	34
3.8	Autumn exceedance	34
3.9	Winter exceedance events for Eskdalemuir, Leuchars and Dyce	35
3.10	Spring exceedance events for Eskdalemuir, Leuchars and Dyce	35

3.11	A boxplot showing the greater variability of winter rainfall depths recorded at Eskdalemuir for the time periods 1981-199 and 2000-2018.	36
3.12	A boxplot showing the greater variability of winter exceedance events recorded at Eskdalemuir for the time periods 1981-199 and 2000-2018.	36
3.13	Summarised regional difference in rainfall pattern for the UK. Figure reproduced from Horswell et al. (2019). Note: NAO + and NAO– describe the negative or positive phase of the NAO index.	39
4.1	The study area for evaluating erosion risk factors along gas pipeline routes. Spatial map created with ESRI (2018) using England and Scotland country boundary by Ordnance Survey (GB) (2017), with oil and gas field data from Oil and Gas Authority (2018). Pipeline data by National Grid (2018).	43
4.2	GIS analysis methodology for assessing the characteristics of the pipeline route and calculating the soil erosion risk map	45
4.3	A simplified Soil texture triangle which give associated names of soil according to the percentage of sand, silt and clay. (DEFRA 2010)	47
4.4	Constructed soil erosion risk maps of (a) A slope risk map which illustrates spatially the moderate and steeply moderate slope class along the pipeline route. (b) A spatial map which illustrates the highest risk category based on land cover classification. (c) A spatial map which illustrates the highest risk category based on soil texture. (d) A spatial map which illustrates the highest risk category based on winter susceptibility to soil erosion. (e) Soil erosion risk map showing both combined risk (excluding rainfall) and the EU erosion risk including rainfall (Panagos et al. 2015). Created in ArcPro (ESRI 2021) using base map imagery from (National Geographic World Map 2011).	50
5.1	The study area for evaluating ground displacement. Maps create with ESRI (2018)	57
5.2	The slope map of the route (in metres), and the elevation profiles of the Gas transmission pipelines that transect the region near Eskdalemuir.	58
5.3	The workflow of processing two Sentinel-1 image pairs into one single stacked image	60
5.4	A diagram defining the pipeline zone and the outer zone. Not to scale.	61

5.5	The ground displacement values for each land category at the Eskdalemuir weather station.	63
5.6	The box plots for each land cover classification and its coherence distribution.	65
5.7	The comparison of sample points across both pipeline zones. . . .	66
5.8	Zone comparison of ground displacement for land cover and soil classes	67
5.9	Constructed soil erosion risk maps of (a) Top 10% of lowest ground displacement values across the study area. (b) The locations of areas 1, 2 and 3 which contain small clusters of ground displacement points. (c) A soil erosion risk map showing winter risk, areas detected in this Chapter, the Winter risk from Chapter 4 and the RUSLE which includes rainfall by Panagos et al. (2015). Created in ArcPro (ESRI 2021) using base map imagery from (National Geographic World Map 2011).	68

List of Tables

2.1	Fluid and hazard categories defined by Bahadori (2016).	9
2.2	Viscosities and API values of popular crude oil blends.	10
2.3	Key global pipelines including details of countries along the route, length and diameter.	11
2.4	Typical pipeline burial depths for the UK and USA.	12
2.5	Comparison of sediment loads from two pipeline sections located within different environmental conditions (Skid road suburban pipeline and a rural cross-country pipeline in West Virginia, USA). From (Edwards et al. 2014)	19
2.6	Recommended values from DVN-RP-F110. The embedment ratio is defined by the pipeline burial depth to pipeline diameter (H/D).	21
2.7	Results of resistance from the pull out tests (Thusyanthan et al. 2008)	22
3.1	Manual quality checking issues, remedy and limitations to the dataset	29
3.2	The location details for each weather station including MIDAS station ID, British National Grid coordinates and the UKCP18 NetCdf grid elements based on 5km OSGB1936 resolution.	30
3.3	Total counts of exceedance events for each season for 1981-2018 water years	33
3.4	Mean values between MIDAS and UKCP18	37
4.1	Data source reference table for chapter 4	44
4.2	The length of the pipeline route under different slope classes and soil erosion rank.	46
4.3	Land cover results for the pipeline route and soil erosion rank.	46
4.4	Soil group results for the pipeline route. Soil triangle imagery defined by Lawley (2011a).	48
4.5	Crop cover type change along the length of the pipeline route. Winter oats were included in Winter wheat statistics prior to 2019.	49
4.6	The length of pipeline evaluated to be at risk.	51
4.7	Literature concerning soil erosion risk in the region of East Scotland	52

5.1	The number of heavy ($\geq 4\text{mm/hr}$) rainfall events recorded at Eskdalemuir weather station. Data obtained via MIDAS (see Chapter 3)	57
5.2	Data, software and references which were used in relation to the ground displacement analysis.	59
5.3	DEFRA and soil texture equivalent. Further information on how soils are classified can be found in Lawley (2011 <i>b</i>)	61
5.4	The number of images processed for each year's autumn and winter period. Defect image is defined by the image not being suitable for further processing due to unusual raster imagery. If an image was found not to be defect then it was checked for offsetting errors.	62
5.5	The offsetting range is determined by rational user judgement and is adjusted based on the following tutorial by Braun & Veci (2021).	62
5.6	The length of the pipeline route under different slope classes in the study area (Eskdalemuir)	63
5.7	The number of pipeline sample locations that were evaluated into each soil class.	64
5.8	The number of sample points for each land cover classification and within each zone of the pipeline corridor. The area around Eskdalemuir is mainly classified as grassland.	64
5.9	Area statistics	69
5.10	Ground displacement velocities observed in a range of previous studies.	70
A.1	The autumn results for the change in rainfall patterns at a seasonal scale for observed (MIDAS) and future simulated (UKCP18) precipitation data. Min = minimum, Max = maximum, M = mean, Ra = range, SD = standard deviation, and SE = standard error.	97
B.1	The winter results for the change in rainfall patterns at a seasonal scale for observed (MIDAS) and future simulated (UKCP18) precipitation data. Min = minimum, Max = maximum, M = mean, Ra = range, SD = standard deviation, and SE = standard error.	100
C.1	The spring results for the change in rainfall patterns at a seasonal scale for observed (MIDAS) and future simulated (UKCP18) precipitation data. Min = minimum, Max = maximum, M = mean, Ra = range, SD = standard deviation, and SE = standard error.	103

D.1	The summer results for the change in rainfall patterns at a seasonal scale for observed (MIDAS) and future simulated (UKCP18) precipitation data. Min = minimum, Max = maximum, M = mean, Ra = range, SD = standard deviation, and SE = standard error. . . .	106
E.1	Sentinel-1 data for 2015	108
E.2	Sentinel-1 data for 2016	109
E.3	Sentinel-1 data for 2017	110
E.4	Sentinel-1 data for 2018	111

Chapter 1

Introduction

1.1 Onshore oil and gas pipelines

Oil and gas production happens at a global scale where products require transportation to refineries onshore using pipelines which can often be located in challenging environments (Sweeney 2016). The research in this thesis is concerned with the risk onshore pipelines may have from soil erosion by water by evaluating the change in rainfall patterns and how satellite data can be utilised to detect areas vulnerable to erosion. These pipelines are major economic infrastructures which are vulnerable to numerous geohazards including flooding (Girgin & Krausmann 2016), landslides (Ferris & Porter 2016, Marinos et al. 2016) and earthquakes (Chakraborty & Kumar 2014, Sahoo et al. 2014). Whilst pipeline transport is considered safe, pipeline failures do occur with exposure through third party activity being the major mechanism of failure (Papadakis 1999, Ramírez-Camacho et al. 2017). The consequence of failure can cause economic damage, impact human lives and contaminate the environment (Cunha 2016, Dai et al. 2017, Otegui 2014, Ramírez-Camacho et al. 2017).

To protect the infrastructure pipelines are buried and protected with soil to prevent exposure and provide enough overbearing weight to mitigate uplift forces acting within the pipeline (Chakraborty & Kumar 2014, Cheuk et al. 2008, Wang et al. 2010). Soil erosion by water poses a threat to the this cover protecting hydrocarbon pipelines. Monitoring pipeline cover requires physical, costly techniques and may not be predictable where there are challenging environments. Pipelines buried in areas vulnerable to rainfall induced soil erosion and surface run-off may be vulnerable to loss of soil cover that potentially exposes pipelines to third party damage (Edwards et al. 2017). Therefore, research evaluating how rainfall has changed over time and how satellite data could be utilised is needed, especially in the context of our changing climate which has the potential for more frequent intense rainfall events linked to climate change (Trenberth 2011).

1.2 The challenges facing buried Onshore infrastructure

There are three main points for consideration when looking at the future safety of onshore pipelines.

1. Population growth and demand for energy

Technological advancement and world population growth has increased energy demand for hydrocarbons throughout the 21st century (British Petroleum 2018). World energy demand is in transition where renewable resources are rising but not at a pace to overtake traditional energy sources such as oil, gas and coal; therefore oil and gas resources are predicted to supply energy demand and dominate total energy supply at least until 2040 (British Petroleum 2018).

2. Environmental capacity, conflict and consequence

Continual hydrocarbon exploration to meet global energy demand increases the requirement for pipeline installation in more challenging environments such as mountainous regions, degraded landscapes (Sweeney 2016) and arable land cover (Batey 2015). Changes in population growth and the need for food security from expanded arable economic activity (Foley et al. 2005) has increased conflict between land owners and pipeline operators (Batey 2015). A major consequence of this is the unknown implication this has on soil erosion rates (Borrelli et al. 2017, Poesen 2018) for the pipeline network.

3. Climate change uncertainty

The rate at which soil erodes is a complex dynamic between slope, climate and land use (García-Ruiz et al. 2015). The IPCC (IPCC 2014) contend that increases in extreme rainfall events are likely linked to human influence (from the increase in greenhouse gas emissions) in a number of regions. There is uncertainty of how rainfall regimes change with each region (Trenberth 2011) and the consequences of a changing climate on built infrastructure (Stewart & Deng 2015).

1.3 Problem identification

The soil cover protects the buried pipeline structure from soil erosion by water and there may be areas along the pipeline route that will be at more risk to soil erosion because of the influence of rainfall, land cover, slope and crop cover (Sweeney 2004). Monitoring the pipeline soil cover involves physical methods which can

be expensive, infrequent and often in targetted areas (Finley et al. 2018b). The East Scotland region is an ideal location to evaluate soil erosion risk as onshore buried pipelines are routed through areas where arable economic activity is strong (Watson & Evans 2007). Defining and evaluating the number of heavy rainfall events in this region can establish risk of soil erosion along the pipeline route. In addition, the recent release of crop spatial data (Centre for Ecology and Hydrology 2016, 2017b, 2018, 2019) and the advancements in satellite technology with the launch of Sentinel-1 (Malenovsky et al. 2012) can be used to create a soil erosion risk map and potentially identify areas where more accurate ground based monitoring work. In addition, the UK Climate Projection 18 simulation data will be considered that can give an idea of future rainfall conditions.

1.4 Aims and objectives

The aim of this research is to evaluate the extent of heavy rainfall events in the area of East Scotland along the onshore pipeline route and use remotely sensed data to perform ground displacement analysis along the pipeline route. The purpose is to evaluate the trend in observed heavy rainfall over a continuous period of time and its likely change in the future using UKCP18 simulations. A recreation of the a soil erosion risk map along the pipeline route, using slope, soils and crop locations, will be created to identify the locations based on risk to soil erosion. Finally, the results from remote sensing to identify areas where soil erosion could be a concern for pipeline failure.

To achieve this aim the objectives are:

1. Define a heavy rainfall event and evaluate the frequency of these events for selected weather stations along the pipeline route. The major criteria for weather station selection is that it must observe hourly records and produce a continuous record for at least 30 years. In addition, UKCP18 data will be used to assess the number of heavy rainfall events predicted in the future (Chapter 3).
2. Create a soil erosion risk map for the pipeline route using environmental data such as soil type, land cover, slope and the new released crop cover plus dataset for years 2016 to 2019. The environmental data will be evaluated along the pipeline length to assess the environmental conditions the buried pipeline is routed in. Based on literature, the environmental variables evaluated along the pipeline corridor will be ranked based on the likelihood of erosion under bare soil conditions (low, medium and high). A raster dataset based on erosion risk along the pipeline route will be produced and compared to a recent released peer reviewed soil erosion dataset (Chapter 4).

3. Use remotely sensed radar interferometry data to quantitatively measure the ground surface displacement along the pipeline route to identify possible soil erosion risk areas. This data will cover the autumn and winter period for the available years of 2015, 2016, 2017 and 2018 in the area of Eskdalemuir which has the highest rainfall along the pipeline route. Sample points will be created along the pipeline corridor route in the G.I.S. environment where two zones will be created that will evaluate the ground displacement immediately close to the pipeline and on the outer edges of the pipeline corridor. A map which averages the ground displacement over all the years is then produced to identify areas which may be vulnerable to soil erosion and can be used to prepare more accurate G.I.S soil erosion maps. In addition the identification of areas where ground displacement was detected have the potential for ground monitoring to target those areas (Chapter 5).

Chapter 2

Literature review

This literature review considers pipeline integrity, installation and threats to changes in depth of soil cover with rainfall induced soil erosion. The first part of the literature review defines how failure is recorded and the picture globally of oil and gas pipelines. The second part of the review considers how pipeline operation may potentially affect vegetation growth which is often the main factor protecting the soil cover above pipelines. The conclusion considers priorities for future research.

2.1 Geohazards contributing to pipeline failure

Natural hazards have the potential to adversely affect the environment and human population in the relation to the safety of hydrocarbon transmission. Pipeline failures caused by natural hazards (landslip, earthquake and flooding) are a type of incident known as natechs, natural hazards triggering technological disasters (Girgin & Krausmann 2015). There is considerable interest in analysing onshore frequencies of pipeline failure with regards to incidents involving geohazards (Girgin & Krausmann 2016, Leir et al. n.d.) including landslides (Ferris & Porter 2016) and earthquakes (Psarropoulos et al. 2012). At present there is no current global framework for defining hazards when recording pipeline failures. However, there has been little attention given to soil erosion as a potential contributor to natechs. Soil erosion and degradation worldwide involve the removal of the fertile top soil and decreases nutrient availability (Lal 2001). This has the potential to affect vegetation cover leaving the soil cover above pipelines more vulnerable to rainfall induced soil erosion and at risk of third-party damage; the leading cause of pipeline failure.

2.1.1 Liquid pipeline failure

In the USA pipeline incidents are recorded by the Pipeline and Hazardous Materials Safety Administration (P.H.M.S.A.). In the USA Girgin & Krausmann (2016) reviewed liquid pipeline incidents from 1986 to 2012 and found that 5.5% of all failures were initiated by natechs which include flooding hazards (36%), landslips (26%), climatic (24%) and hydrological (15%). However, geohazards are complex and triggering is often induced by weather events in the case of landslips. Leir et al. (n.d.) reviewed liquid pipeline failure from 2005 to 2014 and agreed with Girgin & Krausmann (2016) that incidents were caused by both hydrological and geologic actions. In Europe the Concawe database is used to record incidences for gas, water and oil products for pipelines. In Europe the recorded failure for natechs accounted for 4% of all recorded failures in this database representing 20 failure incidences (Girgin & Krausmann 2015). Landslips were the main trigger at 65% with hydrological at 20% and climatic at 10% (Girgin & Krausmann 2015). Whilst natechs account for a small number of incidents, they are also likely to contribute to inadequate soil cover leading to third party damage, though this is not considered specifically in the literature.

2.1.2 Gas pipeline failures

Gas pipeline failure both in the USA and in Europe has been evaluated in recent years. Lam & Zhou (2016) examined pipe incident data between 2002 and 2013 from the PHMSA database and established that there were four leading causes of pipeline failure (1) third party excavation (e.g. by contractors excavating and accidentally damaging the pipeline), (2) external corrosion to the pipeline material, (3) material failure and (4) internal corrosion. Dai et al. (2017) analysed the European Gas Pipeline Incident Data Group (EGIG), United Kingdom Onshore Pipeline Operators' Association (UKOPA) and PetroChina Natural Gas and Pipeline Company (PNGPC) and found that external interference was a leading cause of gas pipeline failure. Golub et al. (1996) highlighted incidences where outside forces acting on the pipeline were due to inadequate depths of soil cover above the pipeline. The importance of maintaining cover depth has been highlighted by the European Gas Pipeline Incident Group (2018) report. Figure 2.1 shows the frequency of pipeline failure with varying depths of soil cover. This figure shows that the higher failure frequency caused by soil cover ≤ 0.8 m has been an issue since the 1970s, but is on a downwards trend. Recognition that reduced soil cover leads to pipeline failure has meant that most pipelines are buried initially with sufficient cover to protect them. However, since 2016 there has been a rise in the frequency of incidence for pipelines with soil cover between 0.8 m to 1 m.

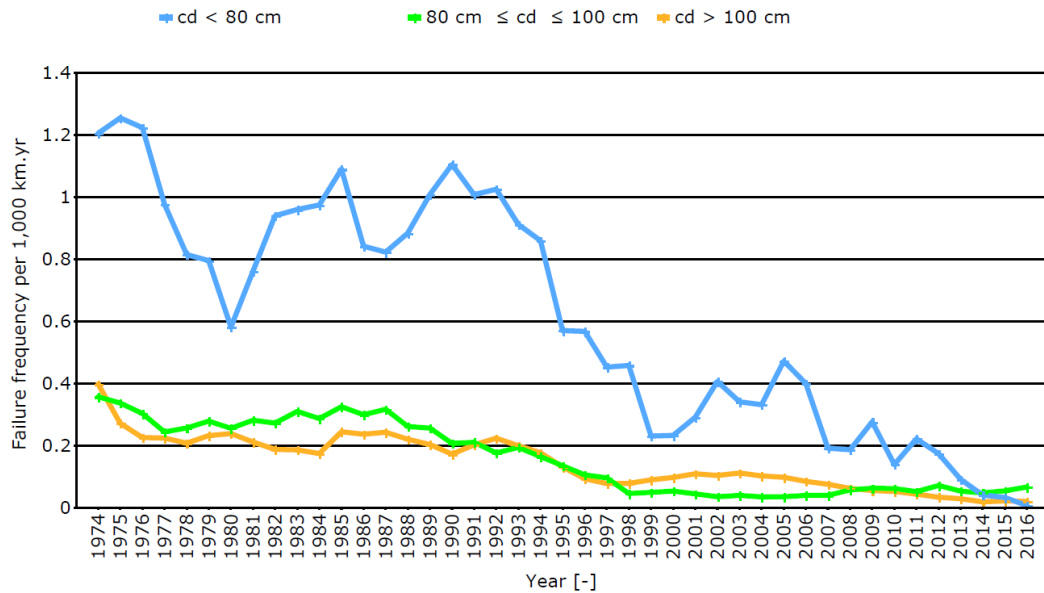


Figure 2.1: The frequency of pipeline failure in relation to depth of cover. (European Gas Pipeline Incident Group 2018)

Historic pipeline failure for liquid pipelines in particular has focussed on primarily sudden impact geohazards (landslip, rainfall and flooding). However, gas pipeline incident data includes soil cover information which shows that reduction in soil cover depth is associated with third party damage. Soil erosion *per se* is not considered empirically in the database, but may contribute *under third party damage* as a reason for failure. Furthermore, the recording of pipeline failure across liquid and gas pipelines requires more robust reporting which is consistent. The evidence shown for pipeline failure due to inadequate soil cover for gas pipelines requires further exploration, in particular to gradual soil erosion as Figure 2.1 shows that pipeline cover depth from 0.80m to 1m are generally more vulnerable to failure in more recent years.

2.2 Pipeline integrity

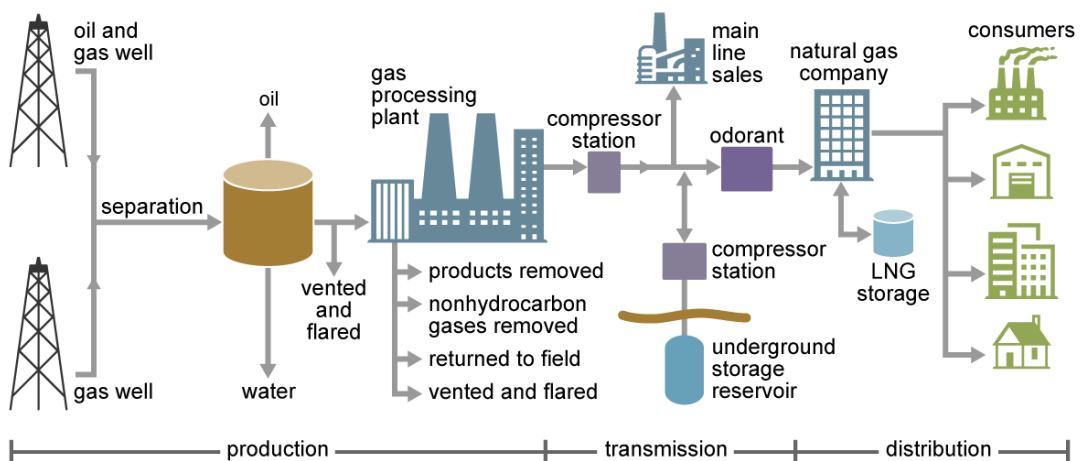
Onshore hydrocarbon pipelines are installed globally, delivering products from oil and gas fields to processing plants and end users for energy consumption. The majority of pipelines are installed in the USA with 2,225,032 km buried pipelines, followed by Russia with 251,800 km, China with 118,400 km and Canada with 110,000 km (Central Intelligence Agency 2018). There are different types of pipelines in the oil and gas industry, varying in diameter and length (Papavinasam 2014).

- **Gathering, flow pipelines or production pipelines** - Used for delivering the hydrocarbon compounds from the production facility to the main transmission pipelines. For example, from production wells to pumping station.

- **Transmission pipelines** - The main arteries of the oil and gas industry transporting to refineries. These pipelines range between 0.9 m to 1 m (36 to 42 inches) in diameter and are laid often over long distances. These pipelines are the most vulnerable to damage and in the case of oil pipelines the location is kept private for national security.
- **Distribution pipelines** - Often smaller in diameter than transmission pipelines they are tasked with bringing the refined product to the end consumer.

Figure 2.2 shows the typical location of these pipelines for a gas transmission network. Compressor stations are situated throughout the network to maintain high pressure for gas delivery. In an oil pipeline network, pumping stations heat the oil and pump at higher pressure for economical delivery.

Natural gas production and delivery




 Source: U.S. Energy Information Administration

Figure 2.2: Diagram showing the types of pipelines in the gas industry (U.S. Energy Information Administration 2020).

2.2.1 Fluid category and API gravity

The type of fluid conveyed in pipelines varies from non-flammable and stable to flammable and unstable which is displayed in Table 2.1. The categories shown range from non-flammable and stable, which poses less of a threat to onshore pipeline failure than unstable and flammable material which is an environmental risk if failure was to occur. Whilst this report has focussed on hydrocarbon pipelines, water, electricity and telecommunications cables are all underground utilities subjected to soil cover removal through soil erosion.

Table 2.1: Fluid and hazard categories defined by Bahadori (2016).

Category	Hazard	Example
A	Non-flammable, stable	Water
B	Flammable, unstable (liquid form)	Crude oil
C	Non-flammable, stable	Nitrogen
D	Flammable, unstable	Natural gas, LPG and ammonia

Liquids are classified into specific gravity, which is the ratio of density of the liquid to the density of water at 4°C. Crude oil is further separated into specific grades known as American Petroleum Institute (API) gravity, defined in the equation 2.1.

$$\text{API Gravity} = (141.5 / \text{specific gravity} - 131.5) \quad (2.1)$$

This measure is an inverse to the liquid density relative to water and is a useful measurement to compare the densities of petroleum liquids. The API of water is 10 where liquids with a great value float on water and liquids with a value of less than 10 sink. Figure 2.3 shows the different grades of oil and the associated API and density. Conventional crude oil, also term medium to light oil, generally fall into the 30-40 API values and flow through pipelines with slight heating.

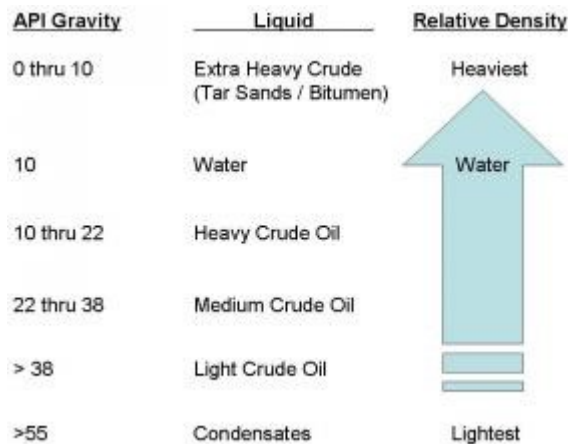


Figure 2.3: The relationship between API gravity and density published by Bahadori (2016).

2.2.2 Thermal and pressure regimes

In gas pipelines the temperature of the gas in the pipelines is typically around 5°C Halmová et al. (2017) and up to 85 bar (8.5 MPa) in pressure (Health & safety executive 2008). In crude oil pipelines, temperature can vary based on the API gravity which influences viscosity. Table 2.2 identifies the properties of established crude oils where viscosity is given in centistoke which is a kinematic viscosity measurement unit where 1 centistoke is equal to 1 centimetre per second (cm^2/s). Their APIs show that these liquids range from light to medium crude oils.

Table 2.2: Viscosities and API values of popular crude oil blends.

Name	Viscosity cSt	API	Reference
Brent	3.45 at 40°C	38	(Chevron 2009)
Forties	3.73 at 30°C	38.9	(Ineos 2019)
West Texas immediate	5 at 16°C	39.6	(Environment Canada Date Unknown ^b)
Arabian light	12 at 26°C	33.4	(Environment Canada Date Unknown ^a)

Heavy and extra heavy oil

Heavy oils display dynamic viscosities ranging from a few hundred to tens of millions of centipoises (1 cP = 1 millipoise second, 1m Pos equivalent to dividing the centistoke unit by the fluid density) under reservoir conditions (Speight 2006). The maximum viscosity of 500 cP can limit its economic value at which many heavy crude oils can be economically pumped through pipelines (Nuñez et al. n.d., Rimmer et al. 1992). Yaghi & Al-Bemani (2002) used a heavy crude with a viscosity of 15,000 cP at 20°C where their experimental work was to bring the viscosity to under 500 cP and at a temperature below 50°C. They found that heating alone was not sufficient, but a combination of 70%-75% oil content (25% - 30% water emulsion) together with heating (30°C-50°C) was sufficient. Such thermal regime for heavy oils challenge pipeline operators and potentially cause environmental heat disturbance (Greenslade et al. 2004).

Key global pipelines

Key onshore transmission pipelines deliver products over long distances within countries for domestic consumption and also crossing international borders for international delivery. To keep the product moving along the pipeline, compressor (for gas) or pump stations (for crude oil) are placed along the pipeline route. The materials composed for individual oil and gas pipelines are not publicised for commercial reasons, but materials are often high grade carbon steel with varying yield strengths to cope with the particular pressure requirements for the pipeline (Witek 2015). Table 2.3 gives details of major global pipelines including diameter and length:

Table 2.3: Key global pipelines including details of countries along the route, length and diameter.

Pipeline	Footprint	Length (km)	Diameter (mm)	Reference
Druzhba	- Russia	4000	420 - 1020	(Transneft 2016)
	- Ukraine			
	- Belarus			
	- Poland			
	- Hungary			
	- Czech republic			
Keystone	- Canada	3461	762-914	(TC Energy 2021)
	- USA			
Forties	- UK	169	914	(Ineos 2018)

2.2.3 Pipeline installation and typical burial depths

Pipeline installation typically takes place during the drier months of the year (April to October) in the UK and is a multistep process detailed in Batey (2015) and outlined below.

1. A strip of land along the pipeline route is fenced off (known as the pipeline right-of-way). It is typically 100m width (50m either side of the pipeline) and is designed to allow initial installation and future maintenance.
2. Top soil is removed and placed alongside the pipeline route for replacement after the laying of the pipeline.
3. A trench is dug for the required depth that accommodates the width of the pipeline and the required depth of soil cover. The subsoil is carefully checked but often soft sand is used as backfill immediately around the pipeline to protect the pipeline surface.
4. The top soil is replaced and re-vegetation of the pipeline route is encouraged to prevent soil erosion (Batey 2015).

Literature which has assessed the impact pipeline installation has on soil properties has found that pH is altered (Soon et al. 2000), soil compaction is prominent (Batey 2015, Landsburg et al. 1996), biodiversity is decreased and alteration of the soil hydrological properties are changed. Typical pipeline burial depths globally are displayed below in the Table 2.4 and show baseline variability with each country. In addition, an embedment depth H/D is given (H being burial depth and D meaning pipeline diameter) during pipeline design. Onshore pipelines generally have a lower H/D ratio below 1.2.

Table 2.4: Typical pipeline burial depths for the UK and USA.

Country	Land use	Depth of cover (m)	Reference
United Kingdom onshore pipeline association	Rural and suburban	0.9 for areas of limited or no human activity and 1.1 for agricultural activity.	(UKOPA 2016)
American Society of Mechanical Engineers	Various locations	0.6 to 0.9	(Landsburg et al. 1996)

2.3 Monitoring and estimating depth of cover

The vulnerability of a pipeline depends on land use and depth of cover. These land use types include: farmland, road crossings, roadways, construction sites and residential property (UKOPA 2016). The monitoring of soil cover depth along a pipeline route takes place by visual inspection, either aerial or by conducting overline surveys in specific areas (UKOPA 2016). Overline surveys target the pipeline route and highlight specific points and areas of concern, which may cause pipeline failure. The limitation for surveying is often cost, time, weather conditions, as well as expertise of the operator to qualitatively assess soil cover. Furthermore, only specific sections of the pipeline can be examined. Remote sensing has been identified as a potential method for monitoring vegetation cover along the route, however research by Bayramov et al. (2016) established that lack of resolution in satellite data and cloud cover hindered a clear assessment of vegetation along the pipeline route.

In recent years pipeline vulnerability and susceptibility mapping of pipeline routes has been used utilising geographical information systems and the Revised Universal Soil Loss Equation (R.U.S.L.E). The revised universal soil loss equation is an updated empirical method for estimating annual rates of soil loss at a given location when considering various factor that contribute to soil erosion. The original equation (2.2) was derived by Wischmeier & Smith (1978):

$$A = R \times K \times L \times S \times C \times P \quad (2.2)$$

Where A is annual soil loss ($t/ha/year^{-1}$), R is rainfall erosivity ($mm \text{ ha}^{-1} \text{ h}^{-1} \text{ yr}^{-1}$), K is soil erodibility ($t \text{ ha h ha}^{-1} \text{ MJ}^{-1} \text{ mm}^{-1}$), L is the length of the slope and S is the steepness (-), C is the coverage (-) and P is practise management (-). Whilst originally derived for farming practises in the USA, the use of the equation has been adopted in pipeline risk monitoring research as a way to estimate empirically soil loss above the pipeline at an annual time scale (Demirci & Karaburun 2011, Panagos et al. 2014, Renard et al. 1997).

2.3.1 Identifying soil erosion risk

One case study by Winning & Hann (2014) used geographical information systems and public domain data where they performed a soil erosion risk analysis for an onshore pipeline corridor where they compared the G.I.S. erosion risk evaluated with a detailed ground truth field examination including soil type, vegetation, slope and local conditions. Figure 2.4 shows the calculated risk classification along the pipeline where areas of high erosion risk were identified. The field evaluation of erosion risk in 69% of cases agreed with the G.I.S examination: ninety five percent of all cases were within +1 unit of the erosion classification. The authors noted that a limitation to this method was the lack of detail in soil data sets for G.I.S., although they stated that the technique may be useful for the early stages of pipeline route design.

2.3.2 Lidar as a technique estimating depth of cover

Lidar has been used recently, with the aim of monitoring depth of cover was trialled by the ROSEN group and National Grid. This method reported in Finley et al. (2018a) used a Digital Terrain Model (DTM) of the ground surface based on Lidar imaging, which is updated quarterly by the Ordnance Survey at a spatial resolution of 5m. Above ground markers using global positioning system and an inspection tool defined the pipe centreline. When combined with the Lidar elevation data, the depth of cover was reportedly estimated to ± 0.15 m root mean square error. The depth of cover report main image (shown in Figure 2.4) identifies the locations vulnerable to third party damage along the pipeline route, which is indicated in red. Limitations to the overall accuracy of this technique are in the placement of the above ground markers (for depth of cover), the digital terrain model (for the ground surface) and the mapping and processing tools. This method detects only major soil loss after the erosion event has occurred. In addition, historic pipeline accidents reporting by European Gas Pipeline Incident Group (2018) highlighted that failure also occurs at medium risk levels (0.8m to 1.1m), whereas the colour coding along the pipeline route assumes cover above 1m is safe despite a small number of failures occurring from the EGIG report. Further risk assessment of how vegetation, soil and rainfall thresholds over a different temporal resolutions can alter the soil cover depth is therefore still required.



Figure 2.4: Aerial image and example of the results from the depth of cover report. Colours along the pipeline indicate cover depth Published in Finley et al. (2018a).

2.4 Threats to changes in depth of cover

2.4.1 Increase in precipitation

Increased global population during the 21st century and the demand for oil and gas (International Energy Agency 2017) mean that pipelines are installed in challenging terrains and environments, in addition to pipelines crossing agricultural land vulnerable to soil degradation (Sweeney 2004). Another major threat to changes in soil cover for pipeline corridor comes from possible increases in rainfall induced soil erosion. Increased emissions of gases from industrialisation has the effect of creating a warmer climate that holds more moisture in the atmosphere. IPCC (2014) reported that precipitation, magnitude, and intensity is likely to increase in higher latitudes and specific regions.

Change in rainfall patterns has been noted as a factor affecting oil and gas infrastructure, and operation in low lying coastal regions due to higher peak stream flows during storm events (Burkett 2011). The process of soil erosion is complex involving climate, soil type, hydrology, land use and human practise where, by the actions of wind and water, the soil particle detaches from the surface and is transported away (Zachar 1982). Soil erosion by water remains the most destructive and leading cause of soil degradation worldwide. The erosivity power of rainfall varies globally, as shown in Figure 2.5. The greatest rainfall erosivity is in South America, the Caribbean countries, Central East Africa and South East Asia (Panagos et al. 2017). Soil erosion rates are expected to change in response to changes in this erosive power (Nearing et al. 2004) and it is argued that future

impact of climate change may increase rainfall erosivity (Shiono et al. 2013).

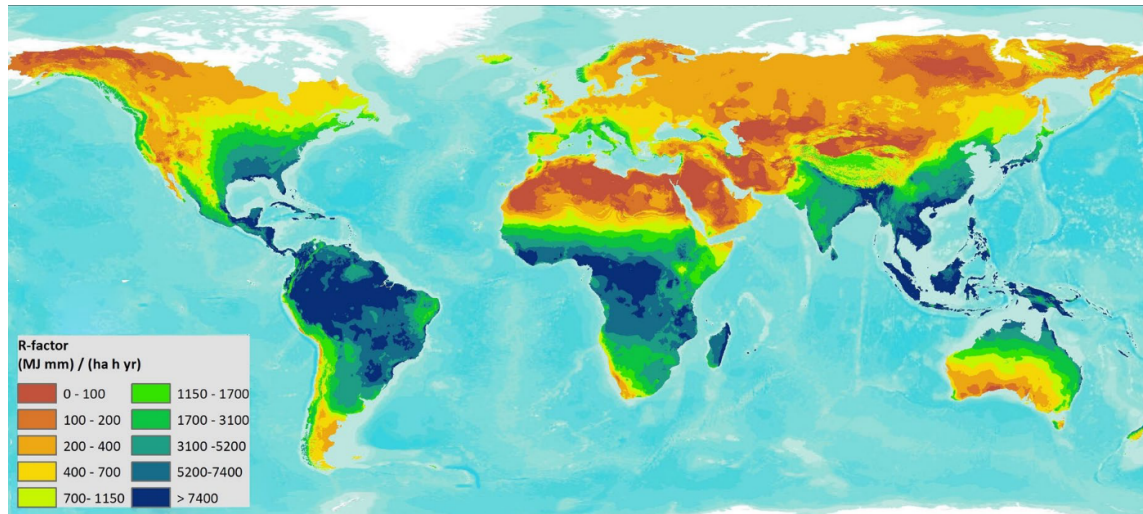


Figure 2.5: Global rainfall erosivity. Published by Panagos et al. (2017)

2.4.2 Changes in the oil and gas industry

Global energy demand is expected to increase by 1.3% per year from 2016 to 2040 with oil remaining the leading global fuel. Oil production will become more concentrated towards the Middle East, USA and Russia (British Petroleum 2018). World conventional oil reserves (where oil can be extracted at an economic cost) are displayed in Figure 2.6 and show that 1697 billion barrels (1 barrel is approximately 159 litres) is in reserve, meeting demand for the next 50 years for production (British Petroleum 2018). Estimates from the International Energy Agency note that at least half of these oil reserves are in the form of heavy oil where Canada and Venezuela are dominant in the heavy oil field (Meyer et al. 2007). Extraction of heavy crude oils has started to become economically viable and research has focussed on how to safely transport heavy crude oils through pipelines (Ashrafizadeh & Kamran 2010, Martínez-Palou et al. 2011). In addition, there is interest in retrofitting existing pipelines by considering different ways to heat the pipeline to decreased viscosity and varying the location of pumping facilities to make them suitable for heavy oil transportation (Diaz-Bejarano et al. 2016).

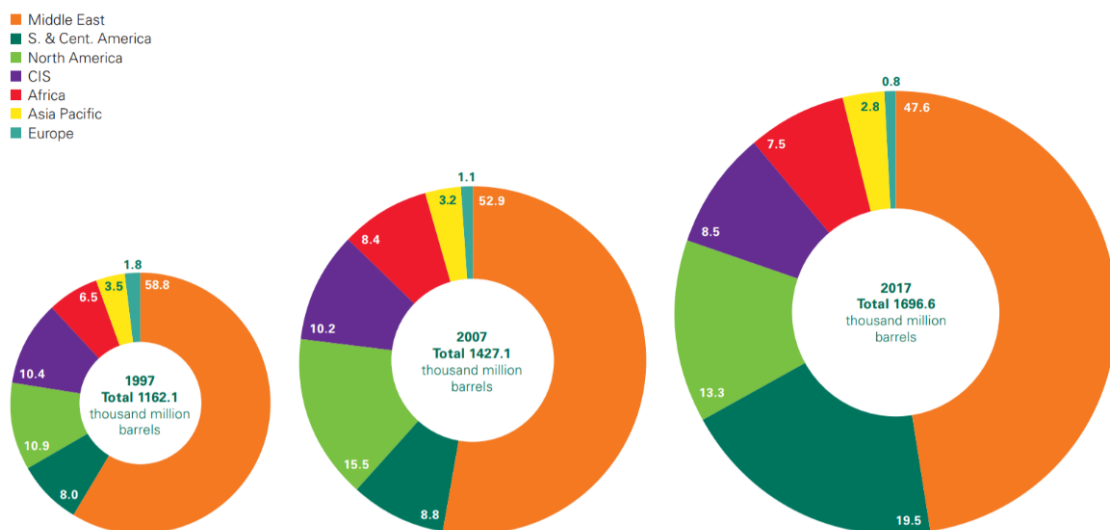


Figure 2.6: Estimation of proven crude oil reserves globally. (British Petroleum 2018)

2.4.3 Vegetation and climate

Vegetation is used to prevent soil erosion along pipeline corridors (Bayramov 2012, Bayramov et al. 2012, Hann & Morgan 2006, Morgan & Hann 2006, Xiao et al. 2016). Change in temperature, rainfall regime and land use management can alter vegetation cover. The increase in atmospheric carbon dioxide may positively increase plant productivity and thus increase vegetation cover (Rosenzweig & Hillel 1998). In contrast, Lobell & Field (2007) examined crop yields at a global scale and found that wheat, maize and barely had a negative response in yields argued to be due to increased global temperatures. Considering precipitation, Jiao et al. (2009) noted that soil erosion by water hinders vegetation development and, in particular, Xiao et al. (2016) noted that vegetation re-establishment within 10 metres of the pipeline route was hindered by heavy rainfall and concluded that environmental factors (sunshine duration and precipitation) were key to vegetation establishment and recovery patterns. Whilst there has been significant research concerning vegetation recovery along newly installed buried pipelines (Bayramov et al. 2016, Bayramov 2012, Olson & Doherty 2012, Xiao et al. 2016) there is a lack of research considering pipeline corridor erosion past the initial installation stage of vegetation establishment. This longer-term consideration is important for pipelines buried in agricultural (especially arable) land as vegetation cover changes throughout the year and the soil be left fallow for extended periods during the winter months.

2.5 Pipeline thermal regime and vegetation growth

Whilst atmospheric temperature affects vegetation cover, there is also a strong possibility that the thermal regime of the pipeline can influence vegetation and plant roots systems directly above the pipeline as well (Yu et al. 2016). Such pipeline temperature effects may have consequences for depth of soil cover. Deaton & Frost (1946) suggested that heated pipelines may create a localised increase in soil temperature if the fluid conveyed in the pipeline is warmer than the surrounding soil. Whilst compaction during pipeline installation could hinder and retard root growth (Soon et al. 2000) there is a lack of research to how roots are affected by the thermal regimes during pipeline operation.

Literature concerning the relationship between thermal regimes and crop yields above oil and gas pipelines is conflicting and is likely to depend on local weather, soil conditions and whether liquid or gas flows through the pipeline. There is a current lack of recent research which considers the relationship between heated oil pipelines and crop yields. In relation to oil pipelines, an earlier study by Culley (1988) found that crop yields were overall lower than in undisturbed fields even up to 10 years post installation for an oil pipeline. Previous to this study, Stewart (1979) evaluated top soil, bulk density on corn growth in a Canadian field for autumn and winter construction. Their results found that corn yields varied based on soil type, time of construction and crop season characteristics, but had no clear indication that thermal regimes from the installed pipeline had an influence on this. Wraith & Hanks (1992) used a buried heated pipeline to stimulate soil temperature and concluded that temperature had little effect on plant growth in the long term. In the short term they contended that early plant growth responded to increased soil temperatures agreeing with other studies.

There are more recent studies of the relationship between the temperature influence on gas pipelines and the surrounding environment. Naeth et al. (1993) found that the soil temperature around the pipeline was affected by pipeline temperature. When considering plant growth they concluded that surface summer temperatures were the main limitation for vegetation growth. Halmová & Feher (2014) and Halmová et al. (2017) contend that soil temperature was also affected by the presence of the gas pipeline which in turn influenced crop yields. They found that soil temperature ranged between 1.1°C to 3.4°C immediately around the pipeline relative to the pipeline corridor, which led to a reduction in soil moisture and an increase in crop yields by up to 14% (Halmová & Feher 2014, Halmová et al. 2017). A limitation for comparing these studies was the lack of information given in the operating pipeline temperature therefore, further investigation on pipeline operating temperatures on crop productivity should be considered as vegetation is recognised as a key method for preventing erosion of the soil cover above the pipeline.

2.6 Soil erosion along pipeline right of way

Assessing soil erosion along a pipeline right-of-way has received little attention in the literature despite knowledge, in particular of gas pipelines, in which a reduction in soil cover depth can lead to failure. Zellmer et al. (1991) looked at a combined erosion control cost method for steep pipeline corridors and found that straw mulch applied at 3.35 t ha^{-1} was economical compared with other erosion methods. Edwards et al. (2014) published a comparison study for sediment loads for two newly installed pipelines in North Central West Virginia where erosion was measured by monitoring the sediment output from waterbars (channels crossing the pipeline right of way to connect run-off). The characteristics of the first site is a skidroad that was constructed over 25 years ago for the purpose of transferring logs with using rubber tyre skidder. The road was not a traffick road, and had an uneven vegetation distribution. Waterbars were installed after logging was completed to control runoff. The second site is also a non traffick road, and is located in an experimental forest area with a recently installed pipeline at 0.8m depth. Once installed, the pipeline was seeded and straw mulch was applied to prevent erosion (Edwards et al. 2014). Table 2.5 compares the physical aspects of each pipeline area (chosen based on similar slope percentages) including slope, length and vegetation cover. On the Skid road pipeline section, the slope is of a lower percentage than the cross-country pipeline section and also in segment 3 and 4 the vegetation cover is greater.

Table 2.5: Comparison of sediment loads from two pipeline sections located within different environmental conditions (Skid road suburban pipeline and a rural cross-country pipeline in West Virginia, USA). From (Edwards et al. 2014)

Section	Slope	Length	Area	Aspect	Vegetation cover	Sediment load per sample period		Mean load across all segments	Total load for each segment
						Mean	Standard error		
	(%)	(m)	(m ²)		(%)	Mean	Standard error	(kg/ha/yr)	(kg/ha/yr)
Skid road pipeline						— kg/ha —			
Segment 1	13.5	32.5	121.6	NE	16.5	72.9	29		2696.4
Segment 2	12.4	26.0	84.0	E	20.2	49.4	13.7		1775
Segment 3	13.3	32.4	125.2	NE	82.1	23.3	6.3		859.4
Segment 4	12.7	28.6	129.3	NE	77.1	21.5	4.7		795.8
								40.7	
Cross-country pipeline								(kg/ha/yr)	(kg/ha/yr)
Segment 1	26.8	18.9	119.7	NW	26.5	10.4	3.2		396.9
Segment 2	20.7	25.6	143.3	NW	47.5	3.08	1.1		110.8
Segment 3	18.6	19.4	110.6	NW	29.3	3.4	1.0		116.2
								5.7	

Table 2.5 displays the results of the sediment load from two pipeline sections in different environmental locations. Edwards et al. (2014) noted that greater soil compaction and poor vegetation resulted in excess runoff and higher rates of soil loss compared to the cross-country pipeline. When considering the reduction in soil cover, using bulk density between 1.3 g/cm³ to 1.5 g/cm³, it is clear from these results that the Skidroad pipeline would undergo a reduction in soil cover (27.1mm to 31.3mm over 8 months) compared to the cross country pipeline (3.8mm – 4.3mm over a year) based on the information given in Table 2.5. Over time it would take If the depth of cover after installation was designed to 1100 mm, then on the Skidroad pipeline section the rate of soil cover reduction would be 2.85% per year. Over time pipelines with soil erosion issues may become vulnerable to pipeline failure as highlighted in section 2.1 once soil cover reduces below 1 metre. In the case of Skidroad it would take between 6.3 years (200/31.3) to 7.4 years (200/27.1) for soil cover depth to reach 0.8 m which is assumed to be at risk for pipeline failure (from Figure 2.1).

2.7 Pipeline uplift

Pipelines which transmit high pressure and high temperature fluids create an internal expansion force within the pipeline causing movement vertically (Chakraborty & Kumar 2013) or horizontally (Jung et al. 2013, Robert et al. 2016). The embedment ratio, defined by the pipeline burial depth to pipeline diameter (H/D), has an influence on the protection offered by soil cover. A major role of soil cover is to provide resistance against pipeline uplift. Onshore pipelines may be vulnerable to changes in cover depth as their H/D ratios are typically below 2 and the current design code DNV-RP-F110 does not offer guidance on how to predict uplift resistance for this H/D ratio (Veritas 2007). Literature involving pipeline uplift has focussed on offshore infrastructure where pipelines are buried at greater depths and in clay (Bransby & Newson 2002, Schaminee 1990, Wang et al. 2009). Pipelines buried onshore are often installed in unsaturated soils conditions where soil moisture varies, but existing design guidelines assumes either dry or fully saturated conditions. The unsaturated soil condition means that there is an additional force between the soil particles which create an additional reinforcement due to suction. Whilst this can add stability for structures, removal of soil cover and potential pipeline uplift forces may be greater than the strength of the soil cover, especially when the soil becomes temporarily saturated.

In the literature, analytical models have been developed to address upheaval resistance from the backfill soil (Schaminee 1990), but these assume peak resistance is developed when the pipeline is displaced by pre-determined mobilization. Peak uplift resistance is given by Det Norske Veritas (DNV) RP F110 for offshore

applications provides peak mobilisation as 0.005H to 0.008H where H is given as the soil cover (Veritas 2007). Table 2.6 shows the recommended values from DNV (Veritas 2007).

Table 2.6: Recommended values from DNV-RP-F110. The embedment ratio is defined by the pipeline burial depth to pipeline diameter (H/D).

Backfill soil type	Mobilisation distance	Pedersen uplift factor	DNV limitation
Loose sand	0.5-0.8%H	0.1-0.3	3.5 <H/D <7.5
Medium or dense sand	0.5-0.8%H	0.4-0.6	2 <H/D <8
Rock	20-30mm	0.5-0.8	2 <H/D <8 particle size (25-72mm)

As noted from the above table, when H/D ratios are less than 2 (typical of onshore buried pipelines), there is a lack of understanding as to how the pipeline mobilises when soil cover is reduced. Wang et al. (2010) assessed low cover diameter ratios for pipeline uplift using a series of full scale and centrifuge testing. Their data found that the vertical slip model and shear contribution remains valid for low H/D ratios when considering compacted sand. This research argues that the vertical slip model still produces a sound enough estimate for maximum uplift resistance. Robert et al. (n.d.) agreed that current analytical models could realistically predict peak uplift for dry and unsaturated soil conditions when H/D ratios were above 2, but there has been a lack of work looking at uplift resistance for H/D ratios below 1.

2.7.1 Vertical displacement

The cover above pipelines is dynamic and changes over time with each erosional event, which has the potential to lessen the resistance offered by the weight of the soil. Such scenarios are slow processes where the pipeline may be displaced minimally vertically or laterally. Research by Thusyanthan et al. (2008) modelled fast and slow pipeline pull-out tests using different cover heights (1.05m and 1.30m) together with a rock dump up to 1m to assess cover depth effects on resistance. Their results are displayed in Table 2.7 and suggest slow vertical pipeline displacement offers substantially less (e.g. one third less) uplift resistance than a fast pull out scenarios, however, further investigation is required on the rate effects of pipeline displacement and soil cover height.

Table 2.7: Results of resistance from the pull out tests (Thusyanthan et al. 2008)

	Test 1	Test 2	Test 3	Test 4
Slow pull out (0.0002 mm/s)	3.13 kN/m	3.25 kN/m	5 kN/m	9 kN/m
Fast pull out (0.2 m/s)	4.63 kN/m	4.75 kN/m	6.88 kN/m	13 kN/m

2.7.2 Lateral displacement

In addition to vertical displacement pipelines buried in soft soil are also subject to lateral displacement through soil erosion. Jung et al. (2013) used finite element modelling to assess the lateral force vs displacement relationship in dry and partially saturated sand. Figure 2.7 shows that displacement force increases with increasing H/D ratios, however it is not well understood for H/D ratios of less than 3 and in the context of soil erosion and removal. Later work by Robert et al. (2016) suggested that in unsaturated soils there may be an underestimation of load from external ground movements. Their finite element modelling showed that an increase in soil suction and stiffness may increase lateral load on pipelines. In addition, there are few studies considering how erosion of soil along the pipeline corridor may affect the potential for lateral displacement.

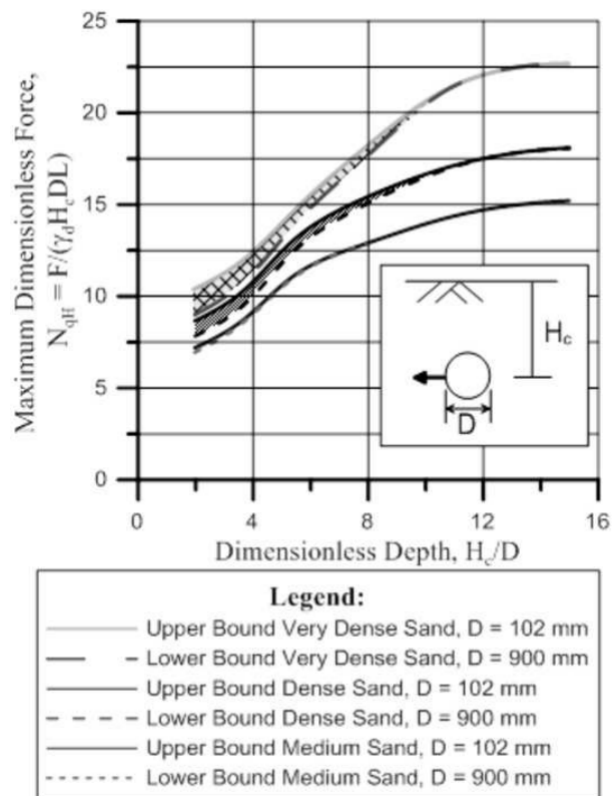


Figure 2.7: Lateral displacement for dimensionless depth H/D Jung et al. (2013)

2.8 Conclusion

There is at present no set standard for recording pipeline failures at a global scale. In the literature third party damage has been cited as the lead cause for failure. The inclusion of cover depth in gas pipeline failure statistics highlights that soil erosion may be is an issue. The reduction in cover depth is has been linked to pipeline failures for 0.8m and 1m cover depth design. The main mechanism for soil loss is intense rainfall events which are predicted to become greater in frequency and magnitude and has the possibility to induce erosion events along pipeline routes which are situated in areas of reduced vegetation cover. Pipeline installation design is commonly based on UK and American guidelines, but ero-sion of the soil surface leaves pipeline areas vulnerable to exposure and third party damage. Monitoring pipelines is expensive and techniques such as LIDAR are a promising method of recording changes in the soil surface and topography, though may lack sufficient resolution. Attempts to estimate soil erosion risk along pipelines using Geographical Information System tools are promising but relatively preliminary. Ideally we need to develop predictive methods for estimating the ef-fect of erosion on soil cover depth (with different soil types and vegetation cover percentages) so that soil cover can be maintained and remediated in areas where erosion and geohazards remains an issue. Understanding how soil erosion and depth of cover changes over time could inform pipeline uplift studies to decrease the risk of pipeline buckling and failure during thermal expansion within a pipeline.

Chapter 3

Evaluating the change in patterns of heavy rainfall events in Eastern Scotland

3.1 Introduction

The frequency rainfall events has been increasing in the UK (Osborn & Hulme 2002) with variability across the country (Brown 2018) and seasonal differences (Champion et al. 2015, Fowler & Ekström 2009). A positive trend in global mean precipitation and temperature was noted by Hulme et al. (1998), who suggested the reason for changing rainfall patterns was attributed to the rise in greenhouse emissions caused by anthropogenic activity, with high latitude regions in the northern hemisphere showing change (Groisman et al. 2005, Scoccimarro et al. 2015) and in particular the UK (Fowler & Kilsby 2003b, Osborn & Hulme 2002). Rainfall intensity is expected to increase as more moisture is held in the atmosphere by a warming climate as predicted by the Clausius-Clapeyron equation (Pall et al. 2006). However, regional studies have suggested that rainfall intensity has increased beyond what is expected (Hanel & Buishand 2010, Lenderink & van Meijgaard 2008). Analysing rainfall at an hourly resolution is important as intensity at this temporal scale can provide information on extreme events such as flash flooding (Archer & Fowler 2018) and aid in climate modelling by establishing the diurnal cycles of precipitation (Blenkinsop et al. 2017, Svensson & Jakob 2002). In Scotland there is asymmetry in rainfall events between the West and East regions, with the West typically wetter than the East (Afzal et al. 2011). Less understood is the increase in single heavy rainfall events using peak over threshold (P.O.T.) analysis, and how this changes over time as such information can be used as a basis for predicting soil erosion by water. These events over time may affect infrastructure such as buried pipelines (Girgin & Krausmann 2016). In addition, the UK Climate Projection hourly dataset was evaluated to give an indication of the

likelihood of heavy rainfall events during the mid and late 21st century.

3.1.1 Peak over threshold selection

Peak over threshold is a type of extreme value analysis which models peak values of independent events (Leadbetter 1991). A method for selecting a threshold for P.O.T analysis is not clearly defined in the literature (Solari et al. 2017). At present there is no clear definition for rainfall intensity categorisation globally and definition varies from meteorological agencies (Met Office 2012) to literature (Osborn & Hulme 2002, Svensson & Jakob 2002). Two types of precipitation have been considered: rainfall and showers. In the UK heavy rainfall, defined by the Meteorological Office, hereafter Met Office, is classed as events meeting or exceeding 4mm/hour intensity Met Office (2012).

3.1.2 Aims and objectives

The aim of the analysis in this chapter is to evaluate the change in heavy rainfall events using observed weather station data that is situated along a pipeline route in East Scotland. Assessment will be made at an annual and seasonal scale to assess if there are any inter-annual changes. This approach is novel and approaching the evaluation of rainfall events differently than just considering rainfall depth totals. The hourly UKCP18 data has been used to comment on the predicted frequency of future heavy rainfall events.

The objectives are to:

1. Acquire and quality check long-term historic hourly precipitation values for three weather stations (Eskdalemuir, Dyce and Leuchars) situated close to a buried gas pipeline network in Scotland. The key criteria for weather station selection was based on hourly resolution of data and the long term availability (more than 30 years).
2. Extract independent rainfall events using thresholds of ≥ 4 mm/hour and analyse the number of rainfall events at an annual and seasonal scale for the period 1980-2018. An annual scale is defined by a hydrological water year which runs from the 1st October to 30th September the following year.
3. Statistically analyse the trend over time and the variability of heavy rainfall events and depth totals (mm) to conclude if rainfall is likely to impact areas susceptible to soil erosion along the pipeline route.

3.2 Materials and methods

3.2.1 Study location

The study area is along the National Grid Gas pipeline network (National Grid 2018) that spans across Eastern Scotland and is an area which contains various hydrocarbon networks that transmit oil and gas from the North Sea to distribution centres in the UK. Onshore oil and gas pipeline routes are often not available publicly online. It is acknowledged that oil and gas pipelines are situated throughout this region of east Scotland due to the location of the North Sea oil and gas fields where the products require processing onshore. The only available public network route is provided by the National Grid and is a gas pipeline which runs throughout the East of Scotland. The Forties pipeline operates in this region and suffered a leak which took weeks to fix and cost the British economy £20 million a day (BBC 2017). Therefore keeping the pipelines buried safely underground is crucial to the environment, safety and the economy. To evaluate historic rainfall patterns weather station data must be used. The main decision for deciding which weather stations to include in this report was based on (1) the availability of long-term hourly precipitation records and (2) proximity to the gas pipeline. Two different sources of hourly precipitation data sets were utilised to 1. evaluate the pattern and change for historic precipitation events and 2. provide an overview of how future climate may change in the context of exceedance events. The data analysis evaluated rainfall amounts against the number of exceedance events within different temporal periods. A combination of Microsoft Excel and the R programming language were used for the processing and analysing each data set.

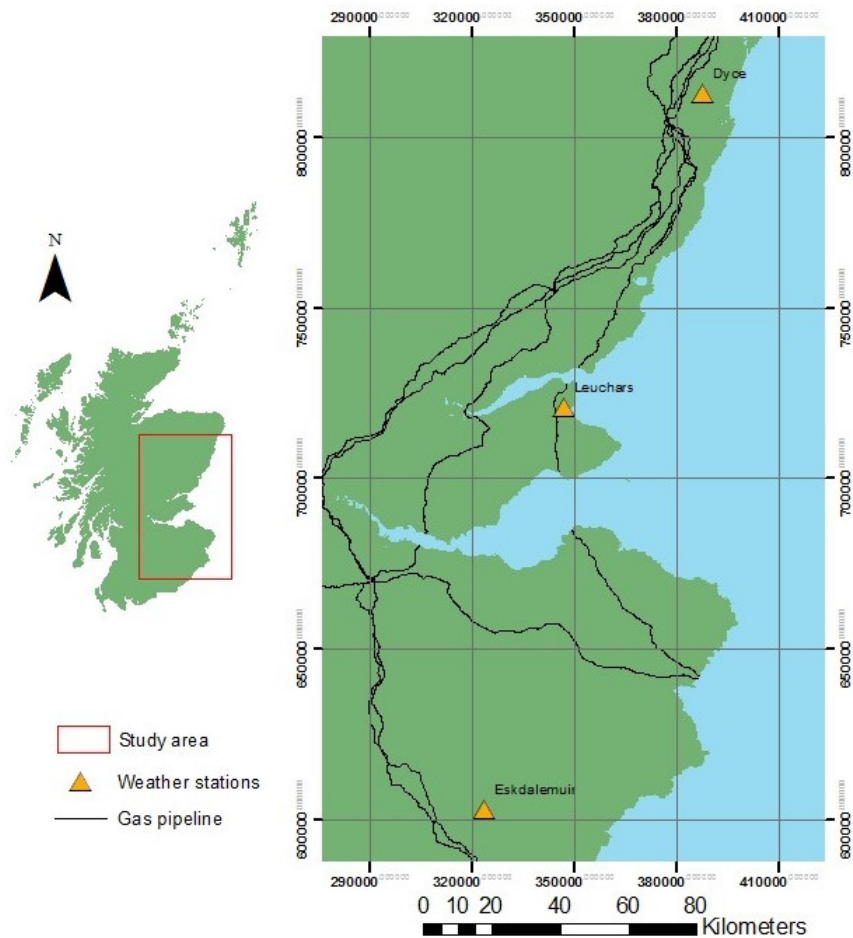


Figure 3.1: The location of the study area, gas pipeline (National Grid 2018) and weather stations based on OSGB1936 British National Grid coordinate system (m).

3.2.2 Data sources and methods

Long term weather station data are free and available to registered users of the Centre for Environmental Data Analysis website (CEDA) where precipitation data is archived as part of the Met Office Data integration Archive System (Met Office 2006). Future climate probabilistic projections have been simulated with collaboration of the Met Office Hadley Centre Climate Programme with UK Government support from the Department of Business, Energy and Industrial Strategy (BEIS) and the Department for Environment, Food and Rural Affairs (Defra). The projections, known as the UK Climate Projection 18 (UKCP18), simulate a range of projections (known as ensembles) based on the current knowledge or how climate reacts to the presence of greenhouse gas emissions. Hourly precipitation models are based on 'business as normal' status, meaning that greenhouse gas emissions are expected to continue to rise through-out the 21st century and these data are referred to as UKCP18 for this report (Met Office Hadley Centre 2019).

Data acquisition

The MIDAS and UKCP18 datasets required different methods of extracting and quality checking the accuracy of data shown in Figure 3.1. Both datasets can be downloaded via the ftp service through the Centre for Environmental Data Analysis (<https://catalogue.ceda.ac.uk/>). The historic observed MIDAS data is a long-term record (Blenkinsop et al. 2017) where advances in equipment used and the way data are presented changed over time which required manual extraction and collation of weather message type across. Furthermore, errors in the raw data records, despite previous quality checking, still returned erroneous information which required further filtering (Blenkinsop et al. 2017). In contrast UKCP18 data is a projected model that is based on uncertainty and under the notion that greenhouse gas emissions will continue as "business as usual" (RCP8.5) and will continue to rise throughout the 21st century (Met Office Hadley Centre 2019).

3.2.3 Method

To utilise and analyse MIDAS and UKCP18 information each dataset required separate processing as MIDAS data required quality checking for erroneous recorded information. These processes are described in the following subsections starting with the MIDAS data.

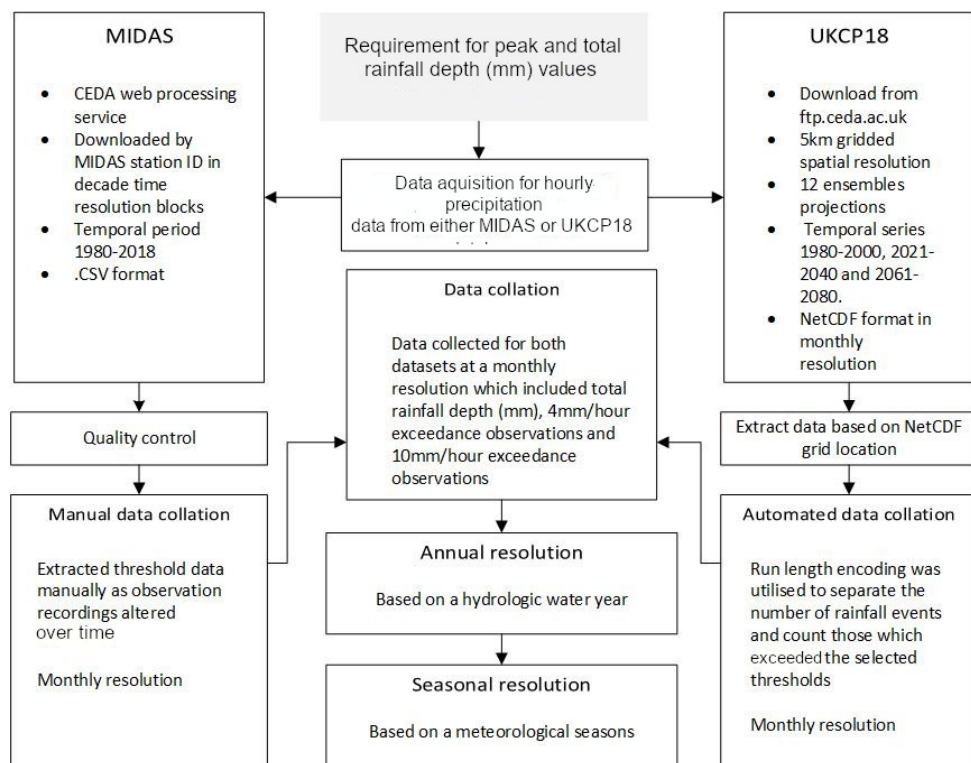


Figure 3.2: Flow chart outlining the different data formats sourced and the steps with justification taken to ensure the data (for MIDAS) is sufficient for data analysis. Microsoft Excel and R Studio (RStudio Team 2021) were used throughout the data mining process.

MIDAS data processing and quality checking

UK hourly rainfall data was downloaded from 1980 to 2018 for Eskdalemuir, Dyce and Leuchars. Manual processing was required to evaluate if the extreme values recorded were true. Microsoft Excel was the choice tool for this as quickly filtering and amending raw data was a more efficient process. Raw data was separated into decade files for quality checking to establish data accuracy. The process required a combination of filtering and IF statements to highlight the extreme values which required validation. Depending on the number of weather stations and years required for analysis, this process can be cumbersome. Table 3.1 identifies the issues, remedies and limitations when processing the data. Appendix A gives a brief example of how data is recorded and why it requires filtering out. Once the quality checking was complete the data for each decade was compiled into one file and saved for each weather station for analysis in R.

Table 3.1: Manual quality checking issues, remedy and limitations to the dataset

Issue	Remedy	Limitation
Various weather messages in the record	Filter specific type of weather messages	Potential overlap of information. Required user judgement where conflicts of data exist
Different weather messages causing splits in continuous data	Separated data for each weather type and amalgamated information into one dataset	Rainfall may have occurred
Missing rainfall data	None Cross check with Met office records and news reports.	Loss of data for the time period where heavy rainfall events may have occurred unrecorded.
Erroneous information recorded (possibly due to snow fall)	Required the user to objectively identify what rainfall is typical and atypical for the region.	Missing data
Rainfall accumulation recorded as excessively large hourly rainfall	Omitted from the dataset	Missing hourly rainfall data

UKCP18 data processing

In contrast to the MIDAS data the UKCP18 data did not require quality checking, but the procedure for extracting and processing UKCP18 data is intensive requiring numerous steps to collate the data into a useable format for R. Like MIDAS, the rainfall depth and event exceedance values were extracted from the data. The complete processing chain was performed solely in the R environment and involved two major steps for each ensemble:

1. The extraction of hourly precipitation data at a monthly scale.

2. Writing a function in R which has the ability to extract a run of values that are counted as one event, find the maximum hour recorded and return a value which counts the number of exceedance events occurring within such a period.

Each UKCP18 monthly NETCdf file holds precipitation in an XY gridded format and for each grid element (given in Table 3.2) 720 values represent hourly precipitation values in a simulated month (24 hours by 30 days). The 5 km dataset was used in this report based on the trade off between processing time and spatial resolution. Within the published R code, indexing was required to ensure the correct spatial information was recorded based on the physical location of the MIDAS weather stations (Table 3.2).

Table 3.2: The location details for each weather station including MIDAS station ID, British National Grid coordinates and the UKCP18 NetCdf grid elements based on 5km OSGB1936 resolution.

Location	MIDAS station ID	British National Grid OSGB1936		UKCP18 NetCDF Grid element	
		X	Y	X	Y
Eskdalemuir	1023	322500	602500	105	128
Dyce	161	387500	812500	118	170
Leuchars	235	347500	722500	110	152

The process of assessing the number of rainfall events and how many equalled or exceeded a certain threshold required the use of a written function in R which tells the software to run a process along a line of code and determine how many precipitation exceedance events are simulated within a certain run of values. The function used in the R environment (R Core Team 2018) utilised Run Length Encoding (RLE) to pick out a run of positive values ($> 0.0\text{mm}$) between periods of at least one hour of zero precipitation. The function is displayed below and was tested on a sample month to make sure it evaluated the number of rainfall events correctly.

```
events <- function(i){
  precip <- as.numeric(i)
  if(sum(precip > 0.0)){
    cons_precip = rle(precip > 0.0)
    rain_id = rep(0.0, length(precip))
    rain_id[precip > 0.0] =
      rep(1:sum(consec_precip$values),
        cons_precip$lengths[consec_precip$values])

    rain_event<-tapply(precip,rain_id,max)
    event_count<-sum(rain_event >= 4.0)
```

```

        return(event_count)
    } else {
        return(0)
    }

```

3.3 Results

3.3.1 Annual rainfall (MIDAS)

A boxplot displaying the total rainfall for the period from 1981 until 2018 by each weather station is shown in Figure 3.3. Eskdalemuir experiences more than double the total rainfall amount than Dyce and Leuchars. The mean total rainfall for Eskdalemuir is 1681 mm where there was a maximum of 2394 mm in one year. The mean rainfall total for Dyce is 794 mm and for Leuchars is 673 mm.

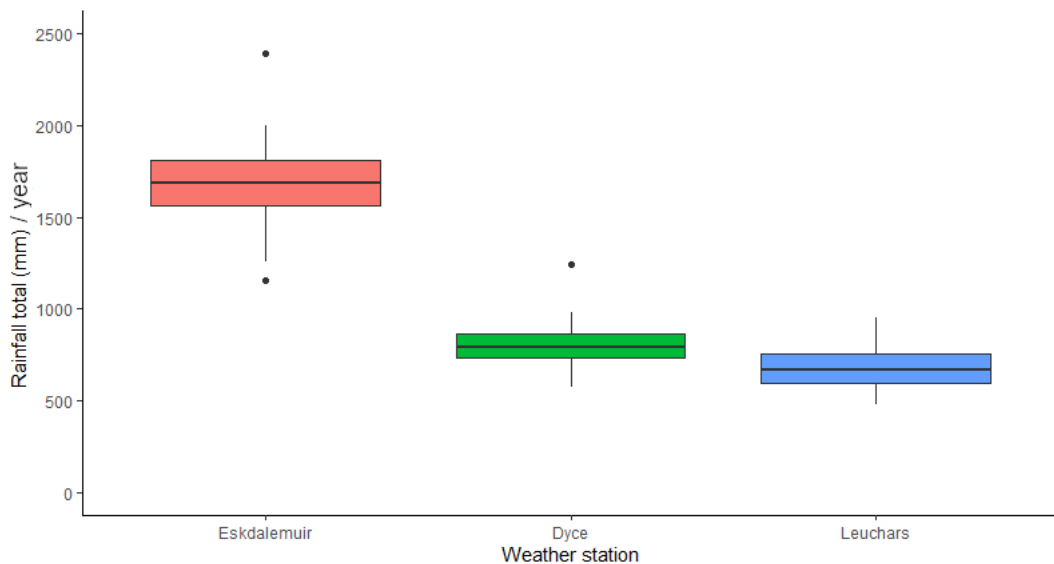


Figure 3.3: Boxplot showing the total rainfall depths (mm) for a given water year across all three weather stations.

Figure 3.4 displays the box plot of heavy rainfall events for each weather station for 1981 until and including 2018. This figure shows that Eskdalemuir experiences about three times as many heavy rainfall events on average compared to Dyce and Leuchars. The mean number of heavy rainfall events occurring in one year at Eskdalemuir is 30 whilst at Dyce it is 11 and at Leuchars it is 9 events.

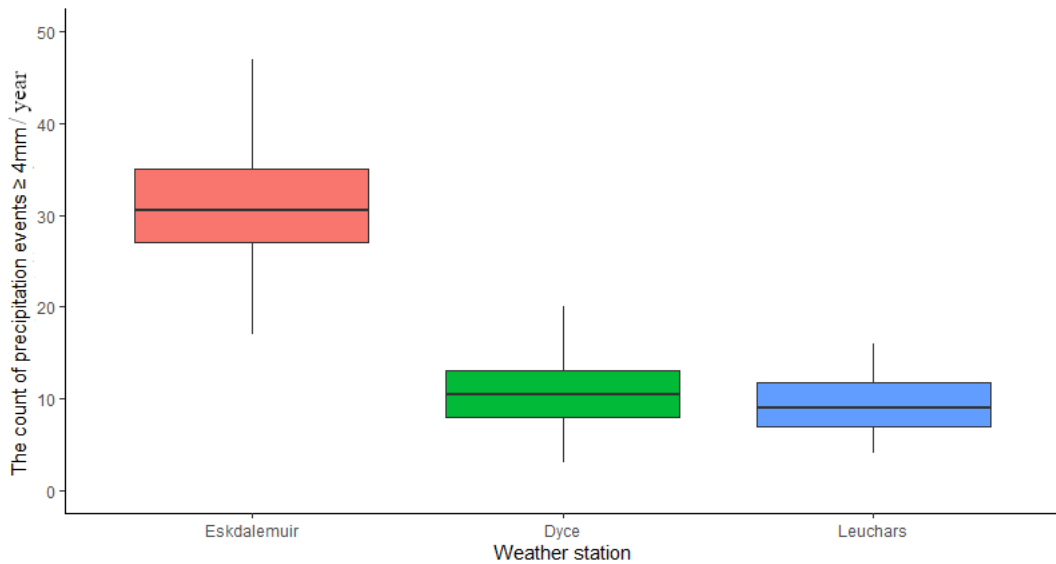


Figure 3.4: Boxplot showing the total rainfall amount for a given water year for all three weather stations.

Total annual rainfall and exceedance over time (MIDAS)

Figure 3.5 and 3.6 display the total rainfall and number of heavy rainfall events over time. Regression analyse of all six datasets indicate positive slope coefficients although the p-values are only approaching significance in the case of Eskdalemuir.

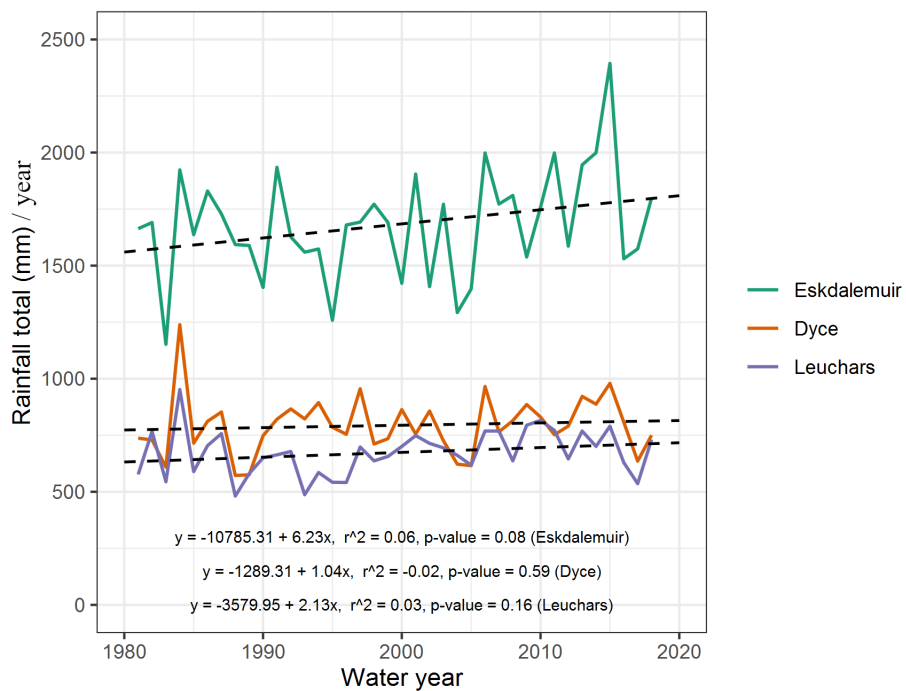


Figure 3.5: Line graph showing total annual rainfall over time

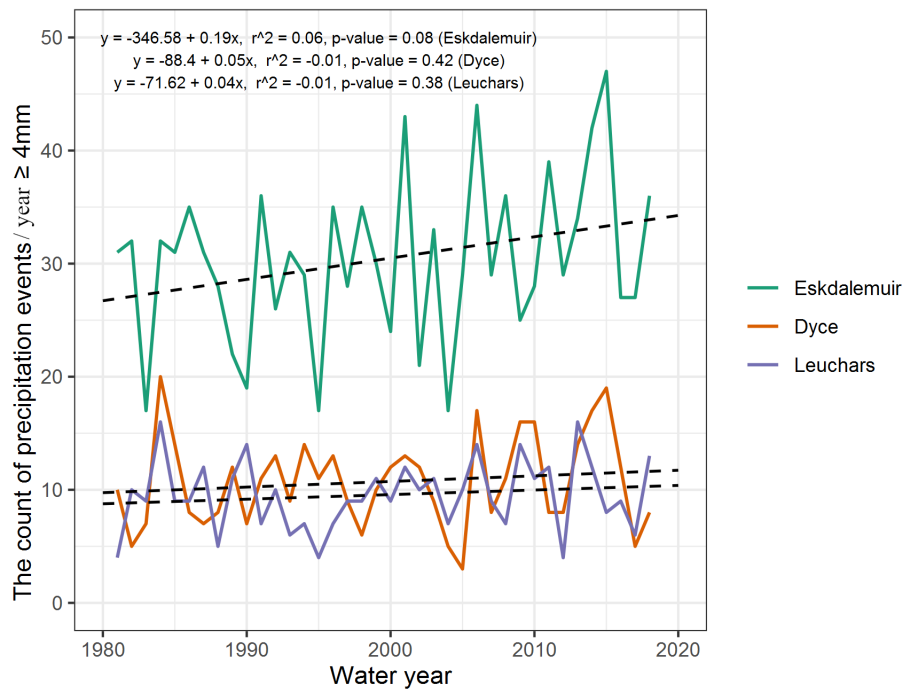


Figure 3.6: Line graph showing the total number of heavy rainfall events over time

3.3.2 Historical seasonal rainfall patterns (MIDAS)

Table 3.3 shows seasonal exceedance counts during 1981-2018. This table shows that there is a seasonal split between the rankings of heavy rainfall events where 58 percent to 75 percent occurred during autumn and summer.

Table 3.3: Total counts of exceedance events for each season for 1981-2018 water years

	Eskdalemuir		Dyce		Leuchars	
	count	rank	count	rank	count	rank
Autumn	348	1	124	2	126	2
Winter	302	3	52	4	51	3
Spring	178	4	59	3	37	4
Summer	327	2	172	1	149	1
Total	1155		407		363	

Autumn and summer exceedance events(MIDAS)

Figure 3.7 displays the count of summer event exceedance throughout the observation period and results show that the increase in exceedance count with time is significant at Leuchars and Eskdalemuir with a positive regression coefficient also at Dyce. It is worth noting that at Eskdalemuir there are two clear peaks of summer exceedance within the second half of the dataset. In contrast, there was

no significant correlation of exceedance frequency with time at Autumn as shown in Figure 3.8.

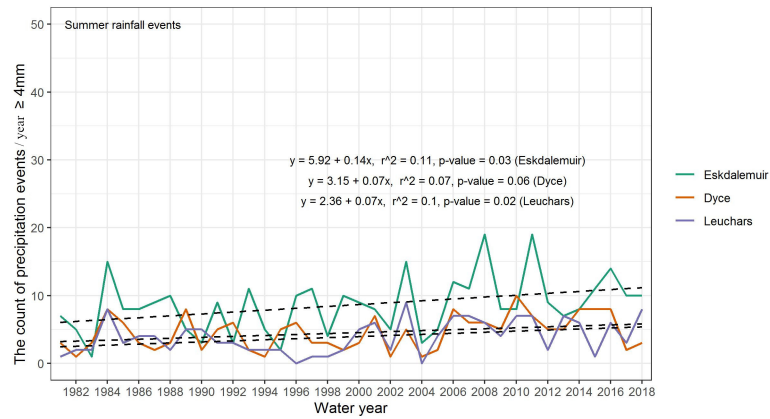


Figure 3.7: Summer exceedance

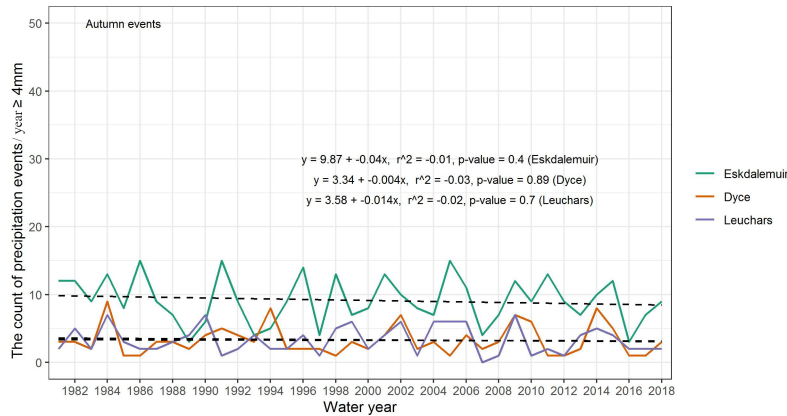


Figure 3.8: Autumn exceedance

Winter and spring exceedance events (MIDAS)

Figure 3.9 illustrates that winter events for Eskdalemuir show greater variability of heavy rainfall events compared to Leuchars and Dyce. The slope of the trend line for Eskdalemuir is positive, but not significant, which is influenced by the 2015 where over 20 heavy rainfall events occurred over the winter period. Figure 3.10 shows the Spring exceedance events trend. Eskdalemuir shows a positive trend due to peaks in 2001 and 2014 whilst Leuchars and Dyce show a fall in trend however, none of the six winter and spring regressions were significant.

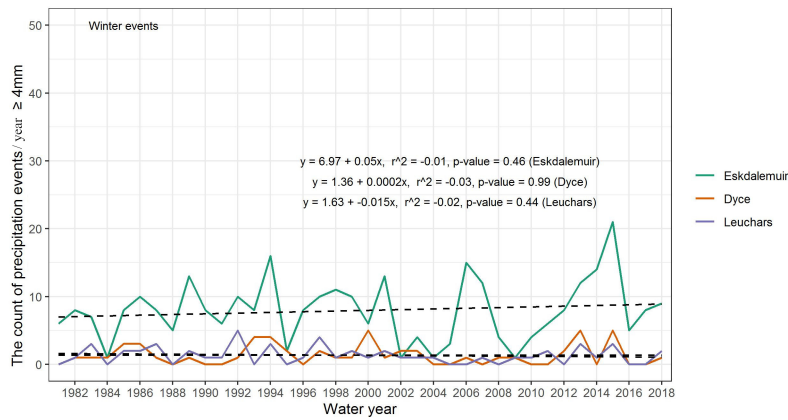


Figure 3.9: Winter exceedance events for Eskdalemuir, Leuchars and Dyce

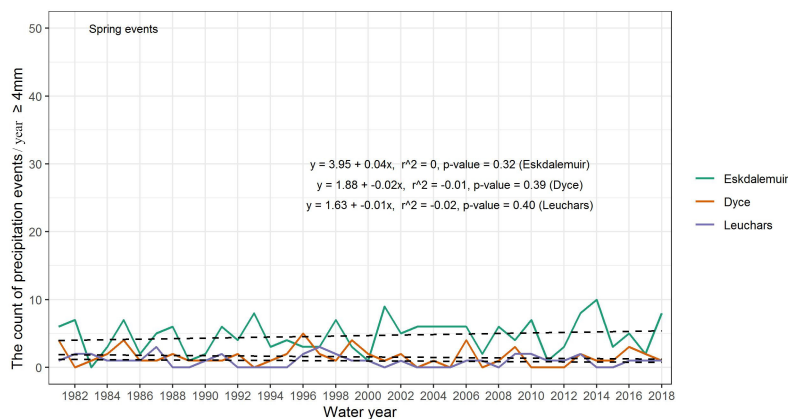


Figure 3.10: Spring exceedance events for Eskdalemuir, Leuchars and Dyce

Eskdalemuir changes by 20 year period

Figure 3.7 demonstrated how summer seasonal rainfall and exceedance events change over time giving a significant positive slope coefficient. Figure 3.11 and Figure 3.12 are box plots of seasonal winter rainfall and exceedance events for Eskdalemuir. Each figure displays a box plot of winter rainfall and exceedance values for each time slice. Winter is considered a vulnerable period for soil erosion as fields have a high possibility of being bare and exposed to rainfall that can induce soil erosion. The data shows that the maximum rainfall depth at Eskdalemuir for the winter period was 709.4 mm during 1981 - 1999 to 1049.4 mm in the later time slice, with the median values being 483.1 mm and 414 mm rainfall depth respectively. The same pattern can be noted for exceedance where in the 1981-1999 there was one winter season with a maximum 16, and this increased to 21 in the later time slice. The variability of rainfall parameters was much greater in the later time period, as shown by the greater inter-quartile spread of values in the box plots.

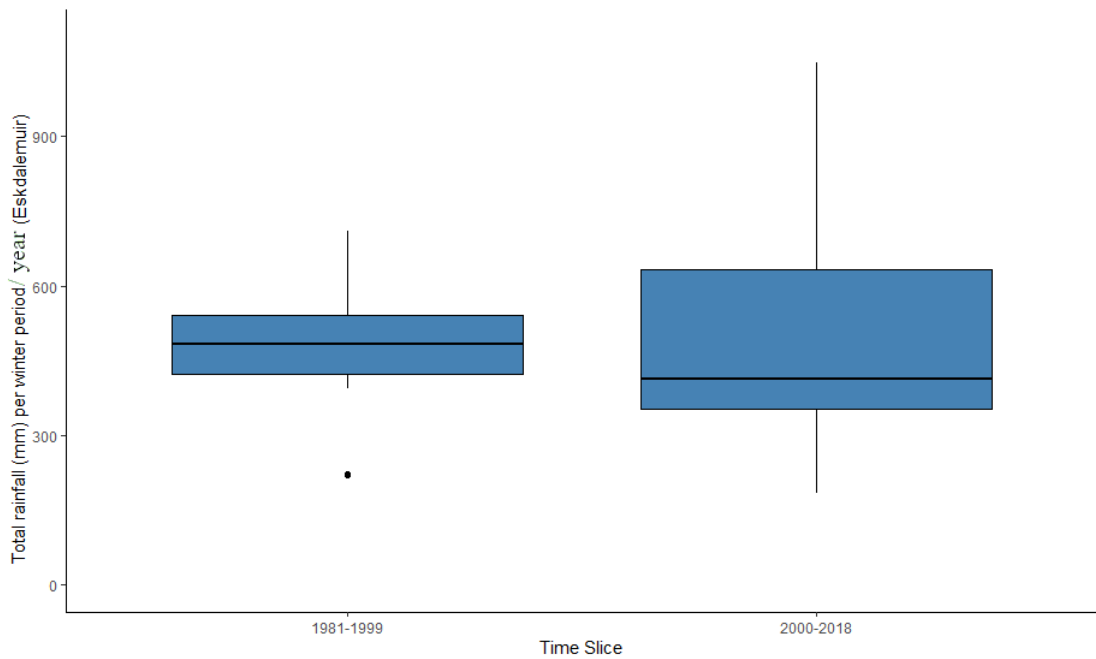


Figure 3.11: A boxplot showing the greater variability of winter rainfall depths recorded at Eskdalemuir for the time periods 1981-199 and 2000-2018.

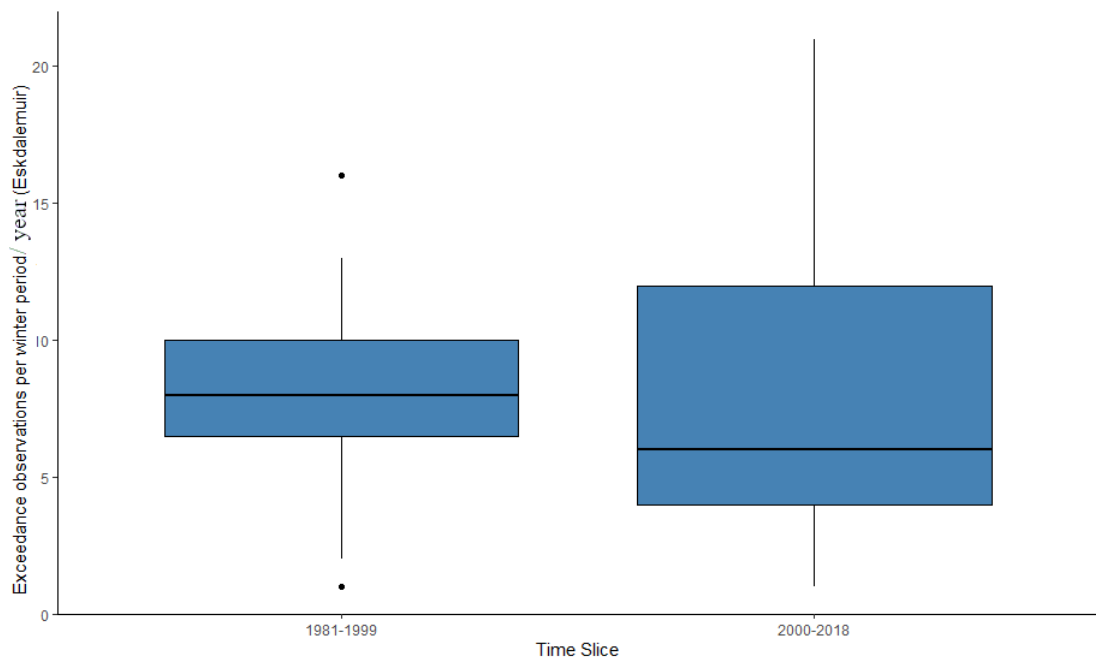


Figure 3.12: A boxplot showing the greater variability of winter exceedance events recorded at Eskdalemuir for the time periods 1981-199 and 2000-2018.

3.3.3 Future annual rainfall projections (UKCP18)

The UKCP18 data are simulated for three time slices that relate to the present day, middle of the century and late century. The data are simulated using 12 different ensembles which account for uncertainty. Table 3.4 shows that for the 1981-1999 period the UKCP18 model rainfall appears to overestimate the historic rainfall total

and exceedance count. Increase in both rainfall parameters with time is predicted into the future.

Table 3.4: Mean values between MIDAS and UKCP18

Weather station	Parameter	MIDAS	MIDAS	UKCP18	UKCP18	UKCP18
		1981-1999	2000-1018	1981-1999	2021-2040	2061-2080
Eskdalemuir	Mean	1631.5	1731.5	1777.7	1833.5	1940.7
Dyce	Rainfall (mm)	786.0	801.3	904.9	920.6	905
Leuchars		636.3	710.1	703.8	728.8	734.8
Eskdalemuir	Exceedance	28.7	32.1	38.9	41.0	42.7
Dyce		10.2	11.2	14.4	16.3	17.6
Leuchars		8.9	10.2	12.7	14.2	15.3

3.4 Discussion

3.4.1 Annual trend

Rainfall is heterogeneous across the pipeline route, which was seen in the weather station data where Eskdalemuir was observed as having greater rainfall depths and exceedance events than Leuchars and Dyce. Afzal et al. (2011) and Kendon et al. (2014) identified the regional differences in precipitation for Scotland with there being a East and West geographic divide. Eskdalemuir is identified as a western weather station in Scotland, agreeing with the higher rainfall depths and events observed at this location (Svensson & Jakob 2002, Afzal et al. 2011). Annually, the results across all stations showed that over a period of 38 years, rainfall depths were increasing with Eskdalemuir increasing at a faster rate than at Dyce and Leuchars. Storms events, such as storm Desmond in 2015 (van Oldenborgh et al. 2015), have been increasing in frequency which has contributed to an increase trend in precipitation events. An increase in rainfall has been observed in other countries and has been attributed to anthropogenic activity and atmospheric circulation (Groisman et al. 2005).

Hourly precipitation observations gave the opportunity to model the number of heavy rainfall events that have occurred over the 38 year period. Heavy rainfall events where at least one hour recorded $\geq 4mm/h$ showed an increase in trend annually, with Eskdalemuir showing a peak of 47 events in 2015. Kendon et al. (2014) predicted from modelling rainfall in East Scotland that there was an increase in the duration of rainfall events which may be more of a threat to soil erosion events than high intensity rainfall events alone. This chapter focussed on the number of events rather than duration, but the findings in this research does show an increase in the number of summer events. However, during the summer

season vegetation cover is at its highest and would pose less of a soil erosion risk to pipelines.

3.4.2 Seasonal change in heavy rainfall events and possible drivers

This chapter evaluated the change in seasonal rainfall events. Over the 38 year period, Autumn and Summer were ranked the top 1 or 2 in number of events across all weather stations, which is consistent with the findings of Blenkinsop et al. (2017). However, this study finds there is no significant trend in Autumn events whilst there is a significant increase in the number of Summer heavy precipitation events. For pipeline operators, the threat of heavy Summer seasonal events to soil cover erosion is reduced as this is the time when vegetation cover is at its greatest in this region. A notable finding which agrees with other studies is the increase in the variability of winter rainfall events. At Eskdalemuir there were 15 events in 2006 and 21 in 2015; which was the period of storm Desmond. For bare fields in this region the number of heavy precipitation events occurring over a short space of time can erode the surface. The explanation in the variability of winter patterns may be correlated with the North Atlantic Oscillation (NAO) index. The NAO is represented by sea-level fluctuations between Iceland and the Azores and is measured in quantitative negative and positive values (Hurrell et al. 2003). Figure 3.13 shows the implications for the UK as a positive NAO value results in wetter winters and a negative value equates to drier winters (Horswell et al. 2019, Hurrell et al. 2003). Being aware of the change in NAO can be useful for pipeline operators in the Eskdalemuir region in relation to soil erosion risk and pipeline cover.

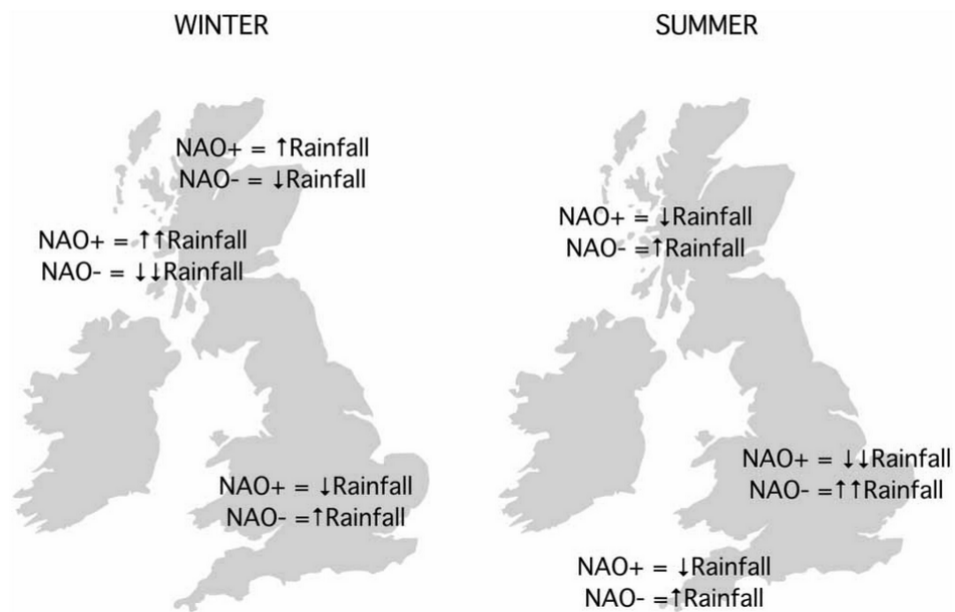


Figure 3.13: Summarised regional difference in rainfall pattern for the UK. Figure reproduced from Horswell et al. (2019). Note: NAO + and NAO- describe the negative or positive phase of the NAO index.

3.4.3 Future simulations and pipeline risk mapping

The UKCP18 CPM (convection permitting model) hourly precipitation dataset for each weather station was evaluated. The idea of these simulations is to give an idea of the rainfall conditions at the present, mid and late 21st century (Met Office Hadley Centre 2019). The UKCP18 data was evaluated with uncertainties and averaged to provide a value to compare to the observed data. In all UKCP18 situations the mean value was greater than the mean of the MIDAS values. Met Office Hadley Centre (2019) argues that this data can provide an estimate for uncertainty in future changes in the climate, although at our three weather stations the UKCP18 data over-estimated historical values. The findings in this chapter show an increasing trend in rainfall events, but this trend is driven by variability more than a consistent increase in values which agrees with other published literature (Fowler & Kilsby 2003b, Fowler & Ekström 2009, Fowler & Kilsby 2003a). It appears that rainfall depths and exceedance events are increasing and likely to continue increasing, but with large variation between years and seasons.

3.5 Conclusion

The results show that rainfall is very variable across the National Grid pipeline route and between years and seasons. There is an increase trend in summer rainfall depth and exceedance events over the 38 year period, greater at Eskdale-

muir than at Dyce and Leuchars. There is increased variability in winter rainfall. When considering the risk of soil erosion for buried pipelines vulnerable areas around Eskdalemuir are at higher risk by rain water action if the ground surface has reduced vegetation cover. The future simulation UKCP18 events did provide average values for rainfall depth and exceedance for mid and late century, however these over-estimated historical datasets (1981-1999) and caution should be used in using these when planning for the long-term.

Chapter 4

Evaluating the soil erosion risk to a hydrocarbon pipeline using G.I.S

4.1 Introduction

Buried onshore hydrocarbon pipelines are subjected to the threat of soil erosion in a changing climate (Sweeney 2004). Transmission pipelines are at the greatest risk to soil erosion as they are often routed in arable land which is sensitive to soil erosion (Qi et al. 2012, Bayramov 2012). Whilst there are new techniques which may mitigate the potential hazards for new pipeline selection (Abudu & Williams 2015), older pipeline installations require ongoing monitoring as they may be routed in areas with soil erosion risk. Modelling soil erosion is complex as influences from rainfall, soil, land cover and anthropogenic activity can impact soil erosion rates. The most established system for predicting soil erosion at an annual rate is the Revised Universal Soil Loss Equation and was devised by Wischmeier & Smith (1978) to estimate soil loss in arable land use in the USA. This equation considers rainfall intensity, soil erodibility, slope characteristics, vegetation cover and land use practises to empirically estimate soil loss. Since the digitalisation of mapping data this model has influenced over 90 soil erosion models (Alewell et al. 2019). In this chapter, the main risk factors for erosion along the National Grid gas pipeline are considered, together with recent information on the crops grown in the area from the Centre of Hydrology and Ecology. The risk factors are considered alongside a recent European map of soil erosion risk (Alewell et al. 2019), identifying the area along the pipeline route. The RUSLE model has been used for assessing soil erosion along a pipeline route (Bayramov et al. 2013, Winning & Hann 2014), but with little detail given about the environment characteristics of the route and risk mapping for a specific season where arable land is at its most vulnerable.

4.1.1 Aims and objectives

The aim of this chapter is consider soil erosion risk factors along the pipeline route. The objectives are to:

1. Acquire data for the project including slope, soil texture, land cover and crop data.
2. Evaluate the attributes of land cover, soil texture, crop type and slope in length (km) along the pipeline route.
3. Identify the most important erosion risk factors and where they are located along the pipeline.
4. Identify where these risks coincide, thereby maximising the chance of erosion events.
5. Compare the areas identified with the highest risk of erosion with risk data from a published EU erosion risk map.
6. Consider the implications of arable crop dataset information from the Centre for Ecology and Hydrology, in relation to seasonal erosion risk.

4.2 Study area

The study area is based on the National Grid gas pipeline network (National Grid 2018). The pipelines that run through the area deliver hydrocarbon products from the North Sea oil and gas fields. Figure 4.1 shows the location of the National Grid pipeline in relation to the North Sea oil and gas fields, through to the route of the pipeline located onshore in Scotland. This region is also productive in agriculture activity where there are areas which coincide with the pipeline route (Watson & Evans 2007). Therefore, this study area provides an opportunity to evaluate the how much of this particular pipeline is in areas of different land types and crop cover. Assessing this information as well as the likelihood of erosion can give an idea about the potential soil erosion risk that may be a threat to the pipeline soil cover.

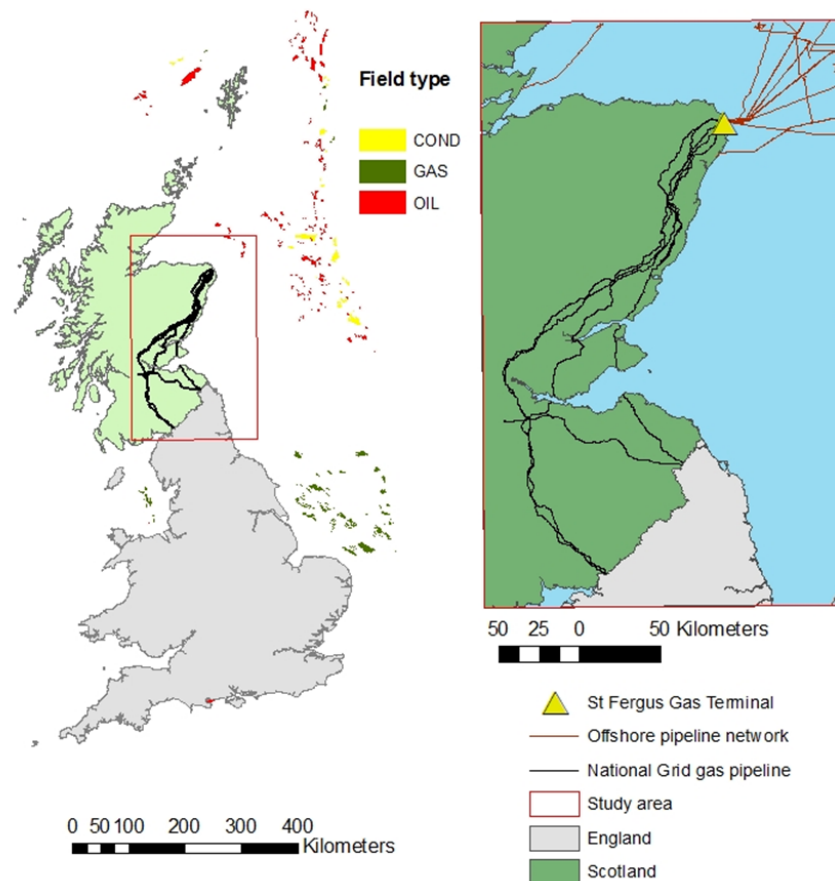


Figure 4.1: The study area for evaluating erosion risk factors along gas pipeline routes. Spatial map created with ESRI (2018) using England and Scotland country boundary by Ordnance Survey (GB) (2017), with oil and gas field data from Oil and Gas Authority (2018). Pipeline data by National Grid (2018).

4.3 Data sources and methods

Table 4.1 provides an overview of the data sources used for creating the soil erosion risk map. This created map will be compared with the EU Soil Data Centre soil erosion by water RUSLE2015 dataset, which is an assessment of soil erosion by over the EU at 100 m scale using a modified version of the Revised Universal Soil Loss Equation. This dataset, published in 2015, has peer reviewed input layers of rainfall, soil, land cover and soil to provide a model for estimating soil loss rates per t/ha per year.

Table 4.1: Data source reference table for chapter 4

Dataset	Date	Format	Description	Resoluton	Reference
National Grid Gas pipeline	2020	Polyline	Spatial dataset of the gas pipeline that is freely available.	N/A	(National Grid 2018)
Slope DTM	2018	Raster	A digital terrain model of the slope which covers the UK.	50 m	(Ordnance Survey 2018)
Land cover	2015	Vecor	A spatial land cover dataset which used machine learning to classify land cover that covers the UK.	50 m	(Centre for Ecology and Hydrology 2017a)
Crop data	2016 to 2019	Vector	A spatial dataset which details different crop locations across the UK using machine learning. This data is cross checked with farmer surveys to ensure accuracy.	2 ha	(Centre for Ecology and Hydrology 2016)
Soil Parent Material Model	2011	Vector	A dataset which covers rock and sediment characteristics which can provide information on soil texture.	1:50 000	(Lawley 2011b)
Soil erosion by water (RUSLE2015)	2015	Raster	An EU wide spatial erosion dataset which considers rainfall, soil erodibility, crop cover and slope that is based on the RUSLE model.	100 m	(Panagos et al. 2015)

The Crop Cover Plus dataset is provided by the UK Centre for Hydrology and Ecology where vector data of crop classification is provided for Great Britain (Centre for Ecology and Hydrology 2016). The method uses a combination of supervised mapping and assessment of accuracy which takes into account records submitted by farmers. It is updated yearly with crop maps available in the Autumn for that particular year.

4.3.1 Methods

The first objective is to evaluate the different risk factor variables within each environmental layer given in Table 4.1. This can be done in the ArcGIS environment (ESRI 2021) where each vector layer is cross tabulated with the pipeline route. As slope data is in raster format the zonal statistics tool was used to evaluate the minimum, mean, maximum and standard deviation of the slope along the pipeline route. The results from this will show how many variables are within each environmental class and a rank can be made for soil erosion risk based on the risk of a variable exposed to bare soil conditions. In the case of slope degrees the soil erosion risk is based on how steep a slope is. The soil erosion risk is based on the ranking system of 1 =low, 2 = medium and 3 = high in relation to slope, land cover and soil texture.

$$RF = LC * S * SG * C \quad (4.1)$$

Equation 4.1 gives a simple qualitative combined Risk Factor(RF) based on Land cover (LC), Slope degree (S), Soil group based on soil parent material (SG) and Crop type (C). This equation is loosely based on the RUSLE equation 2.2 given in the literature review to give a simple indicator of where risk factors are co-located.

4.3.2 G.I.S analysis

The GIS analysis was processed in two parts which is shown in Figure 4.2. The first step was to evaluate the environment along the pipeline route using the cross tabulation tool for vector data (Land cover, soil texture and crop type). The zonal

tool was used to evaluate raster for the pipeline route. The second step of the analysis required all layers to be converted into raster format. The attributes in each layer were then assigned a rank value based on the likelihood of erosion assuming the area is bare. In the case of crop cover, rationale was based on reduced vegetation cover according to season. Rankings are based on low = 1, medium = 2 and high = 3 values and a raster calculation was made using these risk values.

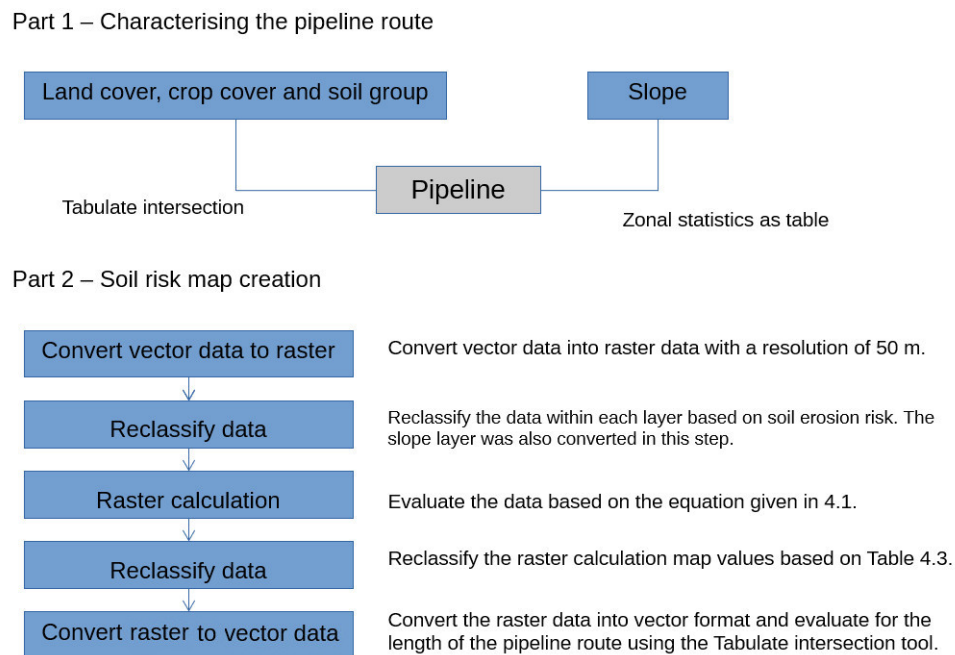


Figure 4.2: GIS analysis methodology for assessing the characteristics of the pipeline route and calculating the soil erosion risk map

4.4 Results

4.4.1 Environment along the pipeline route

Slope is classified based on the classification from Lilly (2018) that is based on soil erosion risk for Scotland. The total length of the pipeline that transects the East of Scotland totals 1611 km. Table 4.2 illustrates that 1330 km of the pipeline is routed in flat terrain. The results from the pipeline route were evaluated as a range from 0 degrees to 22 degrees. The mean value is 3 degrees across this pipeline route with a standard deviation of 3 degrees. Therefore the majority of the pipeline corridor is situated in gentle terrain and is classified as low risk.

Table 4.2: The length of the pipeline route under different slope classes and soil erosion rank.

Slope class	Degrees	Pipeline length (km)	Rank
Almost flat	0 - 2	669	1
Gentle	3 - 5	661	1
Moderate	6 - 10	238	2
Moderately steep	11 - 18	42	3
Steep	18	1	3

Table 4.3 shows the evaluated land cover lengths. The data, based on 2015 surveying, shows that the majority of pipeline consists of arable, horticulture and improved grassland. When evaluating soil erosion risk, the more vulnerable areas are arable and horticulture, bog, freshwater, littoral and saltwater landscapes which total 758 km of the route. Highest soil erosion risk for land cover is based on published literature that recognises water erosion risk for arable land cover (Watson & Evans 2007, Batey 2015), bog and peat cover (Grieve et al. 1995) and pipeline exposure to water (Sawatsky et al. 1998). Improved grassland may have erosion risks (Rickson et al. 2019) as well as woodland areas which have been cleared for pipeline installation, therefore these areas have been given a moderate risk category. Low risk environments were given to urban and suburban areas.

Table 4.3: Land cover results for the pipeline route and soil erosion rank.

Land cover type	Length along pipeline (km)	Rank
Arable and horticulture	739.9	3
Improved grassland	508.3	2
Coniferous woodland	109.1	2
Acid grassland	96.7	2
Broadleaf woodland	57.6	2
Heather grassland	44.4	1
Heather	29.8	1
Bog	15.2	3
Suburban	3.6	1
Supralittoral sediment	2.3	3
Urban	1.5	1
Freshwater	1.4	3
Inland rock	0.8	1
Saltmarsh	0.3	2
Littoral sediment	0.2	3
Saltwater	0.1	3
Fen, marsh and swamp	0.0	1

Soil texture is influential in soil risk erosion as the ratio between sand, silt and clay, can change how likely a soil is to erode along with organic matter content. The soil

texture triangle, shown in Figure 4.3, gives an approximation of the combination of sand, silt and clay in a soil shown in Table 4.4. The British Geological Survey Soil Parent Material Dataset associates soil group is based on a classification system given by the Department for Environment, Food and Rural Affairs (DEFRA). Table 4.4 shows that the majority of the soils in this region are light to medium in soil texture. Soils erosion risk depends on many factors including vegetation coverage and compaction that can risk soil erosion. Therefore the lightest soils have been classified as high risk for soil erosion whilst medium silty to heavy soils are at medium to low risk (DEFRA 2010).

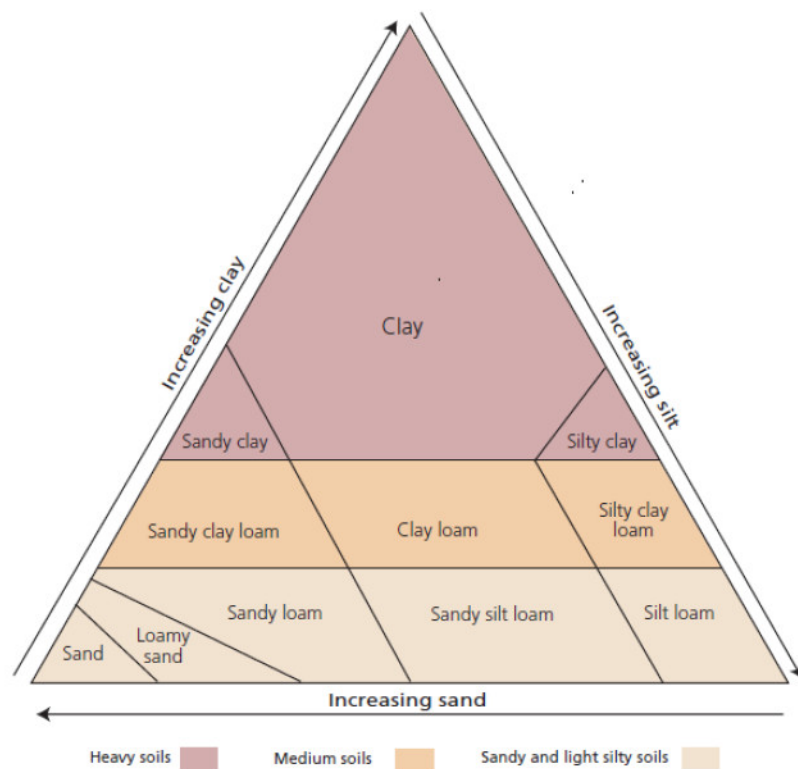
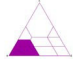



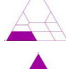
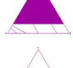


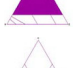
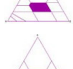

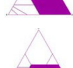



Figure 4.3: A simplified Soil texture triangle which give associated names of soil according to the percentage of sand, silt and clay. (DEFRA 2010)

Table 4.4: Soil group results for the pipeline route. Soil triangle imagery defined by Lawley (2011a).

Soil group (DEFRA classification)	Length along pipeline (km)	Texture triangle	Rank
Light (sandy) to medium (sandy)	869.0		3
Light	272.3		3
All	258.3		2
Heavy to medium (sandy) to light (sandy)	198.6		3
Light (sandy)	171.2		3
Medium to heavy	56.4		2
Light to medium	31.2		3
Medium (silty) to heavy	18.8		2
Heavy to medium	7.4		2
Medium	7.1		2
Medium to light (silty)	6.8		2
Light (silty) to medium (silty) to heavy	2.8		2
Light (silty) to medium (silty)	0.9		2
Not classified	0.3	N/A	1

4.4.2 Changes in crops grown during 2015 to 2019

Fallow (bare) soil is at greatest risk of erosion, as are newly drilled seed beds that give rise to seasonal risks that differ between crops. The total length of crops identified along the pipeline route ranges from 1120 km to 1131 km (70%) of the pipeline route. Table 4.5 shows the change in crops along the pipeline route which is given as length (km). Grass constitutes the majority of the crop data, which does not normally pose a large soil erosion risk. The most notable change in crop cover comes from a shift for spring wheat to spring barley, where the latter become the second highest share of crop cover by 2019. Winter Wheat remains consistent as well as oilseed rape, and potatoes. Risk is categorised by the seasonal likelihood of bare soil cover being vulnerable to intense rainfall conditions. Winter cereals, field beans and oilseed rape drilled in October pose a high risk for soil erosion during the crop establishment in autumn and early winter (Boardman 2013). These crops have been given a high risk value of 3, whilst all other crop types are given a low value of 1. Soil left fallow during rotations is not

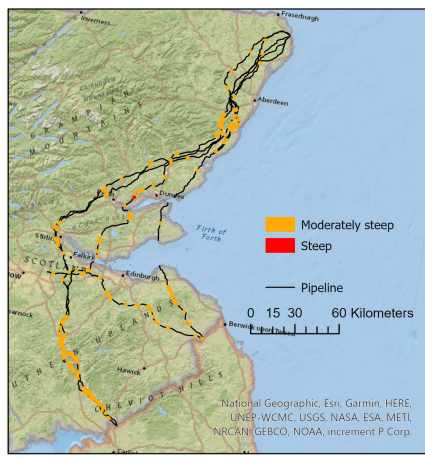
specifically identified in the crop classification, but would be vulnerable to erosion.

Table 4.5: Crop cover type change along the length of the pipeline route. Winter oats were included in Winter wheat statistics prior to 2019.

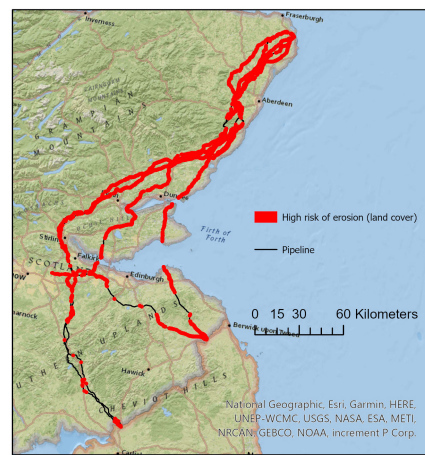
Crop type	Length along pipeline (km)				Planting month	Harvest month
	2016	2017	2018	2019		
Grass	528.8	473.1	502.1	460.3		
Spring wheat	250.1	171.5	42.1	31.5	February to March	July to September
Winter wheat	100.7	107.2	115.9	130.7	October to December	June to August
Other crops	77.0	64.7	56.7	60.7		
Spring barley	57.1	145.2	251.3	252.6	February to March	July to September
Winter barley	46.2	50.7	56.5	72.0	October to December	June to August
Oilseed rape	37.0	49.9	41.6	44.3	August to September	June
Potatoes	25.2	45.8	33.4	42.2	April	August to October
Field beans	7.4	6.3	2.7	7.4	September to October	
Maize	1.4	6.6	18.3		February to May	September to December
Peas				10.8		
Winter oats*				8.2		

4.4.3 Identifying points of high risk

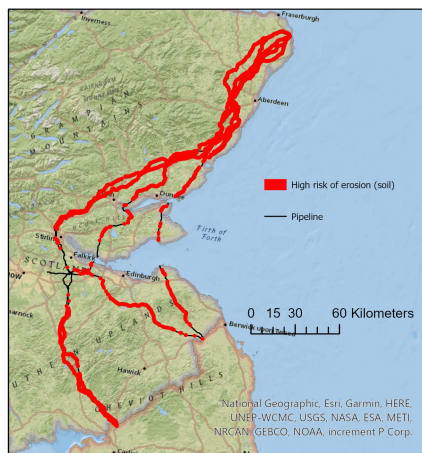
Figure 4.4 is the map which displays the points along the pipeline route which were classified as high risk based. It can be seen that the majority of the points identified as high risk are located in the north of the pipeline route between Leuchars and Dyce. The EU soil data centre erosion RUSLE risk dataset was evaluated along the pipeline route and the values ranged from 0 t/ha/yr to 29 t/ha/yr. The data were separated into 4 equal categories and points were mapped according to the highest risk category which had values between 23 t/ha/yr to 29 t/ha/yr. On Figure 4.4a these show at 3 points near the Eskdalemuir region. In contrast, there were 4 points which were identified as high risk in this region which has typical high rainfall rates.



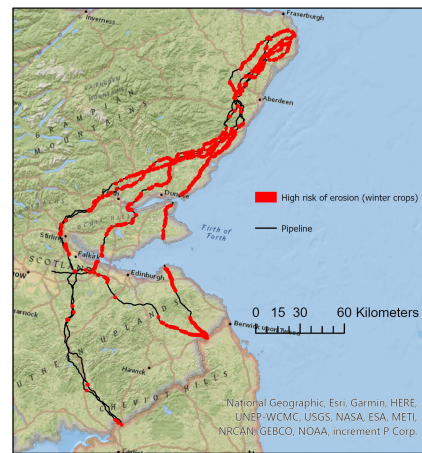
(a) Slope soil erosion risk factor,



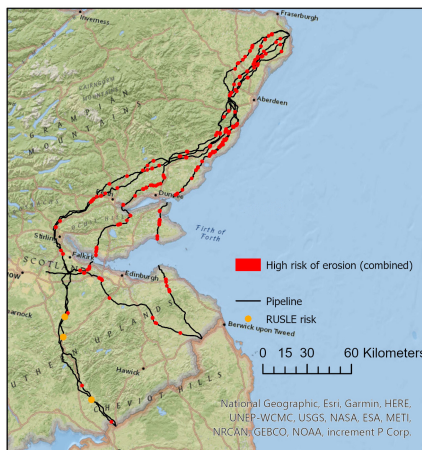
(b) Land cover soil erosion risk factor.



(c) Soil texture risk factor.



(d) Crops at risk during winter.



(e) Combined soil erosion risk map based on equation 4.1 also showing rates identified as high risk by Panagos et al. (2015)

Figure 4.4: Constructed soil erosion risk maps of (a) A slope risk map which illustrates spatially the moderate and steeply moderate slope class along the pipeline route. (b) A spatial map which illustrates the highest risk category based on land cover classification. (c) A spatial map which illustrates the highest risk category based on soil texture. (d) A spatial map which illustrates the highest risk category based on winter susceptibility to soil erosion. (e) Soil erosion risk map showing both combined risk (excluding rainfall) and the EU erosion risk including rainfall (Panagos et al. 2015). Created in ArcPro (ESRI 2021) using base map imagery from (National Geographic World Map 2011).

The length of the pipeline evaluated to be at risk from Figure 4.4 (e) and given in Table 4.3 shows that 169 km of the pipeline corridor is mainly situated in the North of where the majority of the crop and land cover is sown. However, the Eskdalemuir region is not represented in this spatial data.

Table 4.6: The length of pipeline evaluated to be at risk.

Risk category	Length of pipeline (km)
Low - 1	459
Moderate - 2	496
High - 3	169

4.5 Discussion

4.5.1 Land cover and crop change

The benefit of using GIS to analyse quantities of soil erosion risk is that it is simple, efficient and cost effective for identifying large areas of spatial information. The GIS environment has been used to identify risk along pipeline routes including geotechnical hazards (Augusto et al. 2010), ground cover restoration (Bayramov et al. 2016), earthquake mapping (Borfecchia et al. 2015) and soil erosion (Bayramov et al. 2019, Winning & Hann 2014). In this chapter, the GIS environment was used to evaluate the characteristic of the pipeline and for using detailed crop data to identify seasonal areas of erosion. The majority of the pipeline route is situated in land cover that is dominated by arable, horticulture and improved grassland. Whilst most of the pipeline route is situated in flat or gently sloping terrain that is of relatively low risk of soil erosion by water, there is debate in the literature as to the extent of how vulnerable arable areas are to soil erosion by water. The longer term study by Watson & Evans (2007) suggests cereal and oilseed rape were commonly eroded due to winter rainfall storms, whilst Frost & Speirs (1996) argue that there is doubt to the extent of erosion in land cover that is classified as arable. The findings in Table 4.7 evaluated that a substantial portion of the route is arable and traditionally classified as vulnerable, however the recent addition of crop data means spatial data identifying specific crop types can improve the accuracy of seasonal risk mapping.

Table 4.7: Literature concerning soil erosion risk in the region of East Scotland

Year	Location	Detail	Cause	Reference
1993	Strathearn	Erosion was observed on fields with ploughed land and sown autumn cereals	Severe weather conditions during January 1993	(Davidson & Harrison 1995)
1994	Forfar	Erosion was identified in 58% of surveyed fields. Bare soil worked downslope was most effected.	Rainfall in excess of 50 mm/day	(Kirkbride & Reeves 1993)
1995	Southern Uplands	Sampled areas identified peat erosion	Land management: draining, grazing and moorland burning.	(Grieve et al. 1995)
1996	East Lothian	Examined soil erosion after an intense rainfall event in an area with varying topography and arable land cover. Authors found 10 fields out of 265 which were recorded as eroded. Authors doubt risk between arable land and soil erosion.	N/A	(Frost & Speirs 1996)
2006	East Scotland	Authors argue that soil erosion is limited to small areas, but overall no widespread soil erosion issue.	Authors suggest that climate change and an increase in storm events may accelerate soil erosion	(Towers et al. 2006)
1985-2007	East Scotland	A combination of quantitative and qualitative surveys over a 22 year period showed in some years with oilseed rape and cereals being frequently eroded.	Winter precipitation and heavy rainfall	(Watson & Evans 2007)

4.5.2 Identification of vulnerable areas

Between 1113 km and 1120 km of the pipeline route was evaluated in the crop dataset. This study showed that over a four year period (2016 to 2019) there was a change in crop types grown along the length of the pipeline. Winter barley steadily increased over the period, it was seen in Table 4.5 that spring wheat and barley shifted in the share of the pipeline route. In contrast to land cover, the crop dataset requires constant updating as fields are often rotated (Gabriels 2003) and the decision of what to sow is driven primarily by economic decisions (Agriculture and Horticulture Development Board 2019). Therefore, this shows potential for conflict between land owners economic decisions and pipeline operators necessity to protect soil cover. Larger areas of arable crops vulnerable to erosion risk during the winter are situated in the north where the frequency of intense rainfall events is often only a small fraction of that in the Southern Uplands (Chapter 3). The data presented in Chapter 3 established that during the winter period there were few heavy rainfall events for Dyce and Leuchars, however Kirkbride & Reeves (1993) observed fields eroded by low intensity rainfall events in Forfar and Angus. In contrast, the points for the RUSLE erosion risk map (Panagos et al. 2015) identified the region near Eskdalemuir as potential for high erosion rates associated with the more intense rainfall and steeper slopes in this area.

The more detailed information on seasonal crop data from CEH provides an opportunity to improve the accuracy of seasonal risk mapping for erosion along the pipeline route.

4.5.3 Improving soil erosion mapping for pipelines

To improve the accuracy of soil erosion risk maps specialising in the pipeline environment there needs to be accurate ground-truth spatial information which details where erosion has taken place historically. The inclusion of crop data is a welcome step for improving soil erosion risk mapping, however ground-truth data needs to be used for verifying where the erosion has previously occurred (Winning & Hann 2014, Xiao et al. 2016). Modelling using the RUSLE equation comes with challenges regarding the accuracy of predicting where erosion risk are present (Alewell et al. 2019), together with issues regarding its use at a large scale (Evans & Boardman 2016). The analysis in this chapter identified crop patterns shifting over a four year period, which means that there needs to be regular erosion risk mapping based on the location of cropped fields, together with an appreciation that heavy rainfall events vary greatly from year to year with increasing frequency in some areas and seasons. An alternative would be to identify known areas of soil erosion along pipeline routes and construct statistical risk models based on historical and spatial datasets, though the lack of ground-truth data currently limits this approach. It must be remembered that, in the case of soil erosion above pipelines, even a few metres length of substantial erosion along a pipeline corridor could trigger a very expensive failure.

4.6 Conclusion

In north-east Scotland, the pipeline route is situated in land cover that is mainly grass, which has a low erosion rate, and in arable and horticulture land cover. This has the potential to be vulnerable to soil erosion by water for areas where vegetation cover is reduced. The addition of the crop cover plus data offers the opportunity for more detailed seasonal assessment and mapping of soil erosion risks. Maps of slope, soil type and vegetation cover show the main erosion risk factors along the pipeline route in relation to the occurrence of intense rainfall events. In the north of the region, the areas identified as highest risk are subjected to few intense winter precipitation events in contrast to the southern section of the pipeline. However, even if a small area of an individual field is subjected to multiple erosion events which can reduce the soil cover then the pipeline may be at risk of failure. Satellite-based (InSar) ground displacement data offers the potential to map areas where the ground has been eroded along a pipeline route and this is

considered in Chapter 5.

Chapter 5

Estimating ground surface displacement along a hydrocarbon pipeline in Scotland

5.1 Introduction

Satellite missions were originally launched as military applications during the mid-twentieth century (Xue. et al. 2008). Technological advances and the ability of satellites to monitor the Earth means that civilian applications are the main satellite missions of today (Kramer & Cracknell 2008). The launch of NASA LandSat and MODIS (Aqua and Terra) gave the opportunity to monitor the Earth frequently but at low spatial resolution (300m-500m) (Li & Roy 2017). The most recent Sentinel missions launched in 2014 by the European Space Agency (ESA) improved on the temporal and spatial resolution with revisit time of 6-12 days and temporal resolution is of 10m (Malenovsky et al. 2012). Key applications for remotely sensed data include land based management systems and the monitoring of geohazards including earthquakes (Malinowska et al. 2018, Tralli et al. 2005, Polcari et al. 2016) and landslides (Cigna & Tapete 2021) using both optical and InSar (Interferometric Synthetic Aperture radar) radar imagery.

The possibility of utilising ground surface displacement technology for monitoring pipeline routes is attractive as satellite data can cover a large area at modest cost (Sims & Riedmann n.d., Hole et al. 2011). The main limitations for remote sensing technology is the presence of vegetation and cloud cover (Massonnet et al. 1993) which is widespread in Northern Europe, but not for bare fields where soils are particularly vulnerable to erosion. Ground surface displacement is the change in the ground surface height, and is often caused by external influences including soil erosion. This chapter uses InSar ground surface monitoring technology along a pipeline corridor that experiences high rates of rainfall and is generally well vegetated.

5.1.1 Interferometric synthetic-aperture radar

Interferometric synthetic-aperture radar (InSar) is a technique based on radar technology used in geodesy and remote sensing. One of the main applications for this technique is to measure ground displacement on the earth's surface to within mm (Malenovsky et al. 2012). Ground surface displacement is measured as either a positive value (towards the satellite) or a negative value (away from the satellite) and has the potential to identify areas of instability using Differential Interferometry of images from two separate acquisition dates (European Space Agency 2020b). To measure ground displacement over a continuous period there needs to be suitable remote sensing imagery with a constant revisit period with the radar technology being used. The launch of Sentinel-1a in 2014 and Sentinel-1b in 2016 has given the ability to download remotely sensed imagery with acceptable spatial resolution and temporal resolution (from 6 to 12 days revisit time). This opened the possibility of Differential Interferometry in the UK for the Earth observation community (Malenovsky et al. 2012).

5.1.2 Aims and objectives

The aim of this chapter is to present a case study for analysing ground displacement along the national gas pipeline in Scotland, an area where optical imagery is often unavailable due to cloud cover. If successful then InSar would allow changes in the ground surface to be identified and their association with potentially erosive rainfall events to be assessed at a more accurate temporal and spatial scale.

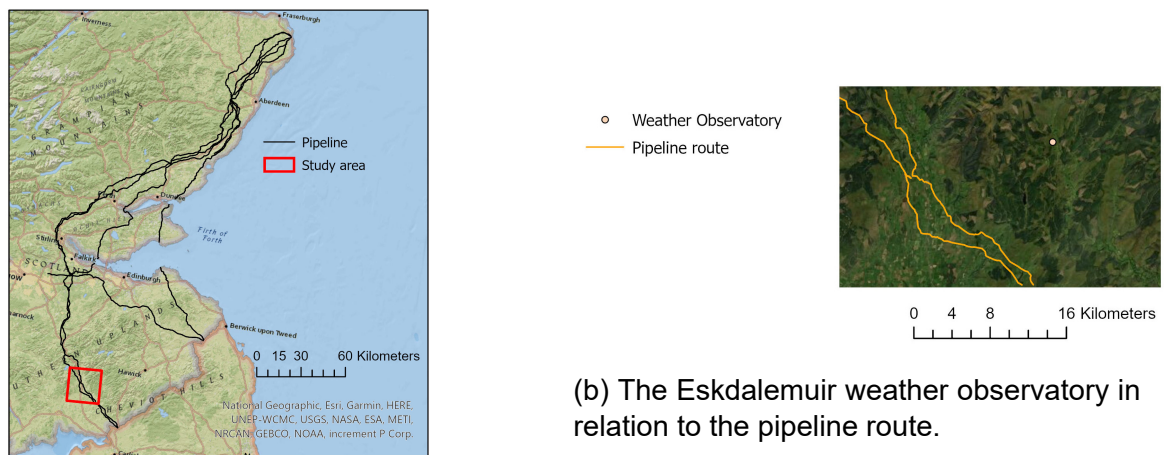
The objectives are to:

1. Ensure that the image processing was carried out correctly by completing the Interferometry tutorial published by Braun & Veci (2021).
2. Process the data at a test site where ground displacement is not expected to change (Eskdalemuir Weather Observatory).
3. Process interferogram images for the winter period between 2015 to 2018 along the pipeline route and evaluate ground displacement.
4. Split the ground displacement data into two zones; the immediate pipeline zone (5m either side of the pipeline), and outer zone (from 5m to 50m either side of the immediate pipeline zone). Compare the ground displacement data in relation to soil texture, land cover and slope.

5.1.3 Study area and reference site

The study area is the National Grid gas pipeline route near Eskdalemuir in Scotland (Figure 5.1) where intense rainfall events have been observed (Chapter 3)

and risk of erosion noted (Chapter 4). Shown in Figure 5.1b, the two National Gas pipelines run adjacent throughout the area, each having a length approximately 35km for this study area. The reference site used to assess this technique for this chapter is the Eskdalemuir Weather Observatory (55°18'44"N, 3°12'22"W) as negligible ground displacement is expected at this location. This region is known for higher than average rainfall rates (Svensson & Jakob 2002) which has the potential for soil erosion by water where pipelines buried in the area could be vulnerable to such risk (Batey 2015). The majority land cover of this study area is improved grassland, with light sandy soil texture and relatively little arable agriculture. The number of heavy rainfall events is shown in Table 5.1, where storm Desmond and unusual conditions over a period of one month, increased the number of heavy rainfall events in December 2015 (van Oldenborgh et al. 2015).



(a) The study area along the pipeline route.

(b) The Eskdalemuir weather observatory in relation to the pipeline route.

Figure 5.1: The study area for evaluating ground displacement. Maps create with ESRI (2018)

Table 5.1: The number of heavy ($\geq 4\text{mm/hr}$) rainfall events recorded at Eskdalemuir weather station. Data obtained via MIDAS (see Chapter 3)

Winter period	Number of heavy rainfall events ($\geq 4\text{mm/hr}$)
2015-2016	29
2016-2017	7
2017-2018	10
2018-2019	16

5.1.4 Pipeline slope profile

The slope map is presented in Figure 5.2 together with the slope profiles. Whilst pipelines are required to be buried in ground which is relatively flat, this can be

a challenge when planning routes in upland terrain. It can be seen in Figure 5.2 that each pipeline runs in undulating terrain, as is shown in the slope profiles.

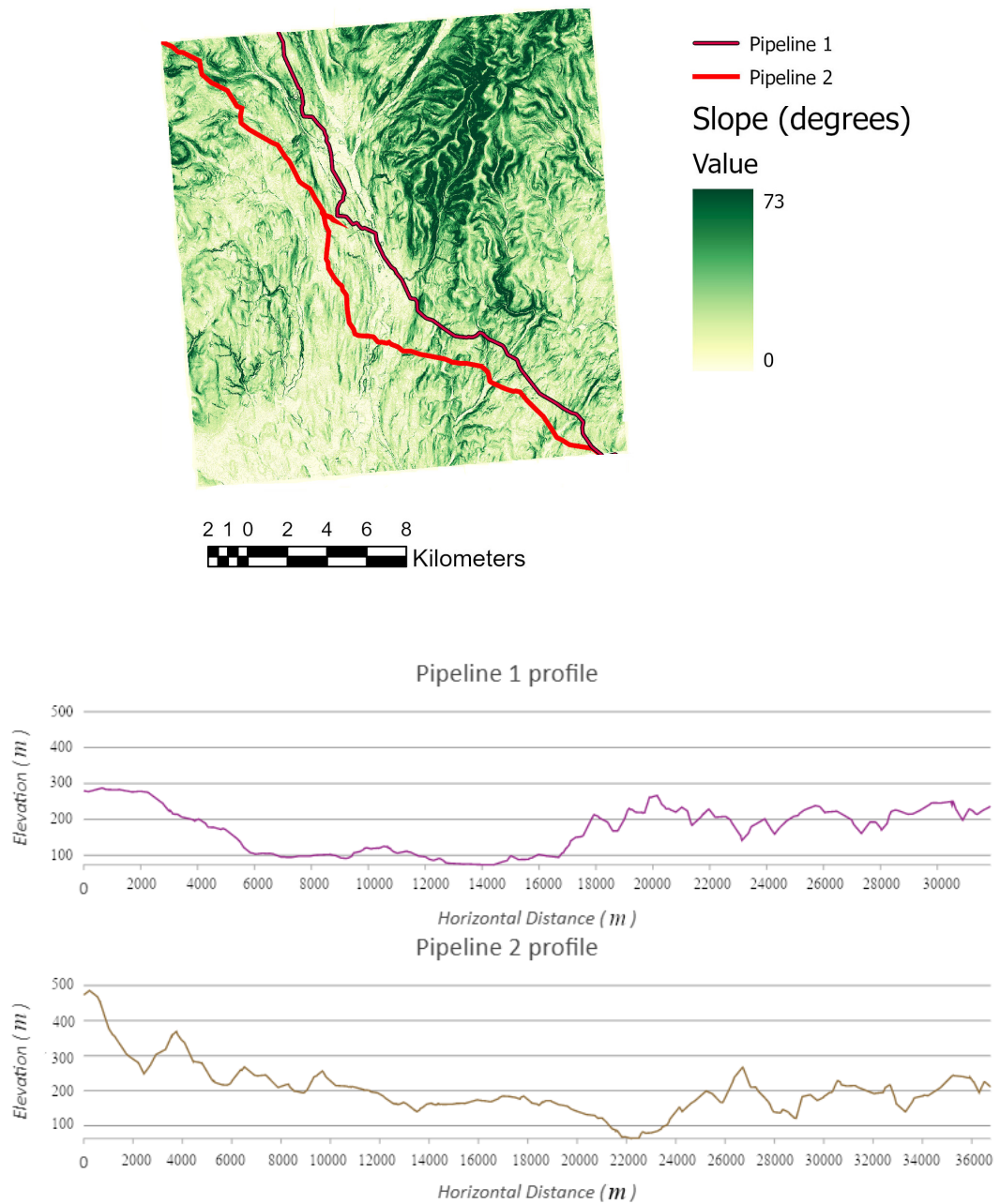


Figure 5.2: The slope map of the route (in metres), and the elevation profiles of the Gas transmission pipelines that transect the region near Eskdalemuir.

5.2 Data sources, software and methods

5.2.1 Database sources and software

Table 5.2 shows the data sources and software used. Each period studied required around 14-17 remotely sensed images for processing. Prior to the pro-

cessing of the ground displacement data, the digital elevation model (DEM), soil parent and land cover datasets were prepared in the ArcPro GIS environment. The pipeline data were buffered (50m either side) along the pipeline corridor and a fishnet sampling technique was used to sample the corridor every 20m totalling 15189 sampling points locations. The DEM, soil parent and land cover datasets were resampled to 10m x 10m to collocate with the sentinel-1 data. Further details of the Sentinel-1 data used for this project can be found in Appendix E.

Table 5.2: Data, software and references which were used in relation to the ground displacement analysis.

Data	Type	Reference
Sentinel-1 imagery	InSar C-Band imagery	(European Space Agency 2020a)
National grid gas pipeline	Vector file	(National Grid 2018)
Land cover	Environmental data	(Centre for Ecology and Hydrology 2017a)
DEM	Digital elevation model	(Ordnance Survey 2018)
BGS Soil parent	Soil texture	(Lawley 2011b)
Software		
SNAP	Software for image processing	(European Space Agency 2020b)
SNAPHU	Software to unwrap images	(Chen 2020)
ArcPro	G.I.S. software for spatial analysis	(ESRI 2021)

Processing each image pair

Figure 5.3 shows the work flow of processing each image pair using the SNAP software. The process works by stacking a pair of images on top of each other where the earlier (by date) is known as the reference image and the later is known as a secondary. This creates one stacked image from which the software produces an interferogram (with a separate coherence layer). The most important step in this processing is the unwrapping of the image which converts the pixels into radians that can then be evaluated to displacement velocities. Unwrapping is a process that may result in errors therefore each image is quality checked for errors. The image then undergoes terrain correction and the final check is to mitigate any offset that occurred during image processing.

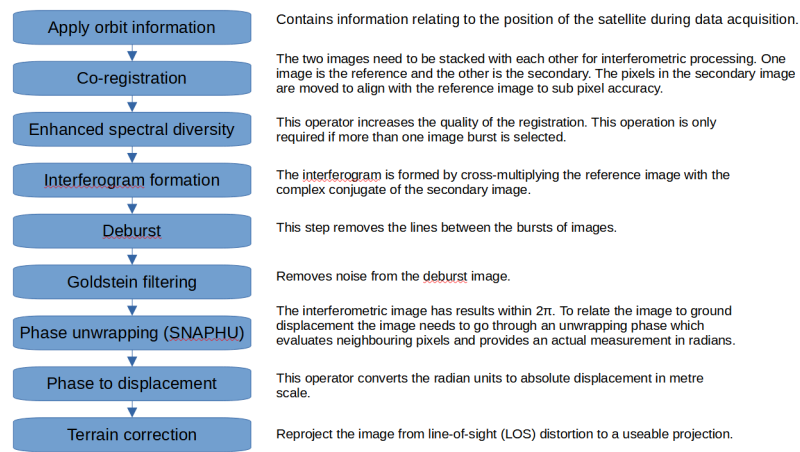


Figure 5.3: The workflow of processing two Sentinel-1 image pairs into one single stacked image

GIS analysis

To represent the pipeline corridor, the area was divided into sample points 20 metres apart totalling 15189 sample points along the pipeline route. These points were then separated into zones representing locations close to the physical pipeline and location in the outer pipeline zone (Figure 5.4). The images were then imported into the ArcGIS environment where soil texture, land cover and slope environmental layers were imported into the environment and the sample tool was used to evaluate the value of each coherence, displacement and environment layer to a pipeline sample point. Each image pair had corresponding coherence layer and only pixels with a coherence ≥ 0.6 were accepted. Rstudio and R code were used to analyse the data for each sample point location across the ground displacement images to evaluate if any spatial patterns occurred.

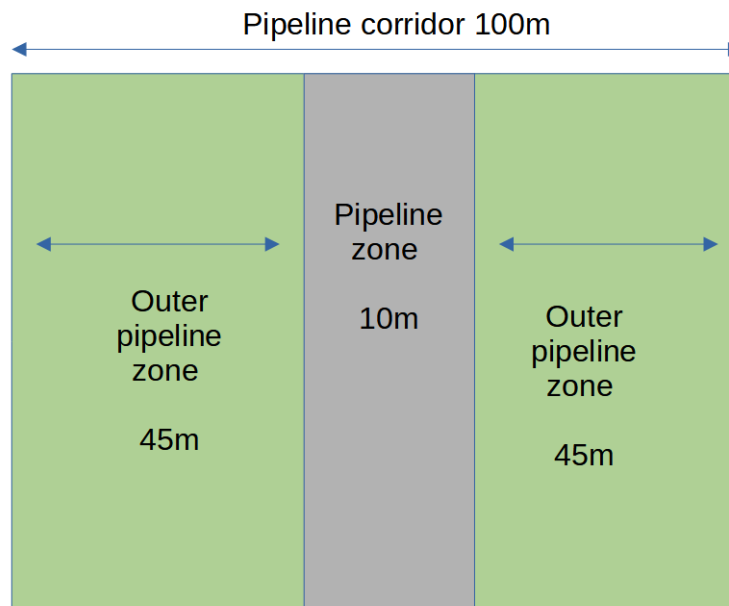


Figure 5.4: A diagram defining the pipeline zone and the outer zone. Not to scale.

The pipeline goes over various soils which are classed in the following table. The Department for Environment, Food and Rural Affairs (DEFRA) soil classes were used for simplicity. Table 5.3 gives information on the equivalent soil textures.

Table 5.3: DEFRA and soil texture equivalent. Further information on how soils are classified can be found in Lawley (2011b)

Defra class	Soil texture equivalent	Texture triangle
Light (sandy)	Sandy soils	
Light (sandy) to medium (sandy)	Sandy loam to sandy clay loam	
Light	Sandy and loamy soils (minimal clay)	
Light to Medium	Sandy to clayey silty loams (minimum 20% sand)	
Medium	Clay loam	
Medium (silty) to light (silty)	Clayey to silty loams	
All	Mixture of Sand, Silt and Clay	

5.3 Results

5.3.1 Data processing

Table 5.4 shows a total of 54 images across four years that were processed for this project. After quality checking each image for errors, there were 13 images which could not be used further due to error in images after the unwrapping phase. From the remaining 41 images, 27 required offsetting where 14 images did not require altering. The break down of post processing offsetting is given in Table 5.4.

Table 5.4: The number of images processed for each year's autumn and winter period. Defect image is defined by the image not being suitable for further processing due to unusual raster imagery. If an image was found not to be defect then it was checked for offsetting errors.

Year	Defect image	Offset required	No offset required	Total images
2015	3	6	4	13
2016	5	6	3	14
2017	5	6	3	14
2018	0	9	4	13
Total	13	27	14	54

The offset of the image were determined by rational user judgement according to criteria in Braun & Veci (2021). Table 5.5 gives the range of values which were used for offsetting. The SNAP software evaluates ground displacement in metres and the offset values are given in the same unit. When converted the range is between 10 mm to 50 mm and a total of 18 images from 41 required offsetting.

Table 5.5: The offsetting range is determined by rational user judgement and is adjusted based on the following tutorial by Braun & Veci (2021).

Year	Offset range (m)
2015	0.01 - 0.02
2016	0.01 - 0.04
2017	0.025
2018	0.01 - 0.05

5.3.2 Weather station - reference point fro all image for all image pairs

The Eskdalemuir weather observatory provided a reference point for the data. The site has a small area and each sample location was mapped to either a building, a field or a vegetated area. Figure 5.5 shows a box plot giving the distribution of ground displacement to each mapped category and shows little difference in

the data with the median close to 0mm. The minimum and maximum values are -20mm and 20mm respectively.

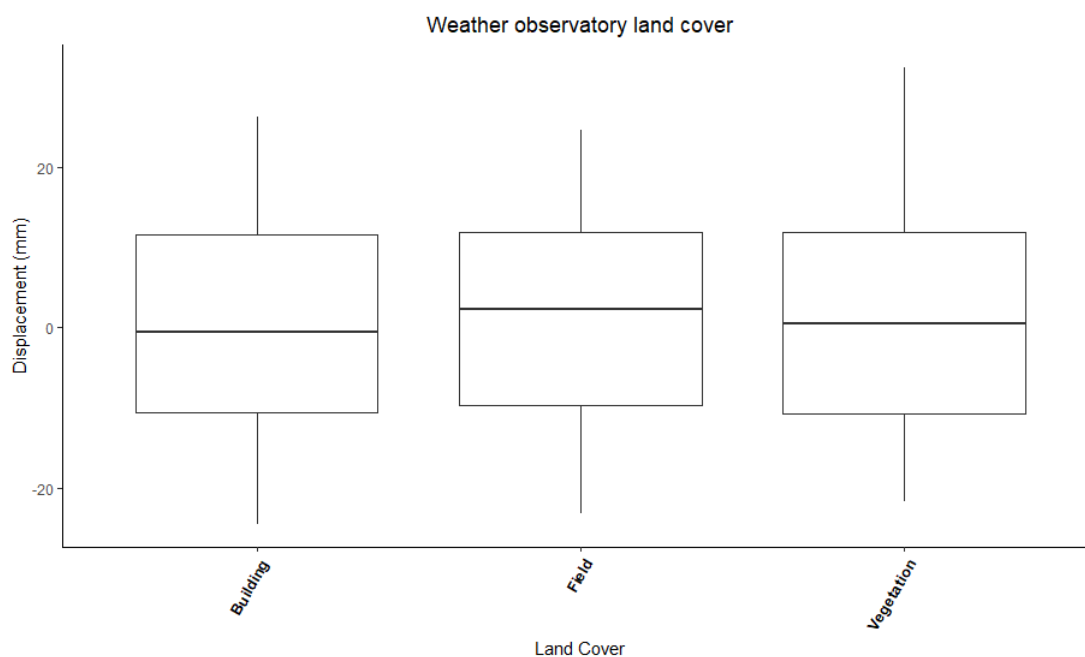


Figure 5.5: The ground displacement values for each land category at the Eskdalemuir weather station.

5.3.3 Pipeline corridor

The total length of the pipeline route totals 63 km. Table 5.6 displays that 36 km of the pipeline route is in moderate to steep elevated conditions. In addition to Table 4.2 this area represented the steeper slope classes across the pipeline corridor in Scotland.

Table 5.6: The length of the pipeline route under different slope classes in the study area (Eskdalemuir)

Slope class	Degrees	Pipeline length (km)
Almost flat	0 - 2	15
Gentle	3 - 5	12
Moderate	6 - 10	26
Moderately steep	11 - 18	9
Steep	>18	1

There was a total number of 15189 sample points representing the pipeline corridor. After G.I.S processing there was a total of 13968 sample points that registered ground displacement values. From these 13968 points 1401 locations were in the immediate pipeline zone and 12567 were the outer zone. Table 5.8 shows that the majority pipeline is situated in improved grassland which is a com-

mon habitat that contains common perennial grasses that lack winter senescence (Centre for Ecology and Hydrology 2017a).

Table 5.7: The number of pipeline sample locations that were evaluated into each soil class.

Soil class	Pipeline corridor	Pipeline zone	Outer zone
Light (sandy)	348	36	312
Light (sandy) to medium (sandy)	1897	186	1711
Light	7905	800	7105
Light to medium	942	100	842
Medium	17		17
Medium (silty) to light (silty)	12		
All	2847	279	2580

Table 5.8: The number of sample points for each land cover classification and within each zone of the pipeline corridor. The area around Eskdalemuir is mainly classified as grassland.

Land cover	Pipeline corridor	Pipeline zone	Outer zone
Improved grassland	8310	858	7452
Acid grassland	2920	315	2605
Coniferous woodland	1876	164	1712
Broadleaf woodland	396	24	372
Arable and horticulture	229	19	210
Inland rock	97	10	85
Suburban	88	7	81
Heather grassland	24	2	22
Bog	22	2	20
Freshwater	5		5
Urban	3		3

The coherence dataset that are produced with the ground displacement images give an indication as to how much vegetation may be on the ground surface to render data suitable for displacement analysis. A high coherence reading indicates bare ground whilst a low coherence suggests a vegetated surface. Figure 5.6 show the distribution of coherence for each land cover category and shows that the majority of coherence values were just over the 0.6 threshold. The values appear reasonably consistent with what is expected from the land cover classes with urban areas having greater coherence..

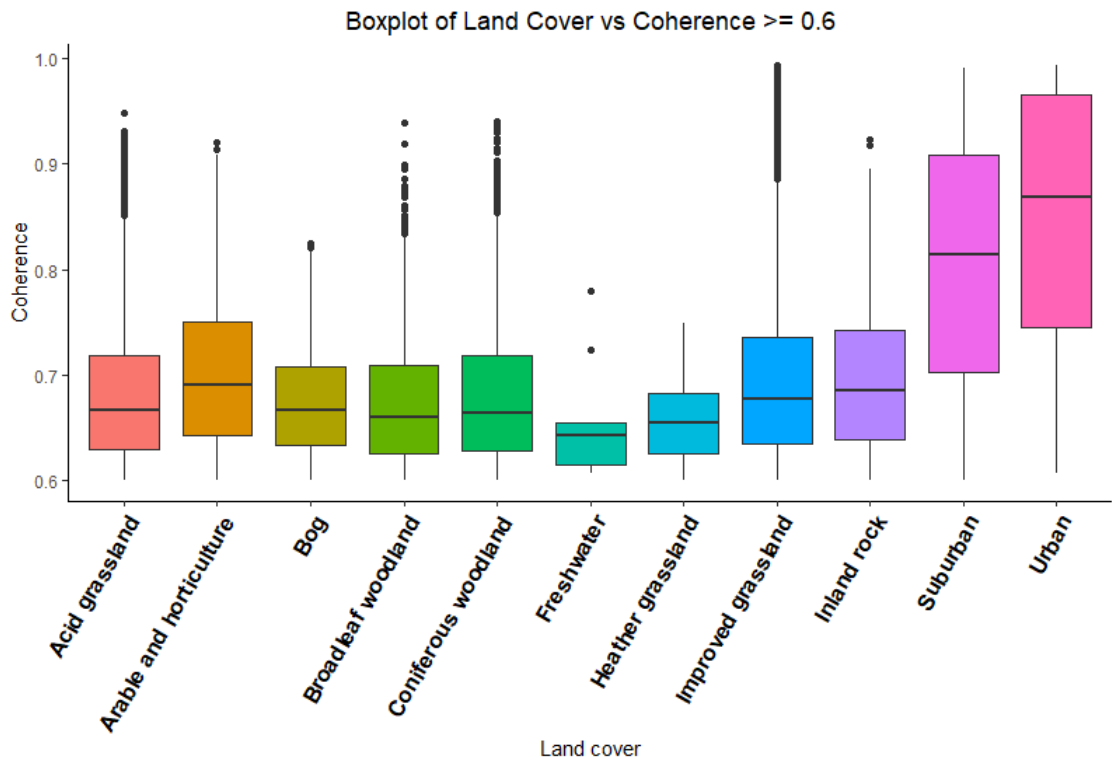


Figure 5.6: The box plots for each land cover classification and its coherence distribution.

Zone comparison

The ground displacement values for Figure 5.7 indicate no difference of ground displacement velocities across each of the pipeline zones. Figure 5.8 shows the box plot distribution for land cover and soil class for each pipeline zone. There was no significant difference in values amongst each class with improved and acid grassland values showing an identical distribution for the pipeline and outer zone. However, there are numerous outliers within each dataset that have the possibility of representing ground displacement $\pm 30mm$.

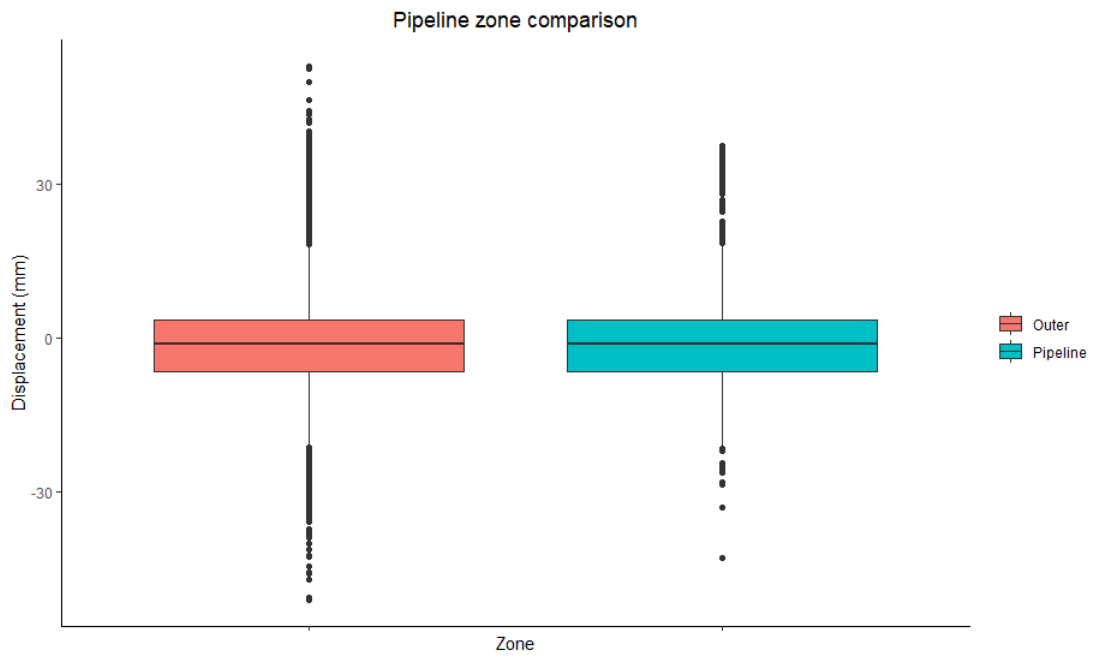


Figure 5.7: The comparison of sample points across both pipeline zones.

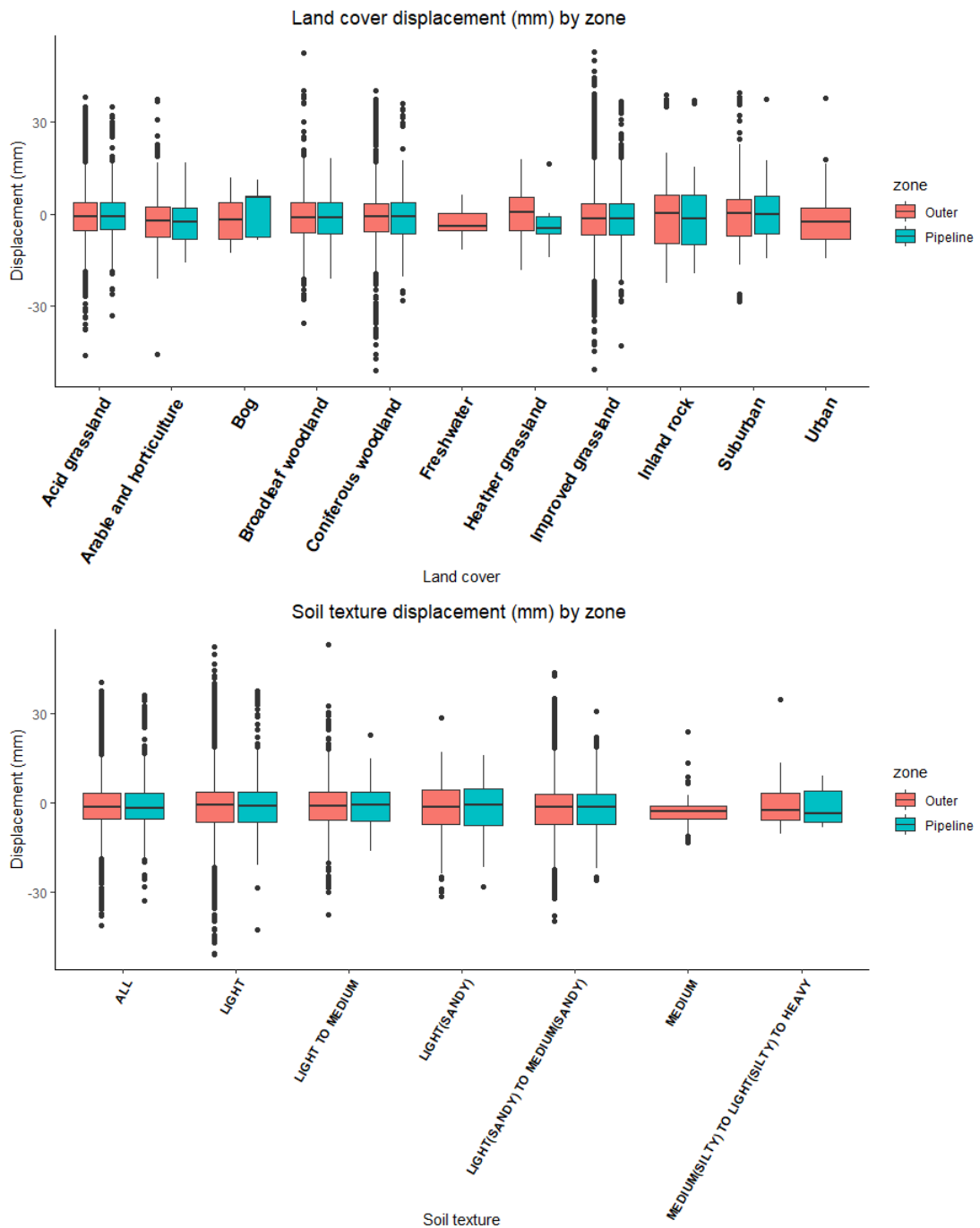
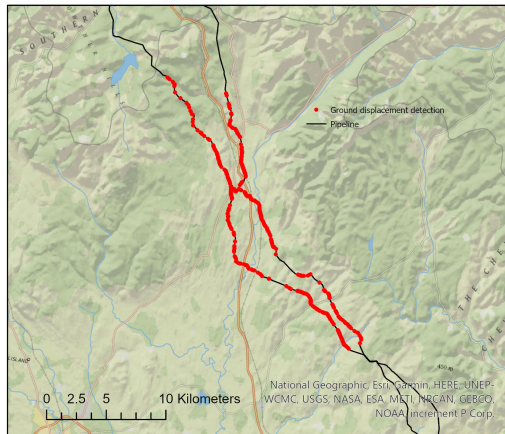


Figure 5.8: Zone comparison of ground displacement for land cover and soil classes

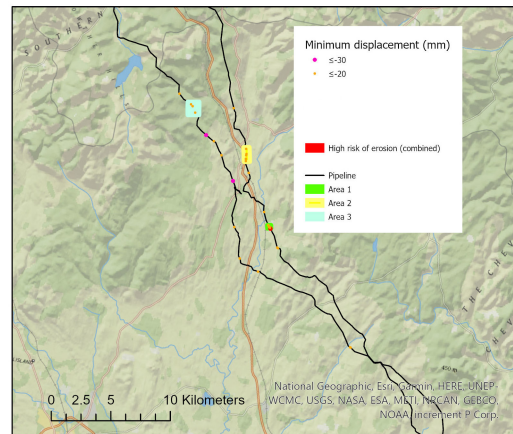
Spatial analysis

Figure 5.9a shows the top 10 percent of the most negative ground displacement values evaluated in the pipeline zone. It illustrates that the lowering of the ground surface is distributed throughout the corridor, which had a range from -43 mm to a maximum of -11 mm and a mean of -14 mm. These values were placed into categories of ground displacement values between -30 mm to -21 mm and -20 mm to -10 mm to determine if there were clusters of ground displacement points. Figure 5.9b shows that there were 3 areas which contained small clusters of points

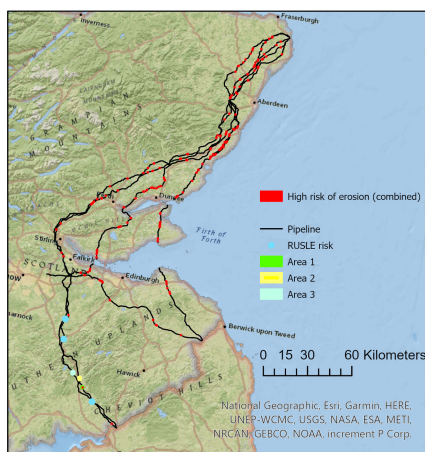
termed Area 1, 2 and 3. These areas were plotted alongside the soil erosion risk data evaluated from Chapter 4. It can be seen from Figure 5.9c that there was one location (Area 1) which co-located with a point that was evaluated in Chapter 4 however, the spatial distribution shown in Figure 5.9a gives an argument for how to include rainfall in risk mapping is important.



(a) Top 10% of lowest ground displacement values.



(b) The locations of areas 1, 2 and 3 which contain small clusters of ground displacement points.



(c) A soil erosion risk map showing risk identified in this chapter and Chapter 4.

Figure 5.9: Constructed soil erosion risk maps of (a) Top 10% of lowest ground displacement values across the study area. (b) The locations of areas 1, 2 and 3 which contain small clusters of ground displacement points. (c) A soil erosion risk map showing winter risk, areas detected in this Chapter, the Winter risk from Chapter 4 and the RUSLE which includes rainfall by Panagos et al. (2015). Created in ArcPro (ESRI 2021) using base map imagery from (National Geographic World Map 2011).

Table 5.9 give detail of the points within each area cluster. Areas 1 and 2 have ground displacement points which are situated on terrain with relatively flat terrain, in sandy soil and improved grassland, which is typical of this region. Area 3 shows possible lowering of the ground surface in mixed soil in coniferous woodland. If

this land cover is accurate then these results could be affected by high vegetation in the area.

Table 5.9: Area statistics

Area	Sample point	Displacement (mm)	Slope (degrees)	Soil texture	Land cover
1	1	-25	6	Light (sandy) to medium (sandy)	Improved grassland
	2	-25	2		
	3	-25	0		
	4	-26	2		
	5	-25	0		
	6	-26	6		
2	1	-21	0	Light (sandy) to medium (sandy)	Improved grassland
	2	-21	0		
	3	-22	0		
	4	-21	0		
	5	-20	0		
	6	-22	5		
3	1	-25	6	All	Coniferous woodland
	2	-26	0		
	3	-28	10		

5.4 Discussion

5.4.1 Challenges and uncertainties in the InSar technique

This chapter used Sentinel-1 InSar image pairs to monitor ground displacement along a selected pipeline route in Scotland. Since the launch of the European Space Agency's sentinel satellites there has been interest in utilising this technology to monitor deformation along hydrocarbon pipeline routes (Bayramov et al. 2020, Sims & Riedmann n.d.). Hole et al. (2011) noted that this technology has the potential to monitor pipelines in challenging environments and Bayramov et al. (2020) demonstrated how this technology can be used to monitor surface deformation along a pipeline route with low vegetation cover. The aim of this chapter has been to use this technology in an area that experiences high rainfall intensities and where cloud cover makes optical imagery challenging. The success of the image processing relies on numerous influences including the quality of the original image, processing technique and atmospheric processes (Wasowski & Bovenga 2014, Strozzi et al. 2018). From a total of 52 image pairs, 11 produced unusable data which hindered continuous data analysis over time due to missing

data. Furthermore, the majority of the images required offsetting, which alters the data based on user judgement unless there is an automated process to handle corrections (Intrieri et al. 2018).

Vegetation in Scotland can hinder successful measurements (Sims & Riedmann n.d., Massonnet et al. 1993). Further uncertainty could be attributed to the coherence values as the majority of the coherence values were just above the threshold of 0.6 which is typical for temperate climates (Fiaschi et al. 2019). The Eskdalemuir weather observatory was used as a reference site where vegetation, buildings and grassed fields were mapped against mean displacement, which was close to zero for all three categories giving some confidence in the method.

5.4.2 Ground displacement along the pipeline route

The top 10% of ground displacement values along the pipeline route showed displacement that ranged from -43 mm to a maximum of -11 mm, with a mean of -14 mm. When these values were categorised it gave the opportunity to identify areas where clusters of ground displacement values could pinpoint locations for further investigation with ground-based monitoring data. There was one area which showed a decreased in ground surface level that was identified high risk in the soil erosion risk map in Chapter 4 and in this Chapter (where Area 1 is). There was no crop data in this area, but the land cover was classified as improved grassland with a maximum slope of 6 degrees and sandy soil texture. Table 5.10 provides information on other literature that has used Sentinel-1 imagery for monitoring surface deformation, which is in a similar range to the velocities found in this study. This technique and the ground displacement results from it have been more widely used in Mediterranean and arid environments where vegetation is relatively sparse. In this study there is uncertainty in applying the method in a vegetated temperate environment, so the values should be treated with some caution.

Table 5.10: Ground displacement velocities observed in a range of previous studies.

Location	Vegetation/area	Velocities (mm/yr)	Reference
Italy	Sparse vegetation and grassland	23	(Cigna & Tapete 2021)
China	Coastal	-30 + 30	(Running et al. 2004)
Azerbaijan	Pipeline corridor	-21.3 and + 14.1	(Bayramov et al. 2020)
Vietnam	Coal mine	14	(Dang et al. 2021)
Argentina	Volcanic complex	20	(Derauw et al. 2020)
Italy	Land subsidence	27	(Ezquerro et al. 2020)
Turkey	Ground deformation	35	(Imamoglu et al. 2019)
Ireland	Landslide	-17	(Fiaschi et al. 2019)
China	Landslide	27	(Intrieri et al. 2018)

5.5 Conclusion and potential use

There is considerable potential for this technique to monitor ground displacement but there needs to be comparison with ground-truth data and observations to establish accuracy of estimates (Bayramov et al. 2020, Strozzi et al. 2018, Carla et al. 2018). The potential spatial and temporal resolutions are of the order of millimetres (Wasowski & Bovenga 2014) which means that large displacements should be easy to identify once the processing of image pairs is becomes error free. However, ground-truth technology needs to be used alongside satellite monitoring to verify the values once a region of interest has been identified.

Chapter 6

Discussion and conclusion

6.1 Results in context

The research presented in this thesis evaluated how to improve soil erosion risk mapping for the oil and gas pipeline industry. It explored changing rainfall patterns and how remote sensing technology could be used to identify areas along the pipeline at risk of soil erosion. Chapter 3 was concerned with the change in rainfall over time. Three weather stations (Dyce, Leuchars and Eskdalemuir) were evaluated for the period 1981 to 2018 and it was concluded that Eskdalemuir experienced more than double the total heavy rainfall total and events than Dyce and Leuchars. Heavy rainfall events ($\geq 4\text{mm/h}$) at Eskdalemuir had a mean value of 30 per year, whilst at Dyce there was a mean value of 11 and 9 precipitation events per year at Leuchars. This split in values across the weather stations is due to the geographic split in rainfall conditions in Scotland which is found in other research work by Afzal et al. (2011) where the results from Chapter 3 can contribute to there being a geographical east/west split in rainfall observations.

Regression analysis showed that Eskdalemuir approached a significant positive trend in total and heavy rainfall events over time at an annual and seasonal scale during the winter and summer. These findings update and support the work by Svensson & Jakob (2002) and Fowler & Kilsby (2003a) that ongoing regional analysis is important to record any significant changes in rainfall patterns for environmental management, in particular to the Eskdalemuir area. The results from chapter 3 illustrate that Eskdalemuir in recent years experienced not only wetter conditions over time, but there is a greater variability in the number of heavy precipitation events at a seasonal resolution for the winter and summer periods. One example of this was during the winter of 2015, where unusual synoptic factors, contributed to 21 heavy rainfall events during this period that led to flooding events in southern Scotland (van Oldenborgh et al. 2015). Such events may be attributed to an increase in seasonal rainfall events to large atmospheric circulation anomalies such as the North Atlantic Oscillation (Horswell et al. 2019). When comparing

historic MIDAS observations with the UKCP18 simulated dataset, there was an over-estimation of annual and seasonal values. It is therefore more reliable for agencies tasked with protecting vulnerable infrastructure, such as pipeline operators, to assess flood risk based on historic observations than simulated data which cannot account for the variability in rainfall.

When constructing a soil erosion risk map, it is efficient to achieve this in a G.I.S. database. The most common method for composing such spatial data in recent time is to combine multiple digital information in the G.I.S. environment using The Revised Universal Soil Loss Equation (RUSLE). Chapter 4 utilised updated land cover, elevation, updated crop and soil texture datasets to outline the environmental constraints along the pipeline corridor and construct a basic soil erosion risk map for a National Grid gas pipeline that traverses through Scotland. The results showed that for the 1611 km length of the corridor, 1330 km was routed in relatively flat terrain and 740 km was classified as arable and horticulture land cover based on 2015 data. The majority of the soil was sandy loam texture and the inclusion of the Crop Cover Plus data evaluated at least 531 km of route to crops such as Spring Cereals, Winter Cereals, Oilseed rape and potatoes. It is noted by Batey (2015) that soil erosion can occur along pipeline routes during installation process where compensation has been paid for damage to crops. However, there is little known about soil erosion events through the lifespan of the pipeline corridor which cross arable land cover. There is debate in the literature with those who argue that single rainfall events can induce soil erosion events in vulnerable land cover (Davidson & Harrison 1995, Kirkbride & Reeves 1993, Watson & Evans 2007) versus those who argue that there is little evidence of widespread soil erosion (Frost & Speirs 1996, Towers et al. 2006). Therefore, the evaluation of environmental characteristics along the pipeline corridor from this study can support future research which investigates the risk of soil erosion to the soil cover protecting buried pipelines for specific crop types and precipitation conditions.

The soil risk erosion map was constructed using soil texture, land cover, crop data and elevation, where the results indicated that soil susceptibility to erosion risk for the pipeline route was greatest in the north, nearer to Dyce and Leuchars. This suggested 169 km length of pipeline corridor was at risk of soil erosion if subjected to intense rainfall. The inclusion of crop cover in Chapter 4 addresses concerns where critique was drawn to crop spatial data not being accurate enough to produce a robust soil erosion dataset (Evans & Boardman 2016, Panagos et al. 2015). The continued release of spatial data annually, specifically crop data, gives the opportunity to continually update soil erosion risk more frequently. Another way to monitor risk would be to use Satellite data as this can cover a large area and recent advancements in spatial and temporal resolution, as this technology can be used to identify potential areas of concern.

Chapter 5 used Satellite technology from the Sentinel-1a and 1b constellations that capture radar imagery to evaluate ground displacement. The Eskdalemuir region was chosen as Chapter 3 evaluated a high number of rainfall events. Whilst there was relatively little crop activity in this region, 33km of the pipeline is routed in moderately to steep elevation conditions. Using InSar technology in generally well vegetated areas is difficult as the radar is unable to penetrate through the vegetated surface. One study in Ireland (Fiaschi et al. 2019) managed to detect ground motion of a landslip with vegetation present successfully, and this study was able to detect potential areas of soil erosion which need further investigation. In Chapter 5, 54 images were processed during the Winter periods of 2015 – 2018 where 13 were defect images and from the remaining 41 images 27 required manual adjustments. Wasowski & Bovenga (2014) argue that a combination of influences such as original data quality and processing technique can influence the success of estimates of ground displacement. The top 10% of ground displacement points were mapped and this resulted in an evenly distribution of ground surface lowering that ranged from -43 mm to -11 mm, with a mean of 14 mm. There were three areas where clusters of ground displacement was detected with one location coinciding with the risk of erosion identified from Chapter 4.

6.2 Implications for the oil and gas pipeline sector

The oil and gas sector in the UK remains crucial to the economy in the short and medium term. The buried onshore pipelines that run throughout Scotland are situated in a region with changing rainfall conditions which can threaten the soil cover protecting such infrastructure. Whilst the UK Climate Projection 18 data has simulated future precipitation conditions, the results historically did not always match observed values. There was a clear trend of increasing rainfall amount and intensity in the Eskdalemuir region, therefore being aware of areas along the pipeline route where rainfall intensities are the greatest can give an indication as to which areas along the pipeline corridor can be affected by soil erosion.

Chapter 4 highlighted that each year crop changes along the route can alter the soil erosion risk depending on what type of crop is sown in a particular year. Such anthropogenic influence can result in erosion risk, but in areas where vegetation is sparse satellite technology can be used to identify problematic areas. However, without ground-truth data to verify data evaluated from Satellite data caution should be used when wholly relying on such a technique to monitor soil erosion risk along pipeline routes.

Whilst renewable energy is becoming increasingly prevalent, the world is still reliant on the oil and gas sector for energy security. A shift to extracting heavy oil, as conventional light oil becomes depleted, means that pipelines require under-

ground heating to ensure safe delivery of an oil to a refinery. At present, there is a lack of research which considers how crops can affect the protection soil offers for buried pipelines, including how heated pipelines affect the integrity of soil cover in regions where crop activity takes place. Such an investigation could be beneficial to the industry as a whole to ensure pipeline failure is reduced as such results have an effect on the environment and economy. The burial of high-tension electricity cables is also increasing with the advent of more wind turbines to generate renewable electricity. This study is also highly relevant to soil erosion issues above cable installations.

6.3 Limits of this study

This study would have benefited from a greater access to the locations of oil and gas pipeline data. Understandably, such data is restricted for safety and security reasons and granted access would have limited the publishing of this thesis. The publicly available National Grid gas pipeline network provided sufficient opportunity to evaluate and perform satellite analysis. It would have been ideal to have used ground-truth data alongside the remotely sensed data in Chapter 5 to verify the results, however much of the land along the pipeline corridor is private and access would be heavily restricted. Areas identified with possible ground displacement issues in Chapter 5 could be used as a starting point of research; in particular the co-located area which was evaluated from both Chapter 4 and 5.

The data used throughout this thesis was sourced from reputable agencies such as the British Geological Survey, The Centre for Ecology and Hydrology and the European Space Agency however, representing data digitally at different spatial scales can create inaccuracies. Whilst working in the G.I.S environment care was taken in converting between vector and raster datasets in order to maintain as much detail as possible. The release of Sentinel-1 data is relatively new and the technique for evaluating ground displacement from radar images is not always successful. Spatial and temporal resolution is improving and important, as for monitoring soil erosion, high resolutions are required. In addition, the rainfall trends evaluated from Chapter 3 were based on long-term (≥ 30 years) hourly data where only three weather stations had long term observations as hourly measurements required manual recordings. Since the mid-1990s there are more weather stations situated along the pipeline route due to the advancement of automatic weather stations that do not require manual recordings. In future, these automatic weather stations can be used to build a more comprehensive evaluation of rainfall along the pipeline route although the data will still require screening for false readings.

6.4 Conclusion

Soil erosion risk mapping is complex because of the numerous influences from soil texture, land cover, crop type and rainfall events that can affect the rate of erosion that can threaten the depth of soil cover protecting infrastructure which transports potentially high risk substances. This study showed that some regions along a long distance pipeline route were exposed to ≥ 40 heavy rainfall events per year in comparison. Areas such as Eskdalemuir also show a great rate of change and variability in the number of heavy rainfall events over a particular season, with a trend for more frequent events with passing decades. This study also showed that pipelines are in conflict with land that is used for other economic activity, such as food security, that can also be classified as vulnerable to soil erosion by water. Satellite analysis that evaluated ground displacement was able to identify areas along the pipeline route where there may be significant risk of soil erosion, but such data would need verifying with ground-truth data. In conclusion, creating soil erosion risk maps is potentially valuable, but at present requires further comparison against ground-truth data.

References

- Abudu, D. & Williams, M. (2015), 'Gis-based optimal route selection for oil and gas pipelines in uganda', *Advances in Computer Science* **4**(4), 93–104.
- Afzal, M., Mansell, M. G. & Gagnon, A. S. (2011), 'Trends and variability in daily precipitation in scotland', *Procedia Environmental Sciences* **6**, 15–26.
- Agriculture and Horticulture Development Board (2019), 'Winter barley and oats on the up in scotland'. Accessed: March 2021.
URL: <https://ahdb.org.uk/news/winter-barley-and-oats-on-the-up-in-scotland>
- Alewell, C., Borrelli, P., Meusburger, K. & Panagos, P. (2019), 'Using the usle: Chances, challenges and limitations of soil erosion modelling', *International Soil and Water Conservation Research* **7**(3), 203–225.
- Archer, D. R. & Fowler, H. J. (2018), 'Characterising flash flood response to intense rainfall and impacts using historical information and gauged data in britain', *Journal of Flood Risk Management* **11**, S121–S133.
- Ashrafizadeh, S. N. & Kamran, M. (2010), 'Emulsification of heavy crude oil in water for pipeline transportation', *Journal of Petroleum Science and Engineering* **71**(3-4), 205–211.
- Augusto, O., Hirai, J. N., Oliveira, A. S. & Liotti, E. S. (2010), 'Gis applied to geotechnical and environmental risk management in a brazilian oil pipeline', *Bulletin of Engineering Geology and the Environment* **69**(4), 631–641.
- Bahadori, A. (2016), '*Chapter 1. Transportation Pipelines*', Gulf Professional Publishing, Gulf Professional Publishing, p. 2.
- Batey, T. (2015), 'The installation of underground pipelines: effects on soil properties', *Soil Use and Management* **31**(1), 60–66.
- Bayramov, E. (2012), 'Evaluation of Revegetation Progress and Erosion-Prone Areas along Oil and Gas Pipelines in Azerbaijan', in '7th Pipeline Technology Conference 2012', PTJ, Hannover, Germany, pp. 1–11.

- Bayramov, E., Buchroithner, M. F. & McGurty, E. (2013), 'Differences of mmf and usle models for soil loss prediction along btc and scp pipelines', *Journal of Pipeline Systems Engineering and Practice* **4**(1), 81–96.
- Bayramov, E., Buchroithner, M. & Kada, M. (2020), 'Quantitative assessment of ground deformations for the risk management of petroleum and gas pipelines using radar interferometry', *Geomatics, Natural Hazards and Risk* **11**, 2540–2568.
- Bayramov, E., Buchroithner, M. & McGurty, E. (2012), 'Quantitative assessment of vegetation cover and soil degradation factors within terrain units for planning, monitoring and assessment of renaturation along oil and gas pipelines', *Geocarto International* **27**(7), 535–555.
- Bayramov, E. R., Buchroithner, M. F. & Bayramov, R. V. (2016), 'Multi-temporal assessment of ground cover restoration and soil erosion risks along petroleum and gas pipelines in azerbaijan using gis and remote sensing', *Environmental Earth Sciences* **75**(3), 1 – 22.
- Bayramov, E., Schlager, P., Kada, M., Buchroithner, M. & Bayramov, R. (2019), 'Quantitative assessment of climate change impacts onto predicted erosion risks and their spatial distribution within the landcover classes of the southern caucasus using gis and remote sensing', *Modeling Earth Systems and Environment* **5**(2), 659–667.
- BBC (2017), 'Forties pipeline shutdown worth £20m a day'. (Accessed on 04/12/2017).
URL: <https://www.bbc.co.uk/news/uk-scotland-north-east-orkney-shetland-42322771>
- Blenkinsop, S., Lewis, E., Chan, S. C. & Fowler, H. J. (2017), 'Quality-control of an hourly rainfall dataset and climatology of extremes for the uk', *International Journal of Climatology* **37**(2), 722–740.
- Boardman, J. (2013), 'Soil erosion in britain: Updating the record', *Agriculture* **3**, 418–442.
- Borfecchia, F., De Canio, G., De Cecco, L., Giocoli, A., Grauso, S., La Porta, L., Martini, S., Pollino, M., Roselli, I. & Zini, A. (2015), 'Mapping the earthquake-induced landslide hazard around the main oil pipeline network of the agri valley (basilicata, southern italy) by means of two gis-based modelling approaches', *Natural Hazards* **81**(2), 759–777.
- Borrelli, P., Robinson, D. A., Fleischer, L. R., Lugato, E., Ballabio, C., Alewell, C., Meusburger, K., Modugno, S., Schutt, B., Ferro, V., Bagarello, V., Oost,

- K. V., Montanarella, L. & Panagos, P. (2017), 'An assessment of the global impact of 21st century land use change on soil erosion', *Nature Communications* **8**(1), 2013.
URL: <https://www.ncbi.nlm.nih.gov/pubmed/29222506>
- Bransby, M. & Newson, T. (2002), 'The upheaval capacity of pipelines in jetted clay backfill', *International Journal of Offshore and Polar Engineering* **12**(4), 280–287.
- Braun, A. & Veci, L. (2021), 'Sentinel-1 toolbox: Tops interferometry tutorial'. Accessed: July 2021.
- British Petroleum (2018), 'Bp energy outlook 2018 global insights'. Accessed on: 06/09/2018.
URL: <https://www.bp.com/content/dam/bp/en/corporate/pdf/energy-economics/energy-outlook/bp-energy-outlook-2018-global-insights.pdf>
- Brown, S. J. (2018), 'The drivers of variability in uk extreme rainfall', *International Journal of Climatology* **38**, 119–130.
- Burkett, V. (2011), 'Global climate change implications for coastal and offshore oil and gas development', *Energy Policy* **39**(12), 7719–7725.
- Carla, T., Farina, P., Intrieri, E., Ketizmen, H. & Casagli, N. (2018), 'Integration of ground-based radar and satellite InSAR data for the analysis of an unexpected slope failure in an open-pit mine', *Engineering Geology* **235**, 39–52.
- Central Intelligence Agency (2018), 'The world factbook'.
URL: <https://www.cia.gov/library/publications/the-world-factbook/fields/383.html>
- Centre for Ecology and Hydrology (2016), 'Land cover plus: Crops (2016) [file-geodatabase geospatial data], scale 1:2500. tiles: Gb. updated: 31 december 2016, centre for ecology and hydrology, uk.'. Accessed at: January 2018.
URL: <http://digimap.edina.ac.uk>
- Centre for Ecology and Hydrology (2017a), 'Land cover map 2015 [tiff geospatial data], scale 1:250,000. tiles: Gb. updated 22 may 2017. version 1.2, centre for ecology and hydrology, uk.'. Accessed at: January 2018.
URL: <http://digimap.edina.ac.uk>
- Centre for Ecology and Hydrology (2017b), 'Land cover plus: Crops (2017) [file-geodatabase geospatial data], scale 1:2500. tiles: Gb. updated: 31 december 2017, centre for ecology and hydrology, uk.'. Accessed at: January 2019.
URL: <http://digimap.edina.ac.uk>

- Centre for Ecology and Hydrology (2018), 'Land cover plus: Crops (2018) [file-geodatabase geospatial data], scale 1:2500. tiles: Gb. updated: 4 december 2018, centre for ecology and hydrology, uk.'. Accessed at: April 2019.
URL: <http://digimap.edina.ac.uk>
- Centre for Ecology and Hydrology (2019), 'Land cover plus: Crops (2019) [file-geodatabase geospatial data], scale 1:2500. tiles: Gb. updated: 22 november 2019, centre for ecology and hydrology, uk.'. Accessed at: September 2020.
URL: <http://digimap.edina.ac.uk>
- Chakraborty, D. & Kumar, J. (2013), 'Vertical uplift resistance of pipes buried in sand', *Journal of Pipeline Systems Engineering and Practice* **5**(1), 04013009–1 – 04013009–10.
- Chakraborty, D. & Kumar, J. (2014), 'Uplift resistance of long pipelines in the presence of seismic forces', *Journal of Pipeline Systems Engineering and Practice* **5**(4), 06014003 – 06014003–7.
- Champion, A. J., Allan, R. P. & Lavers, D. A. (2015), 'Atmospheric rivers do not explain uk summer extreme rainfall', *Journal of Geophysical Research: Atmospheres* **120**(14), 6731–6741.
- Chen, C. W. (2020), 'Snaphu: Statistical-cost, network-flow algorithm for phase unwrapping [software]. version 2.0.4'. Accessed date: October 2020.
URL: <https://web.stanford.edu/group/radar/softwareandlinks/sw/snaphu/>
- Cheuk, C. Y., White, D. J. & Bolton, M. D. (2008), 'Uplift mechanisms of pipes buried in sand', *Journal of Geotechnical and Geoenvironmental Engineering* **134**(2), 154–163.
- Chevron (2009), 'Crude marketing: Brent blend - whole crude properties'. Accessed date: January 2018.
URL: <http://crudemarketing.chevron.com/crude/documents/brent.xls>
- Cigna, F. & Tapete, D. (2021), 'Sentinel-1 big data processing with p-sbas insar in the geohazards exploitation platform: An experiment on coastal land subsidence and landslides in italy', *Remote Sensing* **13**(5).
- Culley, J. (1988), 'Long-term effects of an oil pipeline installation on soil productivity', *Canadian soil science* **68**, 177–181.
- Cunha, S. B. d. (2016), 'A review of quantitative risk assessment of onshore pipelines', *Journal of Loss Prevention in the Process Industries* **44**, 282–298.
- Dai, L., Wang, D., Wang, T., Feng, Q. & Yang, X. (2017), 'Analysis and comparison of long-distance pipeline failures', *Journal of Petroleum Engineering* **2017**, 1–7.

- Dang, V. K., Nguyen, T. D., Dao, N. H., Duong, T. L., Dinh, X. V. & Weber, C. (2021), 'Land subsidence induced by underground coal mining at quang ninh, vietnam: persistent scatterer interferometric synthetic aperture radar observation using sentinel-1 data', *International Journal of Remote Sensing* **42**(9), 3563–3582.
- Davidson, D. A. & Harrison, D. (1995), 'The nature, causes and implications of water erosion on arable land in scotland', *Soil Use and Management* **11**, 63–68.
- Deaton, W. & Frost, E. J. (1946), 'Gas hydrates and their relation to the operation of natural-gas pipe lines', Report BM-Mon-8 United States TIC. TIC English, ; Bureau of Mines, Amarillo, TX (USA). Helium Research Center.
- DEFRA (2010), 'Single Payment Scheme: Cross compliance Guidance for Soil Management', Report PB13315.
- Demirci, A. & Karaburun, A. (2011), 'Estimation of soil erosion using rusle in a gis framework: a case study in the buyukcekmecce lake watershed, northwest turkey', *Environmental Earth Sciences* **66**(3), 903–913.
- Derauw, D., d'Oreye Nicolas, Jaspard, M., Caselli, A. & Samsonov, S. (2020), 'On-going automated ground deformation monitoring of domuyo - laguna del maule area (argentina) using sentinel-1 msbas time series: Methodology description and first observations for the period 2015–2020', *Journal of South American Earth Sciences* **104**, 1–12.
- Diaz-Bejarano, E., Porsin, A. V. & Macchietto, S. (2016), 'Enhancing the flexibility of pipeline infrastructure to cope with heavy oils: Incremental thermal retrofit', *Applied Thermal Engineering* **105**, 170–179.
- Edwards, P., Harrison, B., Holz, D., Williard, K. & Schoonover, J. (2014), 'Comparisons of sediment losses from a newly constructed cross-country natural gas pipeline and an existing in-road pipeline', in '19th Central Hardwood Forest Conference', Vol. General Technical Report NRS-P-142, U.S. Department of Agriculture, Forest Service.
- Edwards, P. J., Harrison, B. M., Williard, K. W. J. & Schoonover, J. E. (2017), 'Erosion from a cross-country natural gas pipeline corridor: The critical first year', *Water, Air and Soil Pollution* **228**(7), 232.
- Environment Canada (Date Unknown), 'Arabian light'. Accessed date: November 2017.
URL: http://www.etc-cte.ec.gc.ca/databases/Oilproperties/pdf/WEB_Arabian_Light.pdf

- Environment Canada (Date Unknown**b**), 'West texas intermediate'. Accessed date: November 2017.
URL: https://www.etc-cte.ec.gc.ca/databases/oilproperties/pdf/WEB_West_Texas_Interm
- ESRI (2018), *ArcMap Desktop: Release 10.6*, Redlands, CA.
- ESRI (2021), *ArcPro Desktop: Release 2.6*, Redlands, CA.
- European Gas Pipeline Incident Group (2018), '10th Report of the European Gas Pipeline Incident Data Group (period 1970 – 2016)', Report Doc. number VA 17.R.0395.
- European Space Agency (2020**a**), 'Copernicus open access hub'. Accessed date: July 2020.
URL: <https://scihub.copernicus.eu/dhus//home>
- European Space Agency (2020**b**), 'Snap download: Sentinel toolboxes, version 8.0.0'. Accessed date: October 2020.
URL: <https://step.esa.int/main/download/snap-download/>
- Evans, R. & Boardman, J. (2016), 'A reply to panagos et al., 2016 (environmental science policy 59 (2016) 53–57)', *Environmental Science Policy* **60**, 63–68.
- Ezquerro, P., Del Soldato, M., Solari, L., Tomas, R., Raspini, F., Ceccatelli, M., Antonio Fernandez-Merodo, J., Casagli, N. & Herrera, G. (2020), 'Vulnerability Assessment of Buildings due to Land Subsidence Using InSAR Data in the Ancient Historical City of Pistoia (Italy)', *Sensors* **20**(10).
- Ferris, G. Newton, S. & Porter, M. (2016), 'Vulnerability of buried pipelines to landslides', *11th International Pipeline Conference* pp. 1–8.
- Fiaschi, S., Holohan, E., Sheehy, M. & Floris, M. (2019), 'Ps-insar analysis of sentinel-1 data for detecting ground motion in temperate oceanic climate zones: A case study in the republic of ireland', *Remote Sensing* **11**(3), 348–378.
- Finley, D., Daniels, S., Kole, K., Roeleveld, M. & Ogden, P. (2018**a**), 'Trial of a process for the identification of reduced depth of cover on buried pipelines', PTC, Berlin, Germany.
- Finley, D., Daniels, S., Kole, K., Roeleveld, M. & Ogden, P. (2018**b**), 'Trial of a process for the identification of reduced depth of cover on buried pipelines', Berlin, Germany, pp. 1–9.
- Foley, J. A., DeFries, R., Asner, G. P., Barford, C., Bonan, G., Carpenter, S. R., Chapin, F. S., Coe, M. T., Daily, G. C., Gibbs, H. K., Helkowski, J. H., Holloway, T., Howard, E. A., Kucharik, C. J., Monfreda, C., Patz, J. A., Prentice, I. C.,

- Ramankutty, N. & Snyder, P. K. (2005), 'Global consequences of land use', *Science* **309**(5734), 570–574.
- Fowler, H. J. & Ekström, M. (2009), 'Multi-model ensemble estimates of climate change impacts on uk seasonal precipitation extremes', *International Journal of Climatology* **29**(3), 385–416.
- Fowler, H. J. & Kilsby, C. G. (2003a), 'Implications of changes in seasonal and annual extreme rainfall', *Geophysical Research Letters* **30**(13).
- Fowler, H. J. & Kilsby, C. G. (2003b), 'A regional frequency analysis of united kingdom extreme rainfall from 1961 to 2000', *International Journal of Climatology* **23**(11), 1313–1334.
- Frost, C. & Speirs, R. (1996), 'Soil erosion from a single rainstorm over an area in east lothian, scotland', *Soil Use and Management* **12**, 8–12.
- Gabriels, D. (2003), 'Assessment of usle cover-management c-factors for 40 crop rotation systems on arable farms in the kemmelbeek watershed, belgium', *Soil and Tillage Research* **74**(1), 47–53.
- García-Ruiz, J. M., Beguería, S., Nadal-Romero, E., González-Hidalgo, J. C., Lana-Renault, N. & Sanjuán, Y. (2015), 'A meta-analysis of soil erosion rates across the world', *Geomorphology* **239**, 160–173.
- Girgin, S. & Krausmann, E. (2015), 'Lessons learned from oil pipeline natech accidents and recommendations for natech scenarios development', Report, European Commission: Joint Research Centre and Institute for the Protection and Security of the Citizen.
- Girgin, S. & Krausmann, E. (2016), 'Historical analysis of u.s. onshore hazardous liquid pipeline accidents triggered by natural hazards', *Journal of Loss Prevention in the Process Industries* **40**, 578–590.
- Golub, E., Greenfield, J., Dresnack, R., Griffis, F. & Pignataro, L. (1996), 'Pipeline accident effects for natural gas transmission pipelines', Technical Report DTRS56-94-C-0006-3, New Jersey Institute of Technology, Newark, NJ.
- Greenslade, J., Nixon, J. & Dyck, D. (2004), 'High Temperature Pipeline Design', in 'International Pipeline Conference', ASME, Alberta, Canada, pp. 833–839.
- Grieve, I., Davidson, D. A. & Gordon, J. (1995), 'Nature, extent and severity of soil upland erosion in scotland', *Land Degradation and Rehabilitation* **6**, 41–55.
- Groisman, P., Knight, R., Easterling, D., Karl, T., Hegrel, G. & Razuvaev, V. (2005), 'Trends in intense precipitation in the climate record', *Journal of Climate* **18**, 1326–1349.

- Halmová, D. & Feher, A. (2014), 'Effect of transit gas pipeline temperature on the production potential of agricultural soils', *Journal of Central European Agriculture* **3**(15), 245–253.
- Halmová, D., Polakova, Z., Koncekova, L. & Feher, A. (2017), 'Impact of operating temperature of gas transit pipeline on soil quality and production potential of crops', *Agriculture* **3**(63), 120–127.
- Hanel, M. & Buishand, T. A. (2010), 'On the value of hourly precipitation extremes in regional climate model simulations', *Journal of Hydrology* **393**(3-4), 265–273.
- Hann, M. J. & Morgan, R. P. C. (2006), 'Evaluating erosion control measures for bio restoration between the time of soil reinstatement and vegetation establishment', *Earth Surface Processes and Landforms* **31**(5), 589–597.
- Health & safety executive (2008), 'Pipelines and gas supply industry: Gb major accident hazard pipeline networks 'dial before you dig' information'. Accessed date: March 2018.
URL: <https://www.hse.gov.uk/pipelines/mahpinfosheet.pdf>
- Hole, J., Holley, R., Giunta, G., Lorenzo, G. & Thomas, A. (2011), 'InSar assessment of pipeline stability using compact active transponders', in 'Fringe 2011 Workshop", ESA, Frascati, Italy.
- Horswell, M., Quinn, N. & West, H. (2019), 'Regional rainfall response to the north atlantic oscillation (nao) across great britain', *Hydrology Research* **50**(6), 1549–1563.
- Hulme, M., Osborn, T. J. & Johns, T. C. (1998), 'Precipitation sensitivity to global warming: Comparison of observations with hadcm2 simulations', *Geophysical Research Letters* **25**(17), 3379–3382.
- Hurrell, J.W, Kushnir, Y. Ottersen, G & Visbeck, M. (2003), 'The North Atlantic Oscillation: Climatic Significance and Environmental Impact', Vol: 134, American Geophysical Union.
- Imamoglu, M., Kahraman, F., Cakir, Z. & Sanli, F. B. (2019), 'Ground Deformation Analysis of Bolvadin (W. Turkey) by Means of Multi-Temporal InSAR Techniques and Sentinel-1 Data', *Remote Sensing* **11**(9).
- Ineos (2018), 'Technical information: Pipeline transport'. Accessed date: April 2018. **URL:** <https://www.ineos.com/businesses/ineos-fps/technical/technical-information/>
- Ineos (2019), 'Forties blend details'. Accessed date: January 2019.
URL: <https://www.ineos.com/businesses/ineos-fps/business/forties-blend-quality/forties-blend/>

- International Energy Agency (2017), 'World energy outlook 2017', report.
URL: <https://www.iea.org/reports/world-energy-outlook-2017>
- Intrieri, E., Raspini, F., Fumagalli, A., Lu, P., Del Conte, S., Farina, P., Allievi, J., Ferretti, A. & Casagli, N. (2018), 'The Maoxian landslide as seen from space: detecting precursors of failure with Sentinel-1 data', *Landslides* **15**(1), 123–133.
- IPCC (2014), Climate Change 2014: 'Synthesis Report. Contribution of Working Groups I, II and III to the Fifth Assessment Report of the Intergovernmental Panel on Climate Change. [core writing team. R.K. Pachairi and L.A. Meyer (eds.)]', Report, IPCC, Geneva, Switzerland.
- Jiao, J., Zou, H., Jia, Y. & Wang, N. (2009), 'Research progress on the effects of soil erosion on vegetation', *Acta Ecologica Sinica* **29**(2), 85–91.
- Jung, J. K., O'Rourke, T. D. & Olson, N. A. (2013), 'Lateral soil-pipe interaction in dry and partially saturated sand', *Journal of Geotechnical and Geoenvironmental Engineering* **139**(12), 2028–2036.
- Kendon, E. J., Roberts, N. M., Fowler, H. J., Roberts, M. J., Chan, S. C. & Senior, C. A. (2014), 'Heavier summer downpours with climate change revealed by weather forecast resolution model', *Nature Climate Change* **4**(7), 570–576.
- Kirkbride, M. & Reeves, D. W. (1993), 'Soil erosion caused by low intensity rainfall in angus, scotland.', *Applied Geography* **13**, 299–311.
- Kramer, H. J. & Cracknell, A. P. (2008), 'An overview of small satellites in remote sensing', *International Journal of Remote Sensing* **29**(15), 4285–4337.
- Lal, R. (2001), 'Soil degradation by erosion', *Land Degradation and Development* **12**(6), 519–539.
- Lam, C. & Zhou, W. (2016), 'Statistical analyses of incidents on onshore gas transmission pipelines based on phmsa database', *International Journal of Pressure Vessels and Piping* **145**(1), 29–40.
- Landsburg, S., Cannon, K. & Finlayson, N. (1996), 'Effects of pipeline construction on soil compaction', in 'International Pipeline Conference', Vol. 2, ASME, Calgary, Alberta, Canada, pp. 1315–1318.
- Lawley, R. (2011a), *The Soil-Parent Material Database*, Nottingham, GB.
URL: <http://digimap.edina.ac.uk>
- Lawley, R. (2011b), *The Soil-Parent Material Database*, Nottingham, GB.
URL: <http://digimap.edina.ac.uk>

- Leadbetter, M. (1991), 'On a basis for 'Peaks over Threshold' modelling', *Statistics and probability* **12**(4), 357–362.
- Leir, M., Leach, M., Haderspock, M., Porter, M. & Ferris, G. (n.d.), 'Updated estimates of frequencies of pipeline failures caused by geohazards', *in* 'Proceedings of the 2016 11th International Pipeline Conference'.
- Lenderink, G. & van Meijgaard, E. (2008), 'Increase in hourly precipitation extremes beyond expectations from temperature changes', *Nature Geoscience* **1**(8), 511–514.
- Li, J. & Roy, D. (2017), 'A global analysis of sentinel-2a, sentinel-2b and landsat-8 data revisit intervals and implications for terrestrial monitoring', *Remote Sensing* **9**(902), 1–17.
- Lilly, A and Baggaley, N. (2018), 'Soil erosion risk map of scotland (partial cover)'.
URL: <https://soils.environment.gov.scot/maps/risk-maps/map-of-soil-erosion-risk-partial-cover/>
- Lobell, D. B. & Field, C. B. (2007), 'Global scale climate–crop yield relationships and the impacts of recent warming', *Environmental Research Letters* **2**(1).
- Malenovsky, Z., Rott, H., Cihlar, J., Schaepman, M., Garcia-Santos, G., Fernandes, R. & Berger, M. (2012), 'Sentinels for science: Potential of sentinel-1, -2, and -3 missions for scientific observations of ocean, cryosphere, and land', *Remote Sensing of Environment* (120), 91–101.
- Malinowska, A. A., Witkowski, W. T., Guzy, A. & Hejmanowski, R. (2018), 'Mapping ground movements caused by mining-induced earthquakes applying satellite radar interferometry', *Engineering Geology* **246**, 402–411.
- Marinos, V., Stoumpos, G., Papathanassiou, G., Grendas, N., Papouli, D. & Papazachos, K. (2016), 'Landslide geohazard for pipelines of natural gas transport', *in* 'Proceedings of the 14th International Congress of the Geological Society of Greece', Vol. 50, Bulletin of the Geological Society of Greece, Thessaloniki, Greece.
- Martínez-Palou, R., Mosqueira, M. d. L., Zapata-Rendón, B., Mar-Juárez, E., Bernal-Huicochea, C., de la Cruz Clavel-López, J. & Aburto, J. (2011), 'Transportation of heavy and extra-heavy crude oil by pipeline: A review', *Journal of Petroleum Science and Engineering* **75**(3-4), 274–282.
- Massonnet, D., Rossi, M., Carmona, C., Adragna, F., Peltzer, G., Feigl, K. & Rabaute, T. (1993), 'The displacement field of the landers earthquake mapped by radar interferometry', *Nature* **364**(6433), 138–142.

- Met Office (2006), 'MIDAS UK Hourly Rainfall Data. NCAS British Atmospheric Data Centre.', Chilton, Oxfordshire, UK.
URL: <https://catalogue.ceda.ac.uk/uuid/bbd6916225e7475514e17fdbf11141c1>
- Met Office (2012), 'Fact sheet no. 3 – water in the atmosphere'.
- Met Office Hadley Centre (2019), 'Ukcp18 convection-permitting model projections for the uk at 2.2km resolution.'. Accessed date: October 2019.
URL: <http://catalogue.ceda.ac.uk/uuid/ad2ac0ddd3f34210b0d6e19bfc335539>
- Meyer, R., Attanasi, E. & Freeman, P. (2007), 'Heavy oil and natural bitumen resources in geological basins of the world', Report, U.S. Geological Survey, Reston, Virginia.
- Morgan, R. P. C. & Hann, M. J. (2006), 'Design of diverter berms for soil erosion control and bioremediation along pipeline rights-of-way', *Soil Use and Management* **21**(3), 306–311.
- Naeth, M., Chanasyk, D., McGill, W. & Bailey, A. (1993), 'Soil temperature regime in mixed prairie rangeland after pipeline construction and operation', *Canadian Agricultural Engineering* **35**(2), 89–95.
- National Geographic World Map (2011), *Sources: National Geographic, Esri, DeLorme, HERE, UNEP-WCMC, USGS, NASA, ESA, METI, NRCAN, GEBCO, NOAA, IPC*, Redlands, CA.
- National Grid (2018), 'Gas pipe [shapefile]. downloaded february 2020. coverage: Great Britain.'. Accessed date: February 2018.
URL: <https://www.nationalgridgas.com/land-and-assets/network-route-maps>
- Nearing, M., Pruski, F. & O'Neal, M. (2004), 'Expected climate change impacts on soil erosion rates: a review', *Journal of Soil and Water Conservation* **59**(1), 43–50.
- Nuñez, G., Guevara, E. & Gonzalez, J. (n.d.), 'Highly viscous oil transportation methods in the venezuela industry', in 'Proceeding of the 15th World Petroleum Congress', pp. 495–502.
- Oil and Gas Authority (2018), 'OGA Offshore Fields WGS84 [Shapefile]', Aberdeen, UK.
- Olson, E. R. & Doherty, J. M. (2012), 'The legacy of pipeline installation on the soil and vegetation of southeast wisconsin wetlands', *Ecological Engineering* **39**, 53–62.

Ordnance Survey (2018), 'OS Terrain 50 [ASC geospatial data]. Scale 1:50000, Tiles: nn10 , nn20, nn30, nn40, nn50, nn60, nn70, nn80, nn90, no00, no10, no20, no30, no40, no50, no60, ns10, ns14, ns15, ns16, ns17, ns18, ns19, ns20, ns21, ns22, ns23 , ns24 , ns25, ns26, ns27, ns28, ns29, ns30, ns31, ns32, ns33, ns34, ns35, ns36, ns37, ns38, ns39, ns40, ns41, ns42, ns43, ns44, ns45, ns46, ns47, ns48, ns49, ns50, ns51, ns52, ns53, ns54, ns55, ns56, ns57, ns58, ns59, ns60, ns61, ns62, ns63, ns64, ns65, ns66, ns67, ns68, ns69, ns70, ns71, ns72, ns73, ns74, ns75, ns76, ns77, ns78, ns79, ns80, ns81, ns82, ns83, ns84, ns85, ns86, ns87, ns88, ns89, ns90, ns91, ns92, ns93, ns94, ns95, ns96, ns97, ns98, ns99, nt00, nt01, nt02, nt03, nt04, nt05, nt06, nt07, nt08, nt09, nt10, nt11, nt12, nt13, nt14, nt15, nt16, nt17, nt18, nt19, nt20, nt21, nt22, nt23, nt24, nt25, nt26, nt27, nt28, nt29, nt30, nt31, nt32, nt33, nt34, nt35, nt36, nt37, nt38, nt39, nt40, nt41, nt42, nt43, nt44, nt45, nt46, nt47, nt48, nt49, nt50, nt51, nt52, nt53, nt54, nt55, nt56, nt57, nt58, nt59, nt60, nt61, nt62, nt63, nt64, nt65, nt66, nt67, nt68, nt69, nt70, nt71, nt72, nt73, nt74, nt75, nt76, nt77, nt80, nt81, nt82, nt83, nt84, nt85, nt86, nt87, nt90, nt91, nt92, nt93, nt94, nt95, nt96, nu00, nu01, nu02, nu03, nu04, nu05, nu10, nu11, nu12, nu13, nu14, nu20, nu21, nu22, nu23, ny00, ny01, ny02, ny03, ny04, ny05, ny06, ny07, ny08, ny09, ny10, ny11, ny12, ny13, ny14, ny15, ny16, ny17, ny18, ny19, ny20, ny21, ny22, ny23, ny24, ny25, ny26, ny27, ny28, ny29, ny30, ny31, ny32, ny33, ny34, ny35, ny36, ny37, ny38, ny39, ny40, ny41, ny42, ny43, ny44, ny45, ny46, ny47, ny48, ny49, ny50, ny51, ny52, ny53, ny54, ny55, ny56, ny57, ny58, ny59, ny60, ny61, ny62, ny63, ny64, ny65, ny66, ny67, ny68, ny69, ny70, ny71, ny72, ny73, ny74, ny75, ny76, ny77, ny78, ny79, ny80, ny81, ny82, ny83, ny84, ny85, ny86, ny87, ny88, ny89, ny90, ny91, ny92, ny93, ny94, ny95, ny96, ny97, ny98, ny99. Updated: 11 June 2013, Ordnance Survey (GB), Using: EDINA Digimap Ordnance Survey Service, <<http://digimap.edina.ac.uk>>. '. Downloaded: 2018-03-05.

URL: <http://digimap.edina.ac.uk>

Ordnance Survey (GB) (2017), '*Boundary-Line™ [SHAPE geospatial data]*', Scale 1:10000, Tiles: GB, Updated: 21 August 2017., Edinburgh, UK.

URL: <http://digimap.edina.ac.uk>

Osborn, T. & Hulme, M. (2002), 'Evidence for trends in heavy rainfall events over the uk', *The Royal Society* **360**, 1313–1325.

Otegui, J. L. (2014), 'Challenges to the integrity of old pipelines buried in stable ground', *Engineering Failure Analysis* **42**, 311–323.

Pall, P., Allen, M. R. & Stone, D. A. (2006), 'Testing the clausius–clapeyron constraint on changes in extreme precipitation under co2 warming', *Climate Dynamics* **28**(4), 351–363.

- Panagos, P., Borrelli, P., Meusburger, K., Yu, B., Klik, A., Jae Lim, K., Yang, J. E., Ni, J., Miao, C., Chattopadhyay, N., Sadeghi, S. H., Hazbavi, Z., Zabihi, M., Larionov, G. A., Krasnov, S. F., Gorobets, A. V., Levi, Y., Erpul, G., Birkel, C., Hoyos, N., Naipal, V., Oliveira, P. T. S., Bonilla, C. A., Meddi, M., Nel, W., Al Dashti, H., Boni, M., Diodato, N., Van Oost, K., Nearing, M. & Ballabio, C. (2017), 'Global rainfall erosivity assessment based on high-temporal resolution rainfall records', *Scientific Reports* **7**(1), 4175.
- Panagos, P., Borrelli, P., Poesen, J., Ballabio, C., Lugato, E., Meusburger, K., Montanarella, L. & Alewell, C. (2015), 'The new assessment of soil loss by water erosion in Europe', *Environmental Science Policy* **54**, 438–447.
- Panagos, P., Meusburger, K., Ballabio, C., Borrelli, P. & Alewell, C. (2014), 'Soil erodibility in europe: a high-resolution dataset based on lucas', *Science of the Total Environment* **479-480**, 189–200.
URL: <https://www.ncbi.nlm.nih.gov/pubmed/24561925>
- Papadakis, G. (1999), 'Major hazard pipelines: A comparative study of onshore transmission accidents', *Journal of Loss Prevention in the Process Industries* **12**(1), 91–107.
- Papavinasam, S. (2014), 'Chapter 2 - Oil and Gas Industry Network', Gulf Professional Publishing, Boston, pp. 41–131.
URL: <http://www.sciencedirect.com/science/article/pii/B9780123970220000029>
- Poesen, J. (2018), 'Soil erosion in the anthropocene: Research needs', *Earth Surface Processes and Landforms* **43**(1), 64–84.
- Polcari, M., Palano, M., Fernández, J., Samsonov, S. V., Stramondo, S. & Zerbini, S. (2016), '3d displacement field retrieved by integrating sentinel-1 insar and gps data: the 2014 south napa earthquake', *European Journal of Remote Sensing* **49**(1), 1–13.
- Psarropoulos, P., Karvelis, P. & Antoniou, A. (2012), 'Geohazard assessment for onshore pipelines in areas with moderate or high seismicity', Curran Associates, Lisbon, Portugal.
- Qi, S. S., Hao, F. H., Ouyang, W. & Cheng, H. G. (2012), 'Characterizing landscape and soil erosion dynamics under pipeline interventions in southwest china', *Procedia Environmental Sciences* **13**, 1863–1871.
- R Core Team (2018), 'R: A Language and Environment for Statistical Computing', R Foundation for Statistical Computing, Vienna, Austria.
URL: <https://www.R-project.org/>

- Ramírez-Camacho, J. G., Carbone, F., Pastor, E., Bubbico, R. & Casal, J. (2017), 'Assessing the consequences of pipeline accidents to support land-use planning', *Safety Science* **97**, 34–42.
- Renard, K. G., Foster, G., Weesles, G., Mccool, D. K. & Yoder, D. (1997), '*Predicting Soil Erosion by Water: A Guide to conservation Planning with the Revised Universal Soil Loss Equation (RUSLE)*', Agriculture Handbook No. 703USDA, Washington DC.
- Rickson, R., Baggaley, N., Deeks, L., Graves, A., Hannam, J., Keay, C. & Lilly, A. (2019), 'Developing a method to estimate the costs of soil erosion in high-risk Scottish catchments | Final Report', Technical report, Department: School of Water, Energy and Environment (Cranfield University) and Environmental and Biochemical Sciences (James Hutton Institute), Aberdeen, UK.
- Rimmer, D. P., Gregoli, A. A., Hamshar, J. A. & Yildirim, E. (1992), '*Pipeline Emulsion Transportation for Heavy Oils*', *Advances in Chemistry*, pp. 295–312.
- Robert, D. J., Soga, K., O'Rourke, T. D. & Sakanoue, T. (2016), 'Lateral load-displacement behavior of pipelines in unsaturated sands', *Journal of Geotechnical and Geoenvironmental Engineering* **142**(11), 04016060–1 – 04016060–13.
- Robert, D. J., Thusyanthan, I. & Li, C. (n.d.), '*Uplift Resistance of Buried Pipelines in Dry and Unsaturated Sands: Comparison of Analytical and FE Model Results with Large-Scale Test Data*', American Society of Civil Engineers, Chicago, Illinois, USA., pp. 298–309.
- Rosenzweig, C. & Hillel, D. (1998), '*Climate change and the global harvest : potential impacts of the greenhouse effect on agriculture*', Oxford University Press, New York.
- RStudio Team (2021), '*RStudio: Integrated Development Environment for R*', Boston, MA.
URL: <http://www.rstudio.com/>
- Running, S. W., Nemani, R. R., Heinsch, F. A., Zhao, M., Reeves, M. & Hashimoto, H. (2004), 'A Continuous Satellite-Derived Measure of Global Terrestrial Primary Production', *BioScience* **54**(6), 547–560.
- Sahoo, S., Manna, B. & Sharma, K. G. (2014), 'Seismic behaviour of buried pipelines: 3d finite element approach', *Journal of Earthquakes* **2014**, 1–9.
- Sawatsky, L. F., Bender, M. J. & Long, D. (1998), 'Pipeline Exposure at River Crossings: Causes and Cures', in 'Volume 1: Risk Assessment and Management; Emerging Issues and Innovative Projects; Operations and Maintenance;

- Corrosion and Integrity Management', International Pipeline Conference, Calgary, Alberta, Canada, pp. 159–163.
- Schaminee, P. Zorn, N. S. G. (1990), 'Soil Response for Pipeline Upheaval Buckling Analyses: Full-Scale Laboratory Tests and Modelling'.
- Scoccimarro, E., Villarini, G., Vichi, M., Zampieri, M., Fogli, P. G., Bellucci, A. & Gualdi, S. (2015), 'Projected changes in intense precipitation over europe at the daily and subdaily time scales', *Journal of Climate* **28**(15), 6193–6203.
- Shiono, T., Ogawa, S., Miyamoto, T. & Kameyama, K. (2013), 'Expected impacts of climate change on rainfall erosivity of farmlands in japan', *Ecological Engineering* **61**, 678–689.
- Sims, R. & Riedmann, M. (n.d.), 'Ground motion monitoring using insar: Example applications for mining and pipeline operations with consideration of potential for deloping countries'.
- Solari, S., Egüen, M., Polo, M. J. & Losada, M. A. (2017), 'Peaks over threshold (pot): A methodology for automatic threshold estimation using goodness of fit p -value', *Water Resources Research* **53**(4), 2833–2849.
- Soon, Y., Arshad, M., Rice, W. & Mills, P. (2000), 'Recovery of chemical and physical properties of boreal plain soils impacted by pipeline burial', *Canadian Journal of Soil Science* **80**, 489–497.
- Speight, J. (2006), *'The Chemistry and Technology of Petroleum'*, 4th edition edn, Taylor Francis Group, LLC., Boca Raton, USA.
- Stewart, A. (1979), 'Effect of Pipeline Construction on Soil and Crops IV. Dept. Renewable Resources. MSc Thesis', Report, Macdonald College, Quebec, Canada.
- Stewart, M. G. & Deng, X. (2015), 'Climate impact risks and climate adaptation engineering for built infrastructure', *ASCE-ASME Journal of Risk and Uncertainty in Engineering Systems, Part A: Civil Engineering* **1**(1).
- Strozzi, T., Antonova, S., Guenther, F., Matzler, E., Vieira, G., Wegmuller, U., Westermann, S. & Bartsch, A. (2018), 'Sentinel-1 SAR Interferometry for Surface Deformation Monitoring in Low-Land Permafrost Areas', *Remote sensing* **10**(9).
- Svensson, C. & Jakob, D. (2002), 'Diurnal and seasonal characteristics of precipitation at an upland site in scotland', *International Journal of Climatology* **22**(5), 587–598.

- Sweeney, M. (2004), 'Terrain and geohazard challenges facing onshore oil and gas pipelines: Historic risks and modern responses', *in* 'International conference on: Terrain and geohazard challenges facing onshore oil and gas pipelines', Institution of Civil Engineers in association with BP Exploration, London, UK, pp. 37–51.
- Sweeney, M. (2016), 'Terrain and geohazard challenges for remote region onshore pipelines: risk management, geoteams and ground models', *Quarterly Journal of Engineering Geology and Hydrogeology* **50**(1), 13–52.
- TC Energy (2021), 'Keystone xl pipeline'.
URL: <https://www.transcanada.com/en/operations/oil-and-liquids/keystone-xl/>
- Thusyanthan, N., Arasu, S., Bolton, M. & Allan, P. (2008), 'Upheaval buckling resistance of pipelines buried in clayey backfill', number Paper No. ISOPE-2008-TPC-499, Vancouver, Canada, p. 7.
- Towers, W., Grieve, I., Hudson, G., Campbell, C., Lilly, A., Davidson, D. A., Bacon, J., Langan, S. & Hopkins, D. (2006), 'Scotland's Soil Resource - Current state and threats', Report, Edinburgh, UK.
- Tralli, D. M., Blom, R. G., Zlotnicki, V., Donnellan, A. & Evans, D. L. (2005), 'Satellite remote sensing of earthquake, volcano, flood, landslide and coastal inundation hazards', *ISPRS Journal of Photogrammetry and Remote Sensing* **59**(4), 185–198. Remote Sensing and Geospatial Information for Natural Hazards Characterization.
- Transneft (2016), 'History'. Accessed date: February 2018.
URL: <https://www.transneft.ru/about/story/>
- Trenberth, K. E. (2011), 'Changes in precipitation with climate change', *Climate Research* **47**(1), 123–138.
- UKOPA (2016), Industry good practice guide: Managing pipelines with reduced depth of cover, Technical Report, Ambergate, Derbyshire, UK.
URL: <https://www.ukopa.co.uk/documents/UKOPA-GPG001.pdf>
- U.S. Energy Information Administration (2020), 'Natural gas explained'.
URL: <https://www.eia.gov/energyexplained/natural-gas/>
- van Oldenborgh, G. J., Otto, F. E. L., Haustein, K. & Cullen, H. (2015), 'Climate change increases the probability of heavy rains like those of storm desmond in the uk – an event attribution study in near-real time', *Hydrology and Earth System Sciences Discussions* **12**(12), 13197–13216.

- Veritas, D. N. (2007), 'Recommended practice. Global buckling of submarine pipelines. Structural design due to temperature/high pressure', Report DNV-RP-F110. Accessed: March 2018.
URL: <https://rules.dnvgl.com/docs/pdf/DNV/codes/docs/2007-10/RP-F110.pdf>
- Wang, J., Armen, R., Haigh, S., Thusyanthan, N. & Mesmar, S. (2010), 'Uplift Resistance of Buried Pipelines at Low Cover-Diameter Ratios', in '2010 Offshore Technology Conference', number OTC 20912, Houston, Texas, USA.
- Wang, J., Haigh, S. & Thusyanthan, N. (2009), 'Uplift Resistance of Buried Pipelines in Blocky Clay Backfill', in 'The Nineteenth (2009) International Offshore and Polar Engineering Conference', Osaka, Japan.
- Wasowski, J. & Bovenga, F. (2014), 'Investigating landslides and unstable slopes with satellite multi temporal interferometry: Current issues and future perspectives', *Engineering Geology* **174**, 103–138.
- Watson, A. & Evans, R. (2007), 'Water erosion of arable fields in north-east Scotland, 1985 – 2007', *Scottish Geographical Journal* **123**(2), 107–121.
- Winning, H. K. & Hann, M. J. (2014), 'Modelling soil erosion risk for pipelines using remote sensed data', *Biosystems Engineering* **127**, 135–143.
- Wischmeier, W. & Smith, D. (1978), 'Predicting Rainfall Erosion Losses: A Guide to Conservation Planning', Technical Report Agriculture Handbook No. 537, Washington D.C., USA.
- Witek, M. (2015), 'Possibilities of using x80, x100, x120 high-strength steels for onshore gas transmission pipelines', *Journal of Natural Gas Science and Engineering* **27**, 374–384.
- Wraith, J. & Hanks, R. (1992), 'Soil thermal regime influence on water use and yield under variable irrigation', *Agronomy Journal* **84**(May-June), 521 – 536.
- Xiao, J., Shi, P., Wang, Y. & Yang, L. (2016), 'The vegetation recovery pattern and affecting factors after pipeline disturbance in northwest China', *Journal for Nature Conservation* **29**, 114–122.
- Xue, Y., Li, Y., Guang, J., Zhang, X. & Guo, J. (2008), 'Small satellite remote sensing and applications – history, current and future', *International Journal of Remote Sensing* **29**(15), 4339–4372.
- Yaghi, B. & Al-Bemani, A. (2002), 'Heavy crude oil viscosity reduction for pipeline transportation', *Energy Sources* (24), 93–102.

Yu, b., Han, F., Liu, W. & Harris, S. A. (2016), 'Geohazards and thermal regime analysis of oil pipeline along the qinghai–tibet plateau engineering corridor', *Natural Hazards* **83**(1), 193–209.

Zachar, D. (1982), '*Soil erosion. Chapter 2 Classification of soil erosion*', Vol. 10 of *Development in Soil Science*, Elsevier, Czechoslovakia.

Zellmer, S., Edgar, D. & Isaacson, H. (1991), 'Erosion control on a steeply sloped pipeline right-of-way in southwestern Pennsylvania', in 'Conference: 22. annual International Erosion Control Association (IECA) conference and trade exposition", Office of Scientific and Technical Information (OSTI), Orlando, Florida, USA.

Appendix A

Autumn results

Table A.1: The autumn results for the change in rainfall patterns at a seasonal scale for observed (MIDAS) and future simulated (UKCP18) precipitation data. Min = minimum, Max = maximum, M = mean, Ra = range, SD = standard deviation, and SE = standard error.

			Autumn											
			Rainfall depth (mm)						4mm exceedance events					
			Min	Max	M	Ra	SD	SE	Min	Max	M	Ra	SD	SE
Location	Time series	Dataset												
Eskdalemuir	1981-1999	MIDAS	222.1	746.9	477.2	524.8	142.8	32.8	3	15	9.2	12	3.9	0.9
	2000-2018		282.6	727.8	504.5	445.2	107.6	24.7	3	15	9.2	12	3.1	0.7
	1981-1999	UKCP18	94.6	925.2	464.6	830.6	136.4	8.8	2	23	11	21	4.3	0.3
	2021-2039		149.6	883.6	476	734	138.5	8.9	3	23	11.7	22	4.4	0.3
	2061-2079		153	1055.4	516.8	902.4	145.7	9.4	2	25	12.9	23	4.4	0.3
	Dyce	1981-1999	MIDAS	110.7	446.9	247.6	336.2	88.8	20.4	1	9	3.2	8	2.2
2000-2018		145.8		441.6	236.5	295.8	77.3	17.7	1	8	3.3	7	2.3	0.5
1981-1999		UKCP18	98.9	558.3	231.3	459.4	75.9	4.9	0	12	3.9	12	2.4	0.2
2021-2039			86.2	517.7	231.8	431.5	71.9	4.6	0	12	4.2	12	2.4	0.2
2061-2079			80.0	461.6	220.3	381.5	65.3	4.2	0	12	5.1	12	2.4	0.2
Leuchars		1981-1999	MIDAS	87.2	373.8	194.8	286.6	67.9	15.6	1	7	3.4	6	1.9
	2021-2039	117.2		317.4	193.2	200.2	61.2	14.0	0	7	3.3	7	2.2	0.5
	1981-1999	UKCP18	50	404.1	183.2	353.1	59.5	3.8	0	10	3.6	10	2.2	0.1
	2021-2039		65.2	380.8	189.2	315.7	60.9	3.9	0	11	3.9	11	2.0	0.1
	2061-2079		66.4	396.3	190.4	329.9	59.8	3.9	0	14	4.8	14	2.5	0.2

Appendix B

Winter results

Table B.1: The winter results for the change in rainfall patterns at a seasonal scale for observed (MIDAS) and future simulated (UKCP18) precipitation data. Min = minimum, Max = maximum, M = mean, Ra = range, SD = standard deviation, and SE = standard error.

			Winter											
			Rainfall depth (mm)						4mm exceedance events					
			Min	Max	M	Ra	SD	SE	Min	Max	M	Ra	SD	SE
Location	Time series	Dataset												
Eskdalemuir	1981-1999	MIDAS	219.8	709.4	482	489.6	126.1	28.9	1	16	8.2	15	3.5	0.8
	2000-2018		182.8	1049.4	481.3	866.6	231.3	53.1	1	21	7.7	20	5.5	1.3
	1981-1999	UKCP18	237.4	1035.4	549.2	798	141.8	9.2	0	67	22	22	4.1	0.3
	2021-2039		186.1	1189.5	602.9	1003.5	181.4	11.7	1	70	26	25	5.1	0.3
	2061-2079		234.5	1188.3	721.5	953.8	186.2	12	3	69	27	24	4.8	0.3
	Dyce	1981-1999	MIDAS	70	353.5	171.3	283.5	68.8	15.8	0	4	1.4	4	1.3
2000-2018		104.8		357.2	189.6	252.4	72.9	16.7	0	5	1.4	5	1.8	0.4
1981-1999		UKCP18	88.2	538.1	245.1	449.9	80.1	5.2	0	8	2.1	8	1.7	0.1
2021-2039			69.5	587.7	255.5	518.1	81.9	5.3	0	10	2.9	10	2	0.1
2061-2079			93.3	654	273.3	560.7	86.3	5.6	0	11	3.5	11	2.2	0.1
Leuchars		1981-1999	MIDAS	87.6	216.9	154.3	130.2	34.7	8	0	5	1.6	5	1.5
	2021-2039	96.2		308.4	159	212.2	59.8	13.7	0	3	1.1	3	1	0.2
	1981-1999	UKCP18	55.3	385.7	178.1	330.4	53.7	3.5	0	7	1.7	7	1.5	0.1
	2021-2039		64.7	416.2	194.5	351.4	60.1	3.9	0	9	2.4	9	1.8	0.1
	2061-2079		61.7	484.7	221	423	67.7	4.4	0	13	3.0	13	2.2	0.1

Appendix C

Spring results

Table C.1: The spring results for the change in rainfall patterns at a seasonal scale for observed (MIDAS) and future simulated (UKCP18) precipitation data. Min = minimum, Max = maximum, M = mean, Ra = range, SD = standard deviation, and SE = standard error.

			Spring											
			Rainfall depth (mm)						4mm exceedance events					
			Min	Max	M	Ra	SD	SE	Min	Max	M	Ra	SD	SE
Location	Time series	Dataset												
Eskdalemuir	1981-1999	MIDAS	128.5	537	340.9	408.5	92.5	21.2	0	8	4.2	8	2.3	0.5
	2000-2018		188.6	432.6	336	244	69.6	16	1	10	5.2	9	2.7	0.6
	1981-1999	UKCP18	73	744.6	549.2	701.6	108.2	7	0	18	6.9	18	0.2	0.2
	2021-2039		140	992.6	602.9	852.5	116.6	7.5	0	22	7.4	22	3.5	0.2
	2061-2079		428.8	693.4	721.5	586	113.2	7.3	1	17	8	16	3.4	0.2
	Dyce	1981-1999	MIDAS	97.5	293.1	186.6	195.6	51	11.7	0	5	1.8	5	1.4
2000-2018		110.4		189.8	154	79.4	22	5.1	0	4	1.3	4	1.2	0.3
1981-1999		UKCP18	80.8	474.8	212.5	394.8	64.5	4.2	0	8	2.3	8	1.6	0.1
2021-2039			60.2	529.9	219.1	469.6	76.2	4.9	0	11	2.8	11	2.0	0.1
2061-2079			74.8	442.2	224.5	369.4	75.5	4.9	0	9	3.1	9	1.9	0.1
Leuchars		1981-1999	MIDAS	62.1	215.4	146.6	153.3	44	10.1	0	3	1.2	3	1
	2021-2039	87.0		195.8	136.8	108.8	29.2	6.7	0	2	0.8	2	0.7	0.2
	1981-1999	UKCP18	34.9	347.9	159.6	313	49.6	3.2	0	8	1.9	8	1.6	0.1
	2021-2039		38.2	357.4	166	319.2	55.8	3.6	0	8	2.2	8	1.6	0.1
	2061-2079		40.3	381.9	171.8	341.6	44	3.8	0	8	2.5	8	1.8	0.1

Appendix D

Summer results

Table D.1: The summer results for the change in rainfall patterns at a seasonal scale for observed (MIDAS) and future simulated (UKCP18) precipitation data. Min = minimum, Max = maximum, M = mean, Ra = range, SD = standard deviation, and SE = standard error.

			Summer											
			Rainfall depth (mm)						4mm exceedance events					
			Min	Max	M	Ra	SD	SE	Min	Max	M	Ra	SD	SE
Location	Time series	Dataset												
Eskdalemuir	1981-1999	MIDAS	120	626.6	331.4	506.6	125.3	28.7	1	15	7.2	14	3.7	0.9
	2000-2018		217.6	666.2	409.6	448.6	123.1	28.3	3	19	10.1	16	4.3	1.0
	1981-1999	UKCP18	151.6	744.8	376	593.2	102.4	6.6	2	29	11.4	27	4.7	0.3
	2021-2039		101.5	818.2	352.4	716.6	113.6	7.3	2	29	11.2	27	4.8	0.3
	2061-2079		65.5	668.1	273.6	602.6	111.9	7.2	2	29	8.6	24	4.1	0.3
	Dyce	1981-1999	MIDAS	87.1	346.5	178.5	259.4	66.8	15.3	1	8	3.8	7	2.2
2000-2018		50.2		316.4	221.1	266.2	78.6	18	1	10	5.3	9	2.7	0.6
1981-1999		UKCP18	76.1	426.4	216	350.2	68.3	4.4	0	15	6	15	3.1	0.2
2021-2039			62	404.7	214.2	342.7	63.4	4.1	1	16	6.5	15	3	0.2
2061-2079			47.4	432	187.1	384.6	69	4.5	0	18	6.0	18	3.2	0.2
Leuchars		1981-1999	MIDAS	67.7	260.1	140.6	192.5	55	12.6	0	8	2.7	8	1.8
	2021-2039	100		344.2	221.1	244.2	81.9	18.8	0	9	5.1	9	2.5	0.6
	1981-1999	UKCP18	73.7	402.9	159.6	329.2	59.2	3.8	0	16	5.5	16	3.1	0.2
	2021-2039		59.6	535	166	475.4	64.6	4.2	0	15	5.7	15	3	0.2
	2061-2079		31.6	421.7	171.8	390.1	67.3	4.4	0	14	5.1	14	2.8	0.2

Appendix E

Sentinel-1 dates

Table E.1: Sentinel-1 data for 2015

Reference	Secondary	Reference image name
4th October 2015	28th October 2015	S1A_IW_SLC__1SDV_20151004T063004_20151004T063031_007999_00B319_B9B6
28th October 2015	9th November 2015	S1A_IW_SLC__1SDV_20151028T062949_20151028T063019_008349_00BC86_84F7
9th November 2015	21st November 2015	S1A_IW_SLC__1SDV_20151109T063003_20151109T063030_008524_00C116_E041
21st November 2015	3rd December 2015	S1A_IW_SLC__1SDV_20151121T062954_20151121T063021_008699_00C610_9112
3rd December 2015	15th December 2015	S1A_IW_SLC__1SDV_20151203T062954_20151203T063022_008874_00CAF3_4F96
15th December 2015	27th December 2015	S1A_IW_SLC__1SDV_20151215T062953_20151215T063021_009049_00CFCD_5E5E
27th December 2015	8th January 2016	S1A_IW_SLC__1SDV_20151227T062953_20151227T063021_009224_00D4C4_6A6D
8th January 2016	20th January 2016	S1A_IW_SLC__1SDV_20160108T062952_20160108T063020_009399_00D9C6_0402
20th January 2016	1st February 2016	S1A_IW_SLC__1SDV_20160120T062952_20160120T063020_009574_00DECB_D8EF
1st February 2016	13th February 2016	S1A_IW_SLC__1SDV_20160201T062950_20160201T063017_009749_00E3EF_0D05
13th February 2016	25th February 2016	S1A_IW_SLC__1SDV_20160213T062951_20160213T063019_009924_00E904_00C6
25th February 2016	8th March 2016	S1A_IW_SLC__1SDV_20160225T062950_20160225T063017_010099_00EE26_1B96
8th March 2016	20th March 2016	S1A_IW_SLC__1SDV_20160308T062952_20160308T063019_010274_00F310_902E
		S1A_IW_SLC__1SDV_20160320T062950_20160320T063017_010449_00F80A_E8E3 (Secondary)

Table E.2: Sentinel-1 data for 2016

Reference	Secondary	Reference image name
8th October 2016	20th October 2016	S1A_IW_SLC__1SDV_20161008T175834_20161008T175901_013402_015646_0266
20th October 2016	1st November 2016	S1A_IW_SLC__1SDV_20161020T175834_20161020T175901_013577_015BD4_E321
1st November 2016	13th November 2016	S1A_IW_SLC__1SDV_20161101T175834_20161101T175901_013752_016137_9C22
13th November 2016	25th November 2016	S1A_IW_SLC__1SDV_20161113T175834_20161113T175901_013927_0166BB_643C
25th November 2016	7th December 2016	S1A_IW_SLC__1SDV_20161125T175834_20161125T175901_014102_016C0B_9B85
7th December 2016	19th December 2016	S1A_IW_SLC__1SDV_20161207T175833_20161207T175901_014277_01718F_3BBC
19th December 2016	31st December 2016	S1A_IW_SLC__1SDV_20161219T175833_20161219T175900_014452_017711_4FE3
31st December 2016	12th January 2017	S1A_IW_SLC__1SDV_20161231T175833_20161231T175900_014627_017C77_FF23
12th January 2017	24th January 2017	S1A_IW_SLC__1SDV_20170112T175831_20170112T175858_014802_0181C5_8A5C
24th January 2017	5th February 2017	S1A_IW_SLC__1SDV_20170124T175831_20170124T175858_014977_018735_F6FF
5th February 2017	17th February 2017	S1A_IW_SLC__1SDV_20170205T175831_20170205T175858_015152_018C94_0FB
17th February 2017	1st March 2017	S1A_IW_SLC__1SDV_20170217T175830_20170217T175857_015327_01920D_05CC
1st March 2017	13th March 2017	S1A_IW_SLC__1SDV_20170301T175830_20170301T175857_015502_019766_9DD1
13th March 2017	25th March 2017	S1A_IW_SLC__1SDV_20170313T175830_20170313T175858_015677_019CB4_14FC
		S1A_IW_SLC__1SDV_20170325T175831_20170325T175858_015852_01A1E6_F345 (Secondary)

Table E.3: Sentinel-1 data for 2017

Reference	Secondary	Reference image name
3rd October 2017	15th October 2017	S1A_IW_SLC__1SDV_20171003T175837_20171003T175904_018652_01F744_1076
15th October 2017	27th October 2017	S1A_IW_SLC__1SDV_20171015T175837_20171015T175905_018827_01FC9A_21C8
27th October 2017	8th November 2017	S1A_IW_SLC__1SDV_20171027T175838_20171027T175905_019002_0201ED_0419
8th November 2017	20th November 2017	S1A_IW_SLC__1SDV_20171108T175837_20171108T175904_019177_020751_8108
20th November 2017	2nd December 2017	S1A_IW_SLC__1SDV_20171120T175837_20171120T175904_019352_020CD3_4977
2nd December 2017	14th December 2017	S1A_IW_SLC__1SDV_20171202T175837_20171202T175904_019527_02124A_D4C1
14th December 2017	26th December 2017	S1A_IW_SLC__1SDV_20171214T175836_20171214T175903_019702_0217C4_3DD5
26th December 2017	7th January 2018	S1A_IW_SLC__1SDV_20171226T175836_20171226T175903_019877_021D2D_8B97
7th January 2018	19th January 2018	S1A_IW_SLC__1SDV_20180107T175835_20180107T175902_020052_0222B0_B030
19th January 2018	31st January 2018	S1A_IW_SLC__1SDV_20180119T175835_20180119T175902_020227_02283E_10BC
31st January 2018	12th February 2018	S1A_IW_SLC__1SDV_20180131T175834_20180131T175901_020402_022DCC_0337
12th February 2018	24th February 2018	S1A_IW_SLC__1SDV_20180212T175834_20180212T175901_020577_02336D_20AF
24th February 2018	8th March 2018	S1A_IW_SLC__1SDV_20180224T175834_20180224T175901_020752_023903_45BF
8th March 2018	20th March 2018	S1A_IW_SLC__1SDV_20180308T175834_20180308T175901_020927_023E86_F878
		S1A_IW_SLC__1SDV_20180320T175834_20180320T175901_021102_024413_C530 (Secondary)

Table E.4: Sentinel-1 data for 2018

Reference	Secondary	Reference image name
10th October 2018	22nd October 2018	S1A_IW_SLC__1SDV_20181010T175844_20181010T175911_024077_02A1AE_99CC
22nd October 2018	3rd November 2018	S1A_IW_SLC__1SDV_20181022T175844_20181022T175911_024252_02A760_733E
3rd November 2018	15th November 2018	S1A_IW_SLC__1SDV_20181115T175844_20181115T175911_024602_02B3A3_7717
15th November 2018	27th November 2018	S1A_IW_SLC__1SDV_20181115T175844_20181115T175911_024602_02B3A3_7717
27th November 2018	9th December 2018	S1A_IW_SLC__1SDV_20181127T175843_20181127T175910_024777_02BA1D_7EF
9th December 2018	21st December 2018	S1A_IW_SLC__1SDV_20181209T175843_20181209T175910_024952_02BFF5_8BB9
21st December 2018	2nd January 2019	S1A_IW_SLC__1SDV_20181221T175843_20181221T175910_025127_02C64A_5DBA
2nd January 2019	14th January 2019	S1A_IW_SLC__1SDV_20190102T175842_20190102T175909_025302_02CC99_BE94
14th January 2019	26th January 2019	S1A_IW_SLC__1SDV_20190114T175842_20190114T175909_025477_02D2E3_CE39
26th January 2019	7th February 2019	S1A_IW_SLC__1SDV_20190126T175841_20190126T175908_025652_02D951_6D2C
7th February 2019	19th February 2019	S1A_IW_SLC__1SDV_20190207T175841_20190207T175908_025827_02DF93_8638
19th February 2019	15th March 2019	S1A_IW_SLC__1SDV_20190219T175841_20190219T175908_026002_02E5D1_1A74
15th March 2019	27th March 2019	S1A_IW_SLC__1SDV_20190315T175841_20190315T175908_026352_02F281_FE61
		S1A_IW_SLC__1SDV_20190327T175841_20190327T175908_026527_02F8EE_BF91 (Secondary)